Direct Functionalization of Carboxylic Acids by Boron Catalysis

ホウ素触媒によるカルボン酸直接修飾反応の開発

SUN KAI

2024

Contents

General Introduction

1. Value of carboxylic acids

Carboxylic acids exist ubiquitously in living bodies and the surrounding environment. Despite their different molecular structures, they play critical roles in various biological processes that are crucial in keeping the form of the world.

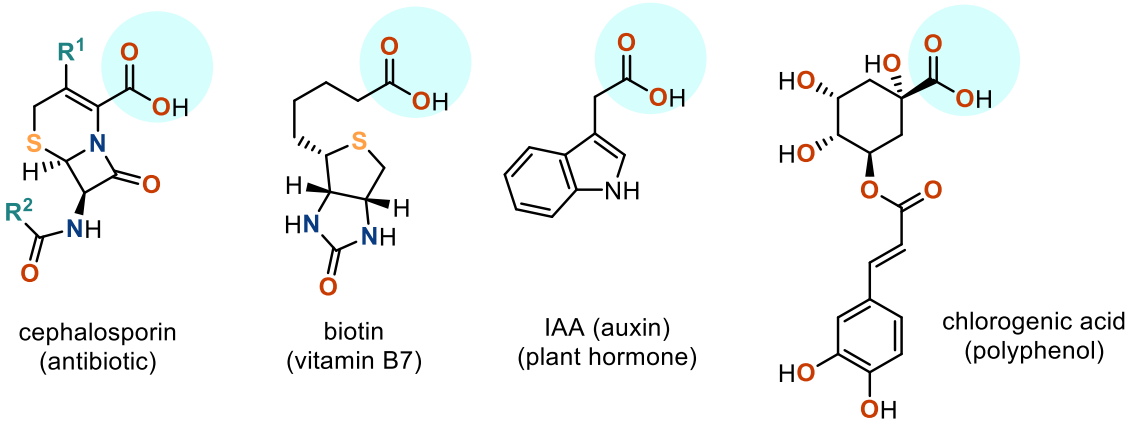

Fig 1 Examples of natural products containing carboxy group

Inspired by naturally occurring bioactive molecules, pharmaceuticals based on carboxylic acid have been widely developed. For example, they constitute a category of NSAIDs (Non-Steroidal Anti-Inflammatory Drugs).

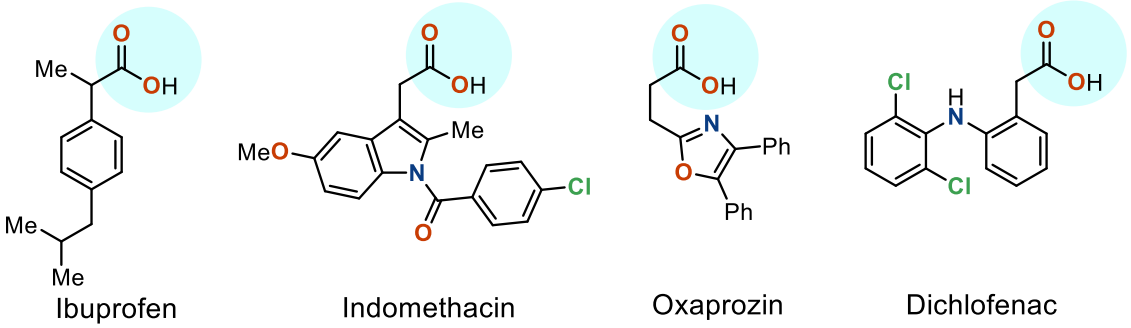

Fig 2 Carboxylic acids developed by human as pharmaceuticals: NSAIDs

Besides their direct usage, carboxylic acids also act as important synthetic precursors and intermediates. Carboxy groups can be readily converted into amido groups, ester groups and so on. Additionally, they can also be removed by decarboxylation to reveal the carbon skeleton. Versatile reactivity bestows them synthetic utility leading to a wide variety of products. As an illustrative example, carboxylic acid has been known as an important intermediate in the synthesis of cabotegravir,[1] which is used to treat

HIV/AIDS.

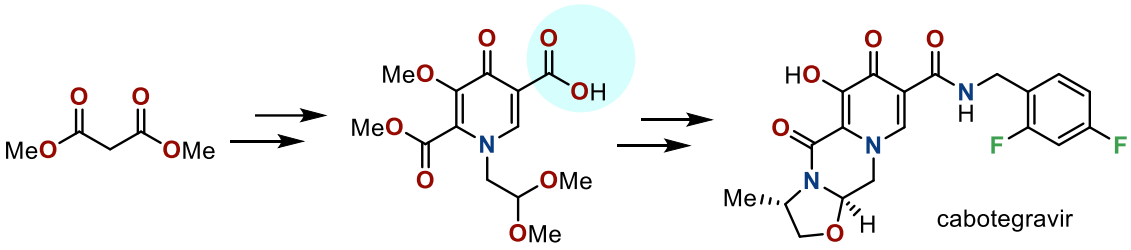

Fig 3 Synthetic route of cabotegravir

Masami Okabe and coworkers[2] reported an efficient synthetic route for Ro 28-2653, a highly selective barbiturate class of matrix metalloproteinase inhibitor. Their synthesis started from a carboxylic acid compound Felbinac, which is also a commercially available, well-known pharmaceutical.

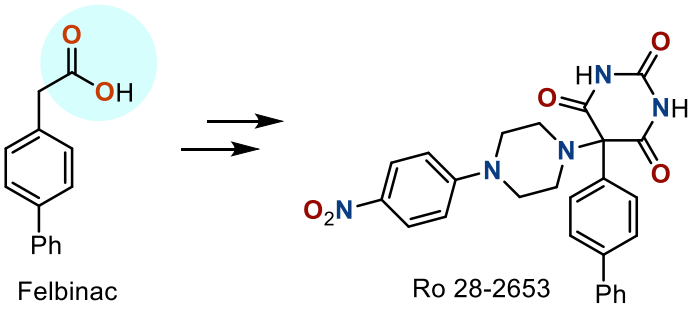

Fig 4 Synthesis of Ro 28-2653 from Felbinac

Based on the above-mentioned reasons, convenient and efficient functionalization of carboxylic acids has been highlighted among organic chemists. Functionalization of carboxylic acids can provide people with more synthetic flexibility to generate more value-added products.

2. Direct functionalization of carboxylic acid

Carboxylic acid features an active hydrogen atom, which is acidic and can thus be easily removed as proton. This character can fail many approaches by deactivating the reactants or catalysts, inducing unwanted byproducts, or causing solubility issues.

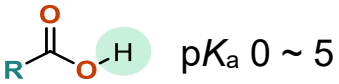

Fig 5 Typical acidity of carboxylic acids

Conventional strategy to solve this problem is to remove this hydrogen by protection

prior to the functionalization. However, this procedure requires two additional steps, i.e. protection and deprotection. At the same time, the stoichiometric reagent used for protection is doomed to cause low atom economy.

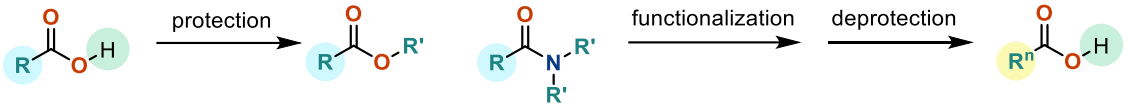

Fig 6 Conventional procedure of carboxylic acid functionalization

In this context, direct functionalization of carboxylic acids becomes a great interest of chemists. To achieve this goal, one approach is to develop a method that simply tolerates carboxy group, which is beyond the scope of discussion here. Another strategy is to utilize carboxy group, in which metal or metalloid atoms are widely used to replace hydrogen and form a transient species. Such species are active in the reaction whilst quenched by a simple work-up procedure.

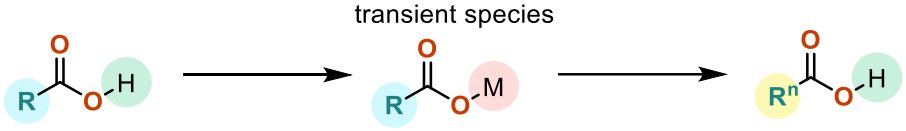

Fig 7 Direct functionalization of carboxylic acids

Kazuaki Ishihara and coworkers[3] reported an enantioselective conjugate addition of carboxylic acids. This reaction features using chiral amine-boronic acid cooperative catalysis. In this reaction, the boronic acid catalyst forms a mixed anhydride to activate α,β-unsaturated carboxylic acid.

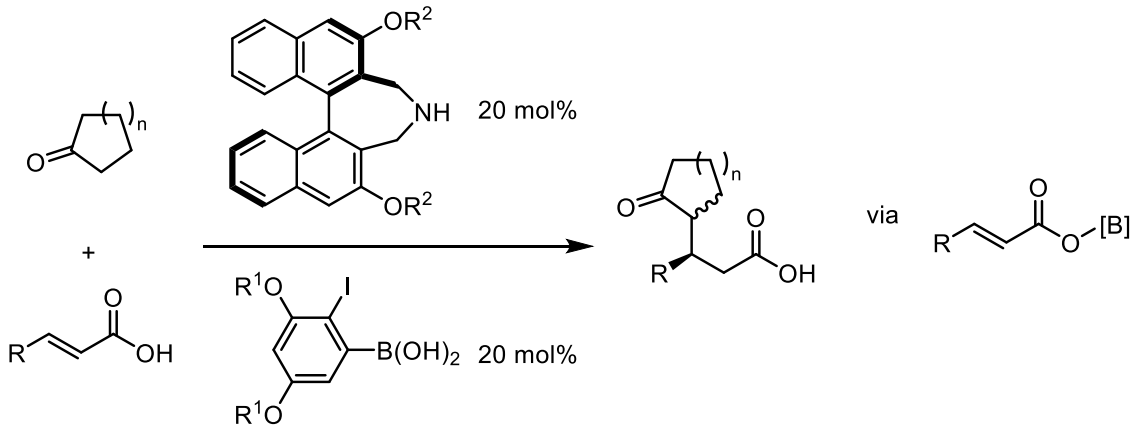

Fig 8 Enantioselective conjugate addition of carboxylic acids

Jin-Quan Yu and coworkers[4] reported a Pd-catalyzed β-C-H activation, which

forms C-C bonds by using carboxyl group itself as the directing group. This reaction is applicable to not only benzoic acid derivatives but also aliphatic acids, which was an unanswered challenge.

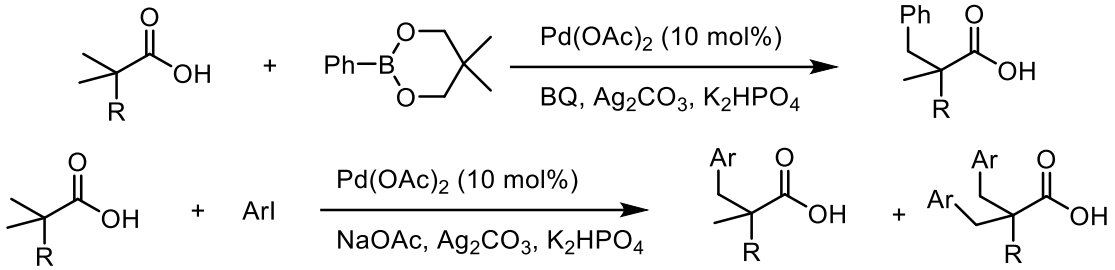

Fig 9 Pd-catalyzed β-C-H activation

Among these methods for the direct functionalization of carboxylic acids, direct α-functionalization is an attractive category. The strategy is to generate the semi-stable enolate by further removing α-H. The enolate intermediate then reacts with a variety of reagents, typically electrophiles, to introduce new functional groups including alkyl, aryl, carbonyl, amino, hetero atoms and so on.

Due to its high utility and adjustability, chemists have examined various metals or metalloids for these transformations. For example, alkali metals such as Li, Na, alkali earth metals such as Mg, metalloids such as B, Si as well as transition metals such as Fe.

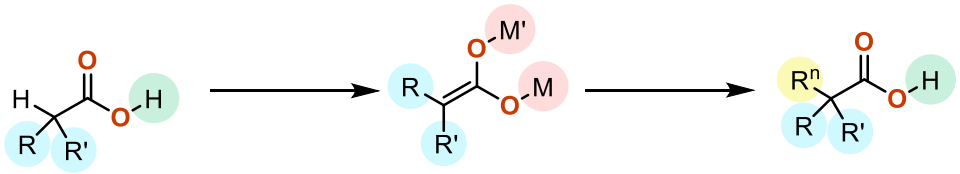

Fig 10 Direct α-functionalization of carboxylic acids via enolate

Atsunori Mori and coworkers[5] reported an arylation of arylacetic acid with Pd catalyst. The reaction first generates magnesium enolate using Grignard reagent as a base, followed by the treatment of Pd catalyst and aryl bromide to afford corresponding diarylacetic acid.

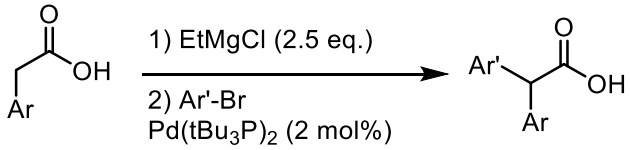

Fig 11 Magnesium enolate used for arylation

David B. Collum, Armen Zakarian and coworkers[6] reported several reactions

including alkylations, Michael additions, and aldol reactions using lithium enolates as the intermediate. Chiral lithium amides were used as transient auxiliaries, which form mixed aggregates in situ. Such aggregation posts an influence on the lithium enolate and gives high enantioselectivity. In addition, the chiral amine used in the reaction can be recovered after the reaction.

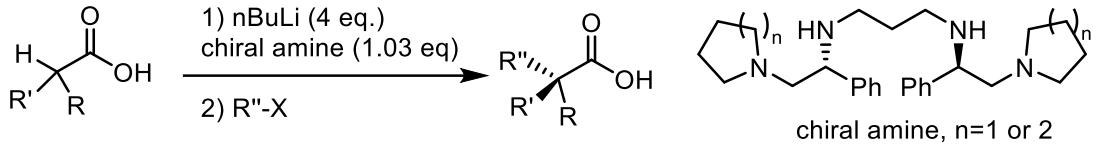

Fig 12 Enantioselective quaternary carbon center construction with lithium enolates

The Hartwig group[7] reported a palladium-catalyzed α-arylation of carboxylic acids, which can be applied to a variety of carboxylic acids as well as a range of aryl bromides. In the reaction, the carboxylic acid was tentatively protected by the silyl group, which can be removed easily after the reaction. This reaction is also effective at gram-scale synthesis, bestowing its utility and practicality.

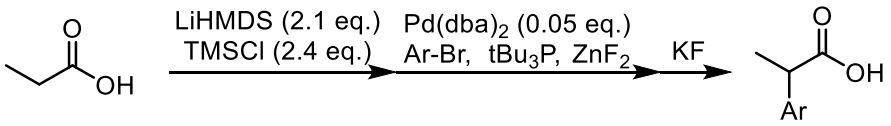

Fig 13 Traceless protection with the silyl group

Shunsuke Kotani, Makoto Nakajima and coworkers[8] reported an enantioselective aldol reaction between carboxylic acids and aldehydes. $SiCl_4$ was used to generate bis(trichlorosilyl)enediolates as intermediates *in situ*. A chiral bis(phosphine oxide) was used as a Lewis base catalyst to induce enantioselectivity. The protocol extended to the reaction with an α-ketoester was also showcased.

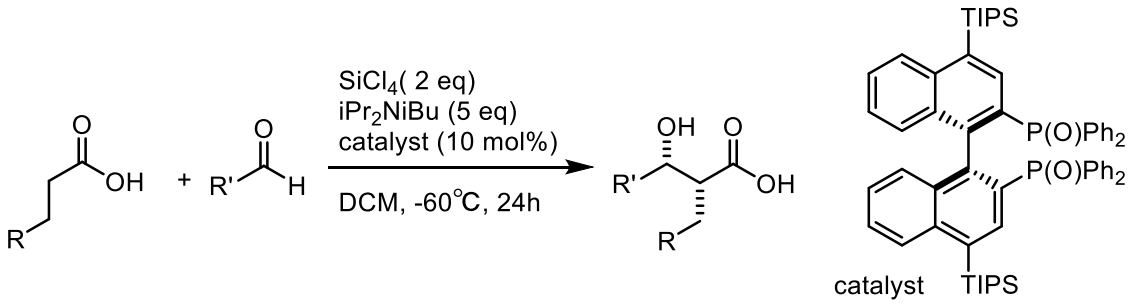

Fig 14 Silicon mediated enantioselective aldol reaction

These reactions all feature the generation of a stoichiometric amount of enolate,

followed by catalytic or stoichiometric reaction with enolate. Catalytically generated enolate has also been reported to achieve α-functionalization.

Ryo Yazaki, Takashi Ohshima and coworkers[9] reported an α-oxidation of carboxylic acids by using $Fe(OAc)_2$ as the catalyst. Iron- and alkali metal ions derived from molecular sieves participated in the forming of enolate. Such species are redox active and react with stable oxyl radicals, TEMPO and its derivatives, to give the product.

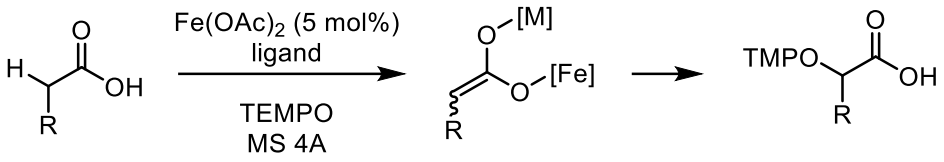

Fig 15 Catalytic reaction using Fe species as the catalyst

3. Boron catalysis in direct functionalization of carboxylic acid

Boron reagents are well known to efficiently generate enolate from carboxylic acid, and subsequent functionalization can be achieved using this strategy. Compared with other metals or metalloids, boron has several special merits in the functionalization of carboxylic acids. For example, boron has good ability of ligation so its reactivity and selectivity can be easily tuned for desired reaction. Furthermore, boron catalyzed carboxylic acid functionalization usually features mild conditions, which allow for broader reaction scope. In addition, boron can be removed by a simple workup, while silicon and another metalloid used in carboxylic acid functionalization require fluorides for complete removal. Also, boron has good abundance on earth and good accessibility from ores, which contributes to the lower cost for boron catalysis. Last but not least, boron has lower toxicity comparing with heavy metals, which makes it more environmentally friendly and promising to be used at a larger scale in industry. Besides, boron has higher electronegativity and smaller radius compared with other metals and metalloids, which give boron unique properties in the functionalization of carboxylic acids.

As an example of the application of stoichiometric boron reagent in the functionalization of carboxylic acids, D. A. Evans and coworkers[10] reported a stereoselective aldol condensation via boron enolates. Dialkylboryl triflates were used with carboxylic acid derivatives or ketones to generate boron enolates, while carboxylic acids generate dialkylboryl enediolates.

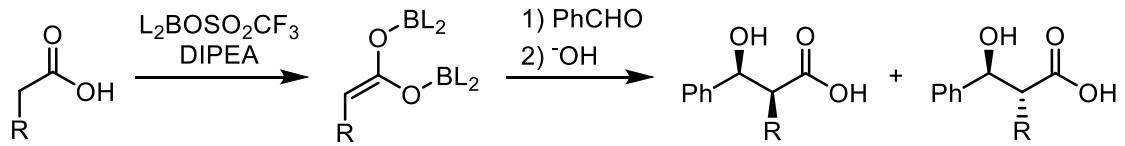

Fig 16 Aldol condensation of carboxylic acids via dialkylboryl enediolates

P. Veeraraghavan Ramachandran and coworkers[11] reported an anti-selective enolboration-aldolization of propionic acid. Boron reagent cyh_2BBr was used to enolize the propionic acid, allowing further aldol reaction with aldehydes.

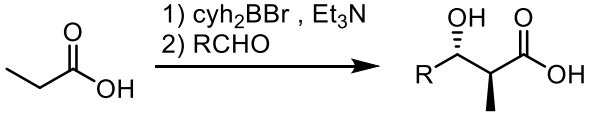

Fig 17 Stoichiometric example of boron application

Research over the past decade employing boron as a catalyst in the functionalization of carboxylic acid will be highlighted here.

Yohei Shimizu, Motomu Kanai, and coworkers[12] developed a Mannich-type reaction using carboxylic acid as the substrate and borane as the catalyst. In this reaction, the carboxylic acid was activated by a catalytic amount of BH_3•SMe_2, which was further deprotonated by DBU to generate the enolate. The enolate can act as nucleophile to furnish Mannich-type reactions. Additionally, chiral ligands are implemented to induce enantioselectivity in this reaction.

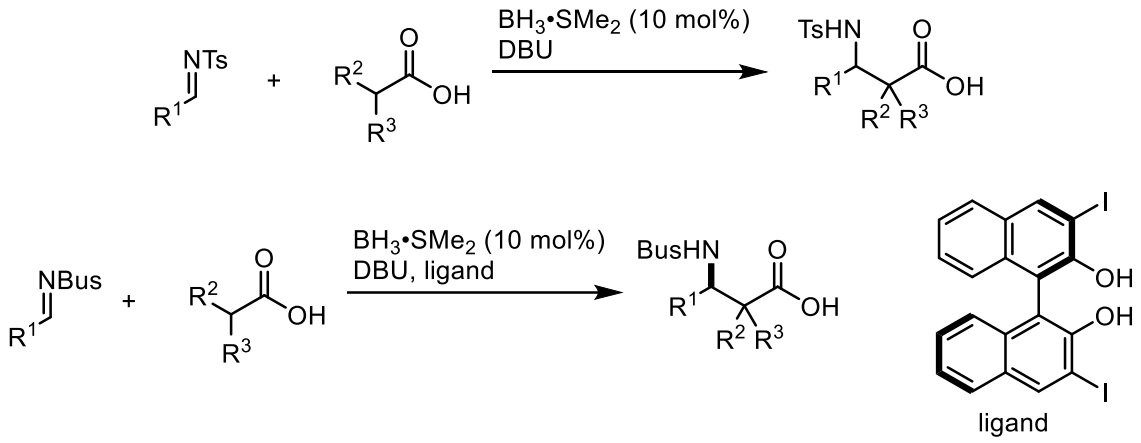

Fig 18 Boron catalyzed Mannich-type reaction

Yohei Shimizu, Motomu Kanai, and coworkers[13] reported a selective aldol reaction between carboxylic acids and trifluoromethyl ketones. The functionalization occurs only at the α-position of the carboxylic group, while ketone, ester or amide functional groups remain inert.

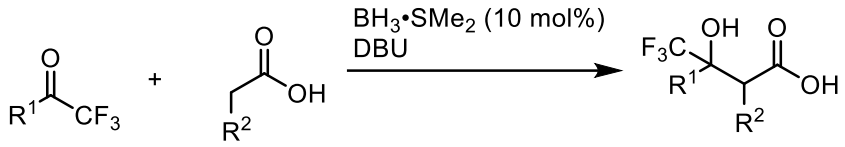

Fig 19 An aldol reaction example

Masaya Sawamura, Yohei Shimizu, and coworkers[14] reported an α-amination using diisopropylazodicarboxylate (DIAD) as an electrophilic aminating reagent. This reagent reacts with the catalytically generated boron enolates, yielding amino acid derivatives. The product can be further derivatized with ease. In addition, enantioselective reaction is possible by introducing a chiral ligand on the boron catalyst.

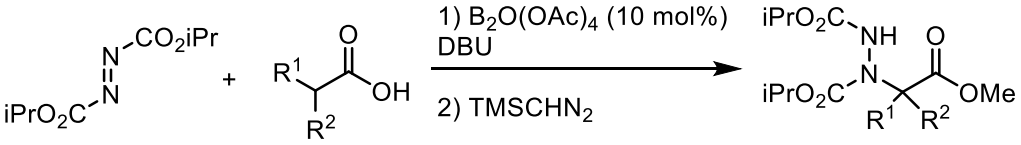

Fig 20 Boron catalyzed α-amination with DIAD

In some special cases, hybrid catalysis using boron along with another metal or metalloid gives unique reactivity.

Yohei Shimizu, Motomu Kanai, and coworkers[15] reported a hybrid catalysis consisting of palladium and boron complexes. The reaction generates acyclic quaternary carbon centers chemo- and enantioselectively at the α-position of the carboxylic acid. Boron enolate acts as nucleophile, while π-allyl palladium acts as an electrophile. Two chiral ligands were crucial in tuning the selectivity of this reaction.

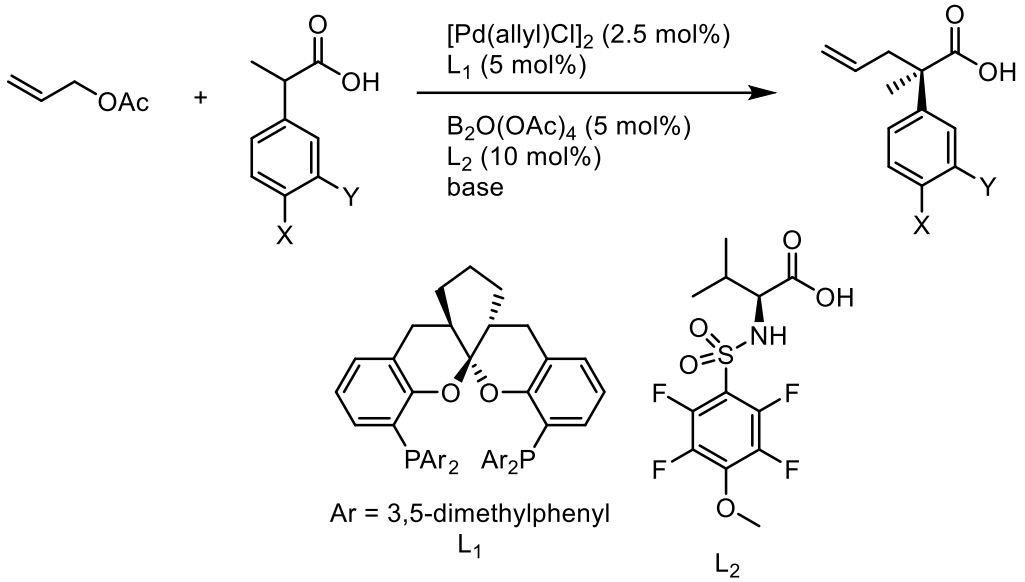

Fig 21 Pd/B hybrid catalysis of carboxylic acid functionlization

Harunobu Mitsunuma, Motomu Kanai, and coworkers[16] reported a chemo-selective asymmetric aldol reaction between carboxylic acids and aldehydes catalyzed by boron catalyst, where siloxy esters are formed in situ to activate the carboxylic acid. Si/B enediolates were proposed to be the active species. The reaction is applicable to multifunctional substrates to enable late-stage functionalization.

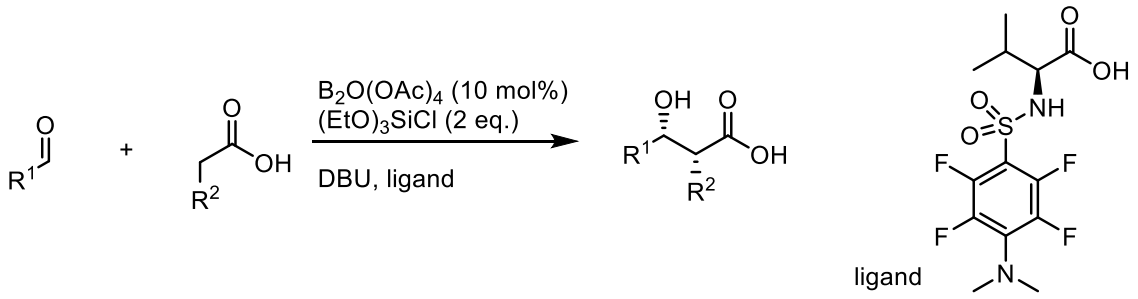

Fig 22 Boron catalyst and silicon reagents utilized in carboxylic acid functionalization

Based on these advantages of boron catalyzed functionalization of carboxylic acid, Further development of this method can bring people new transformations and better utilization of carboxylic acid. Importantly, most of the boron-catalyzed functionalization of carboxylic acids focuses on α-functionalization. Although Michael additions of α,β-unsaturated carboxylic acids have been frequently reported, β-functionalization of saturated carboxylic acids is rarely developed. Such research can be useful in expanding the synthetic utility of carboxylic acids.

4. References

[1] Hughes, D. L., *Org. Process Res. Dev*. **2019**, *23*, 716–729.

[2] Daniewski, A. R.; Liu, W.; Okabe, M., *Org. Proc. Res. Dev*. **2004**, *8*, 411–414.

[3] Horibe, T.; Hazeyama, T.; Nakata, Y.; Takeda, K; Ishihara, K., *Angew. Chem. Int. Ed*. **2020**, *59*, 17256 –17260.

[4] Giri, R.; Maugel, N.; Li, J. J.; Wang, D. H.; Breazzano, S. P.; Saunders, L. B.; Yu, J. Q., *J. AM. CHEM. SOC*. **2007**, *129*, 3510-3511.

[5] Tanaka, D.; Tanaka, S.; Mori, A., *Eur. J. Org. Chem*. **2014**, 4254–4257.

[6] Yu, K.; Lu, P.; Jackson, J. J.; Nguyen, T. D.; Alvarado, J.; Stivala, C. E.; Ma, Y.; Mack, K. A.; Hayton, T. W.; Collum, D. B.; Zakarian, A., *J. Am. Chem. Soc*. **2017**, 139, 527−533.

[7] He, Z. T.; Hartwig, J. F., *J. Am. Chem. Soc*. **2019**, *141*, 11749−11753.

[8] Kotani, S.; Yoshiwara, Y.; Ogasawara, M.; Sugiura, M.; Nakajima, M., *Angew. Chem. Int. Ed*. **2018**, *57*, 15877 –15881.

[9] Tanaka, T.; Yazaki, R.; Ohshima, T., *J. Am. Chem. Soc*. **2020**, *142*, 4517−4524.

[10] Evans, D. A.; Nelson, J.V.; Vogel, E.; Taber, T.R., *J. Am. Chem. Soc*. **1981**, *103*, 3099-3111.

[11] Ramachandran, P. V.; Chanda,P. B.; Otoo, B., *Tetrahedron Letters*, **2014**, *55*, 1289–1291.

[12] Morita, Y.; Yamamoto, T.; Nagai, H.; Shimizu, Y.; Kanai, M., *J. Am. Chem. Soc*. **2015**, *137*, 7075−7078.

[13] Ishizawa, K.; Nagai, H.; Shimizu, Y.; Kanai, M., *Chem. Pharm. Bull*. **2018**, *66*, 231–234.

[14] Morisawa, T.; Sawamura, M.; Shimizu, Y., *Org. Lett*. **2019**, *21*, 7466−7469.

[15] Fujita, T.; Yamamoto, T.; Morita, Y.; Chen, H.; Shimizu, Y.; Kanai, M., *J. Am. Chem. Soc*. **2018**, *140*, 5899−5903.

[16] Fujita, T.; Yamane, M.; Sameera, W. M. C.; Mitsunuma, H.; Kanai, M., *Angew. Chem. Int. Ed*. **2021**, *60*, 24598– 24604.

Chapter 1
Light-driven α-Allylation of Carboxylic Acids[17]

1.1 Introduction

Although nucleophilic reactions of carboxylic acid have been studied for a long time by chemists, radical pathways for carboxylic acid functionalization are rarely reported. Recently, photoinduced radical reactions for the functionalization of other carbonyl compounds have been reported.

In 2010, the MacMillan group[18] reported an enantioselective aldehyde α-benzylation. A chiral imidazolidinone was used as the catalyst. The aldehyde substrate first condenses with imidazolidinone catalyst during the reaction to form a π-nucleophilic enamine, which further reacts with benzyl radical generated by Ir photocatalyst.

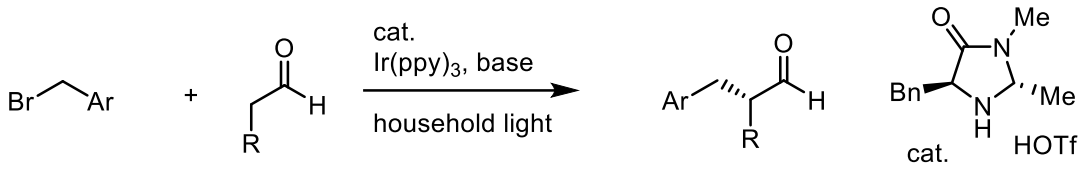

Fig 1.1 Aldehyde α-benzylation

Paolo Melchiorre and coworkers[19] reported a visible-light-driven, stereoselective α-alkylation of aldehydes. The chiral amine catalyst participated in both photochemical activation of the substrates and the stereo-determining C–C bond formation. The difficulty of accomplishing asymmetric α-alkylation of aldehydes under thermal conditions was conquered by applying the radical mechanism.

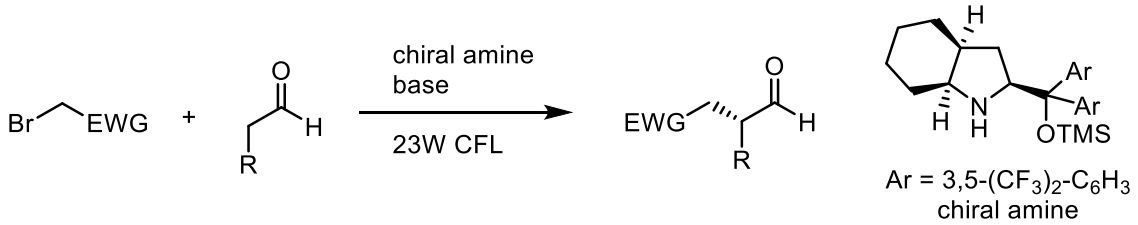

Fig 1.2 Visible-light-driven a-alkylation of aldehydes

The Melchiorre group[20] later also reported an aromatic perfluoroalkylation and trifluoromethylation of α-cyano arylacetates. This method features a metal-free approach. The electron donor-acceptor (EDA) complexes formed in situ were activated by visible-light irradiation under ambient temperature.

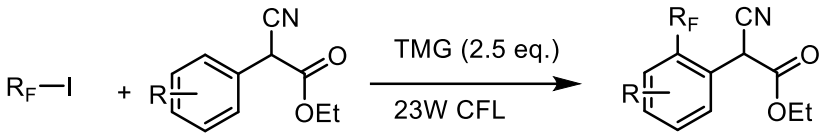

Fig 1.3 Perfluoroalkylation and trifluoromethylation

In recent years, α-functionalization of carboxylic acid via radical pathway has also been reported.

David W. C. MacMillan and coworkers[21] reported an α-arylation of several carbonyl compounds, including α-chlorocarboxylic acids, by a manner of cross-electrophile coupling. The reaction proceeds through a halogen atom abstraction and a nickel radical-capture mechanism. A wide range of aryl bromide coupling partners can be tolerated. However, the reaction with carboxylic acid requires an α-chloro substituent, which is a limitation in the aspect of carboxylic acid functionalization.

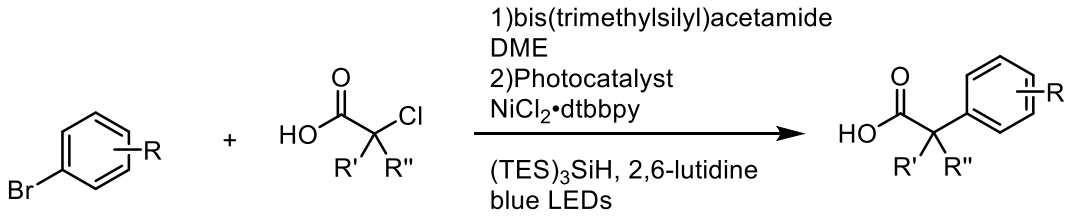

Fig 1.4 α-Arylation via a radical process

Ryo Yazaki, Takashi Ohshima, and coworkers[9] reported an α-oxidation of carboxylic acids, as introduced in previous paragraph. Although this reaction tolerates a wide range of carboxylic acid substrates, the requirement of stable free radicals as the coupling partner limits its further application.

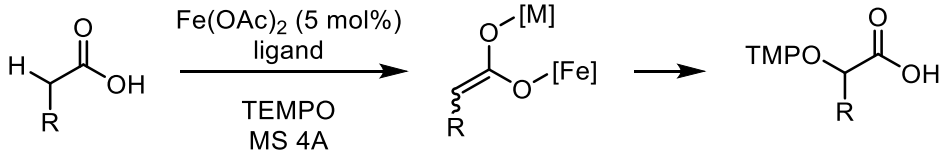

Fig 1.5 Catalytic reaction using Fe species as the catalyst

α-Alkylation via radical pathway have until now not been reported yet. Although nucleophilic α-alkylation is well-developed, those reactions require very strong bases to remove α-H, thus severely limiting the scope.

1.2 Hypothesis

Boron catalysis for α-functionalization of carboxylic acid had been proven to proceed under mild conditions. However, α-alkylation with alkylation reagent is not preferable because the carboxylate forms rapidly, while α-functionalization is slow due to the low concentration of enolate species. A radical pathway may solve the problem.

Allyl sulfones are good intermediates for the synthesis of pharmaceuticals. They are also used as reagents for allylation reactions[22][23][24]. Thus, the allyl sulfones were chosen as the coupling partner to develop a boron-catalyzed α-allylation reaction.

I envisioned that π-conjugation with enolate and ligand on the boron can enable its single electron transfer (SET) to electron-accepting allyl sulfones and generate allyl radicals, thus providing further allylation product by radical coupling.

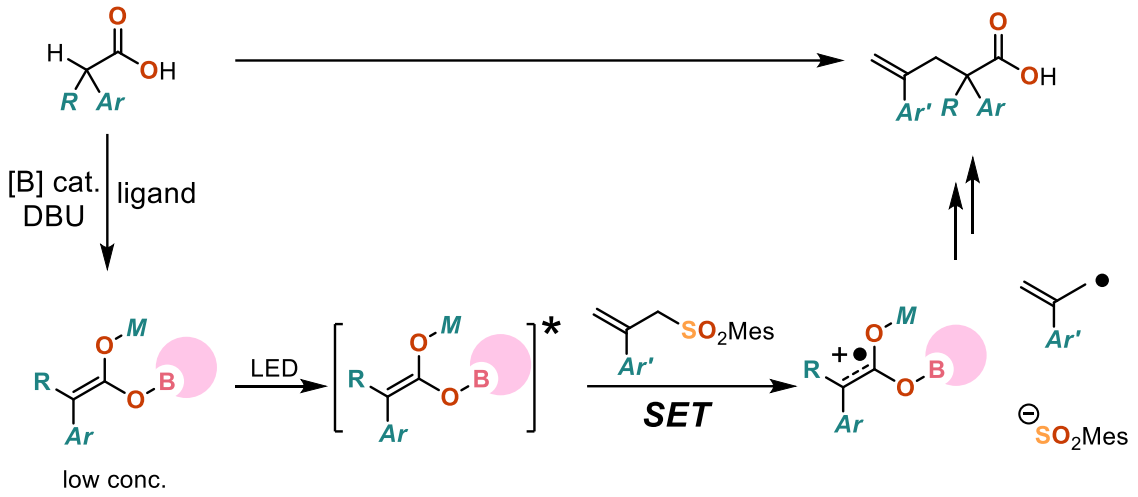

Fig 1.6 Proposed reaction scheme

1.3 Screening

1.3.1 ligand

Considering the π-conjugation affect the photoexcitation efficiency, different ligands with various π-system had been tested. At first, α-disubstituted carboxylic acids were chosen to be the substrate. It can be clearly noticed that ligands with larger π-conjugation gave higher yield, which is consistent with the hypothesis. It was also found that iodine atom as the substitution on the ligand affects the yield. Unfortunately, substitution patterns that provided superior yields were not found. Finally, the **L1** was shown to be the optimal ligand.

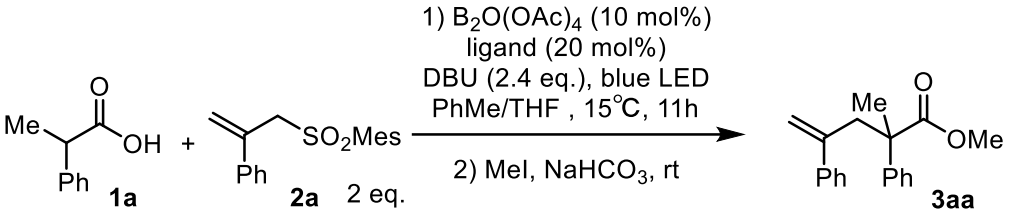

entry	ligand	yield / %
1	**L1**	69
2	**L2**	56
3	**L3**	29
4	**L4**	43
5	**L5**	8
6	**L6**	2
7	none	7

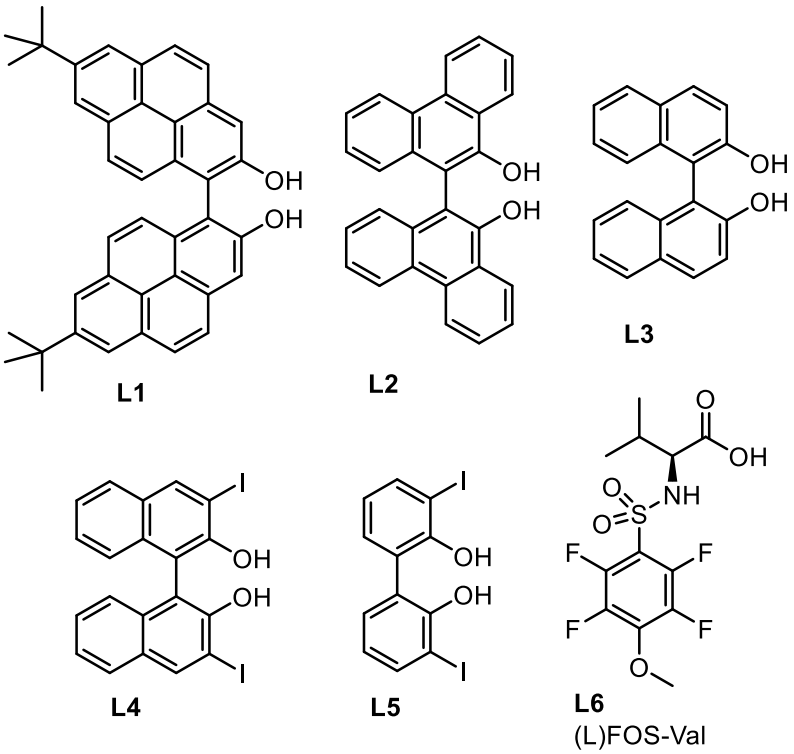

Fig 1.7 Ligand screening for α-disubstituted carboxylic acid

However, for α-monosubstituted carboxylic acid, π-conjugation effect of the ligand was not as prominent. At the same time, the substituents on the ligand play important roles. So **L4** was chosen to be the best ligand for the reaction of α-monosubstituted carboxylic acid.

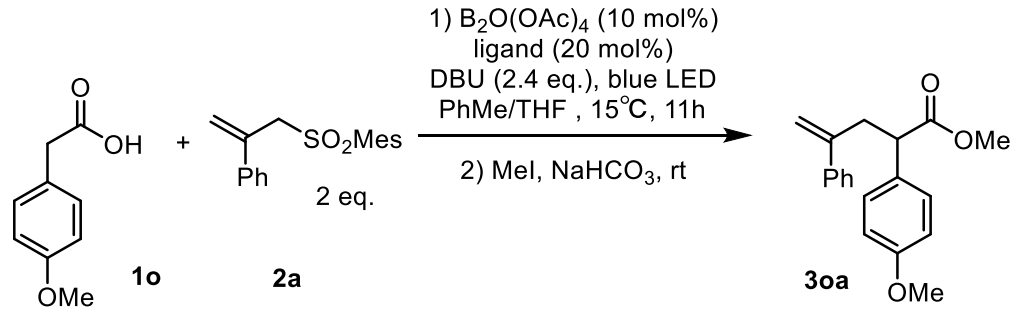

entry	ligand	yield / %
1	**L1**	54
2	**L2**	37
3	**L3**	25
4	**L4**	59
5	**L5**	37
6	**L6**	7

Fig 1.8 Ligand screening for α-monosubstituted carboxylic acid

1.3.2 leaving group on sulfone

The leaving group on the sulfone was screened with the optimal ligand **L1**. It was found that the identity of the leaving group of sulfones was very important to the reaction. However, the relationship between the leaving group and the allylation was unclear.

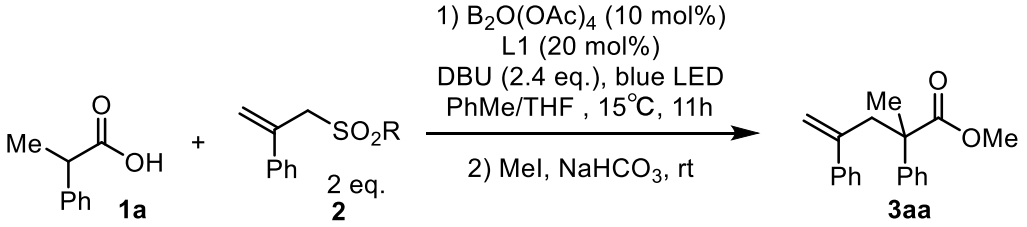

entry	R	sulfone	yield / %
1	Mes	**2a**	69
2	p-Tol	**2a'**	12
3	Me	**2a"**	0

Fig 1.9 Screening of the leaving group on the sulfone

1.3.3 base

Several organic and inorganic bases having different basicity and structures were tested. It was found that DBU gave good yield exclusively, which may be due to its basicity, steric hinderance, and solubility.

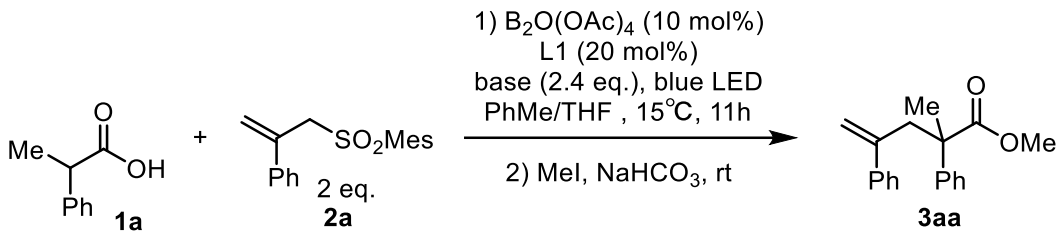

entry	base	yield / %
1	DBU	69
2	DBN	0
3	iPr_2NEt	0
4	Cs_2CO_3	0

Fig 1.10 Base screening

1.4 Scope

With the optimized conditions, the scope of this reaction was investigated.

1.4.1 α,α-disubstituted carboxylic acid scope

Substrates bearing para- or meta- substituents on the α-aryl rings were well tolerated, while the ortho-substitution was not allowed (**3la**). This is probably due to the steric hinderance that hampers the conjugation of enolate with the ligand. The nonreactivity of the α,α-dialkyl substrate (**3ma**) may also be due to the lack of conjugation in the enolate intermediate . Heterocycles such as α-thiophenyl substrate (**3fa**) were also suitable for this reaction. α-Ethyl substrate (**3ha**) was shown to have similar reactivity as α-methyl substrate. This utility of reaction was demonstrated for the transformation of pharmaceuticals such as Naproxen or Loxoprofen (**3ja**, **3ka**).

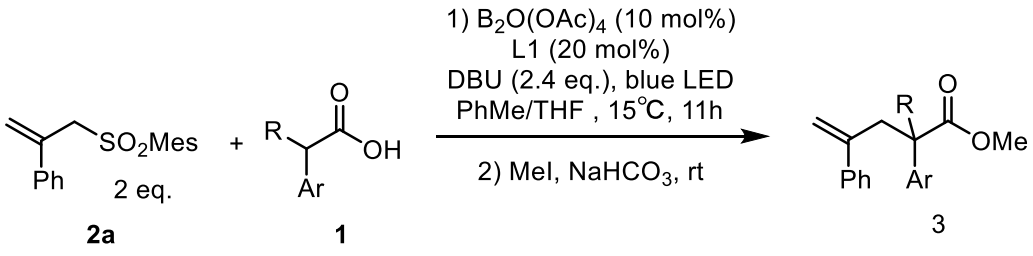

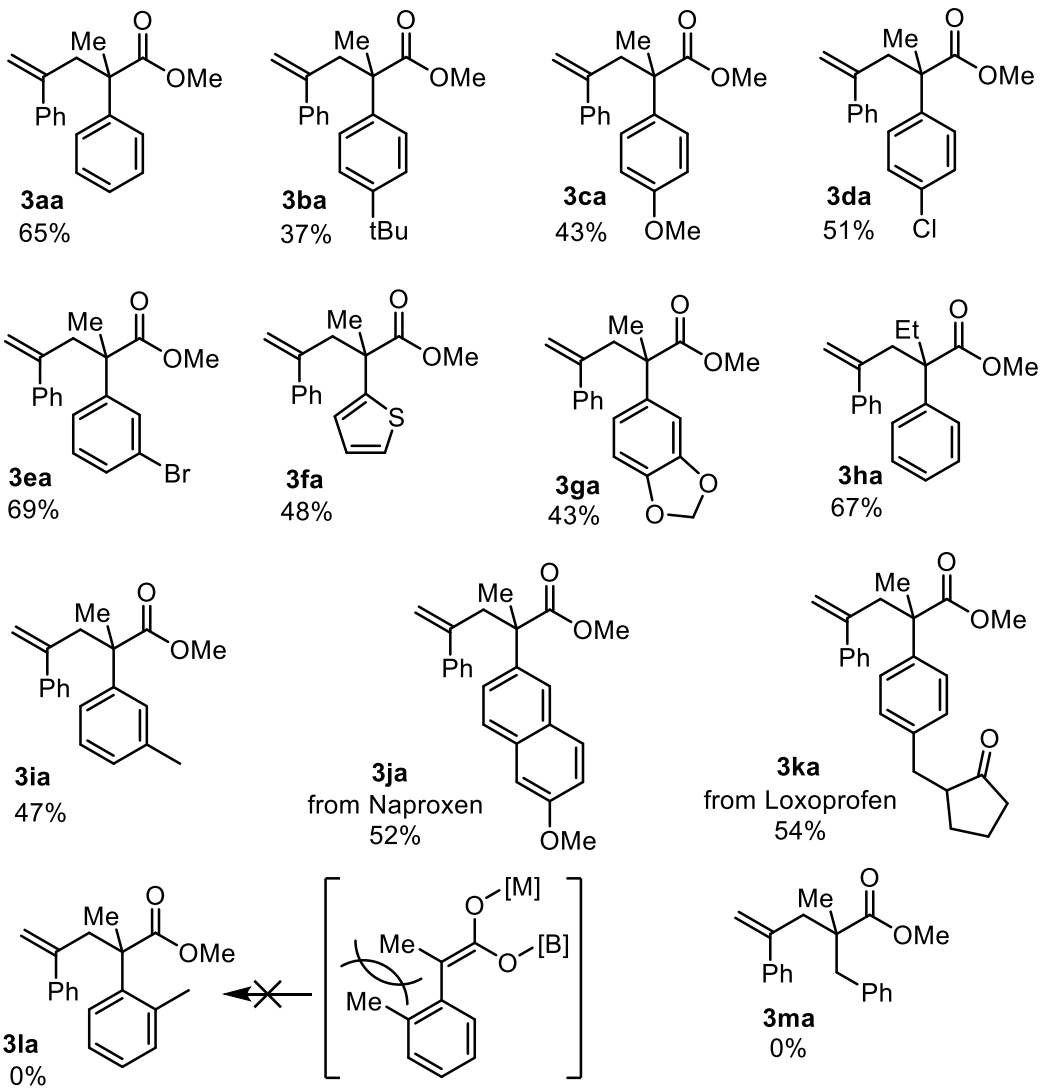

Fig 1.11 α,α-Disubstituted carboxylic acid scope
isolated yield is shown

1.4.2 α-monosubstituted carboxylic acid scope

The scope of α-monosubstituted carboxylic acids was also briefly investigated. Both electron-withdrawing (**3pa**) and -donating (**3oa**) groups on the phenyl ring were tolerated.

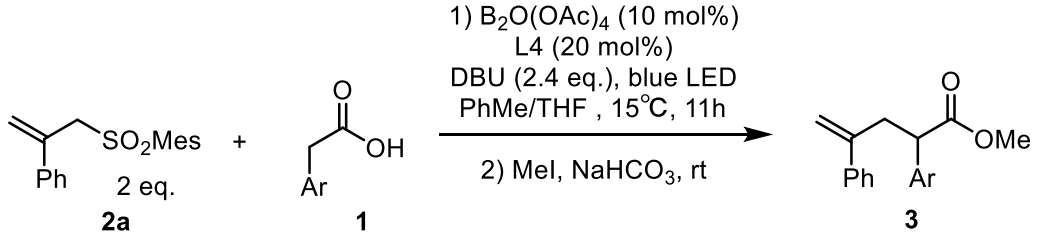

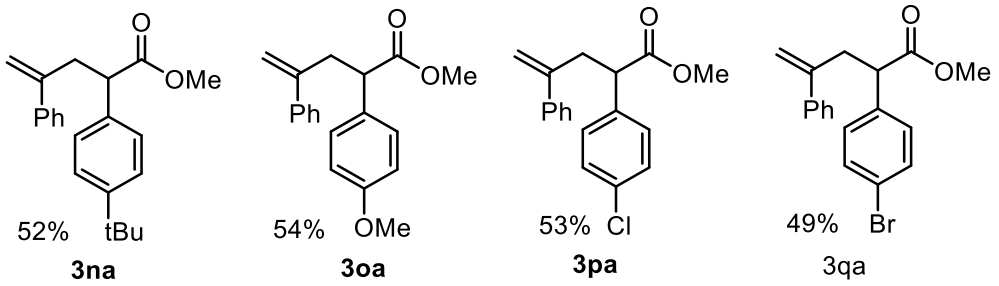

Fig 1.12 α-Monosubstituted carboxylic acid scope
isolated yield is shown

1.4.3 sulfone scope

At last, the sulfone scope was investigated. Substituents at the para- or meta- position were well tolerated. It is noteworthy that acetyl group, which is enolizable, remained untouched during the reaction (**3dc**). Meanwhile an ortho-substitution on the phenyl ring inhibited the reaction (**3dg**). It was also found that the phenyl group on the allyl group is crucial to the reaction, thus the allyl sulfone without phenyl ring on the allyl group all gave 0% yield (**3dh**, **3di**, **3dj**).

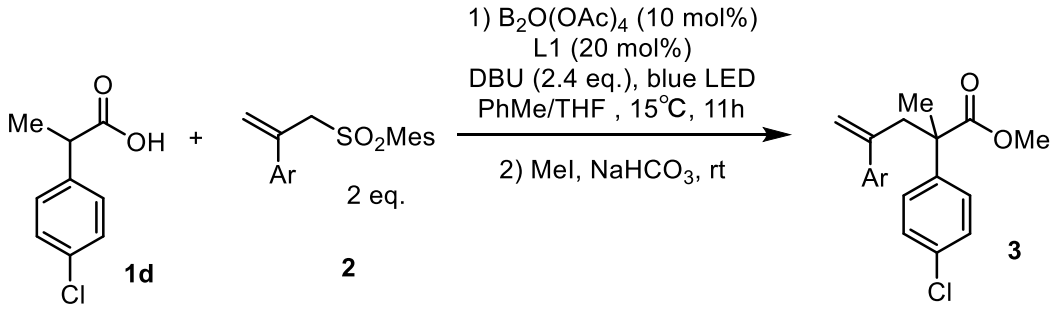

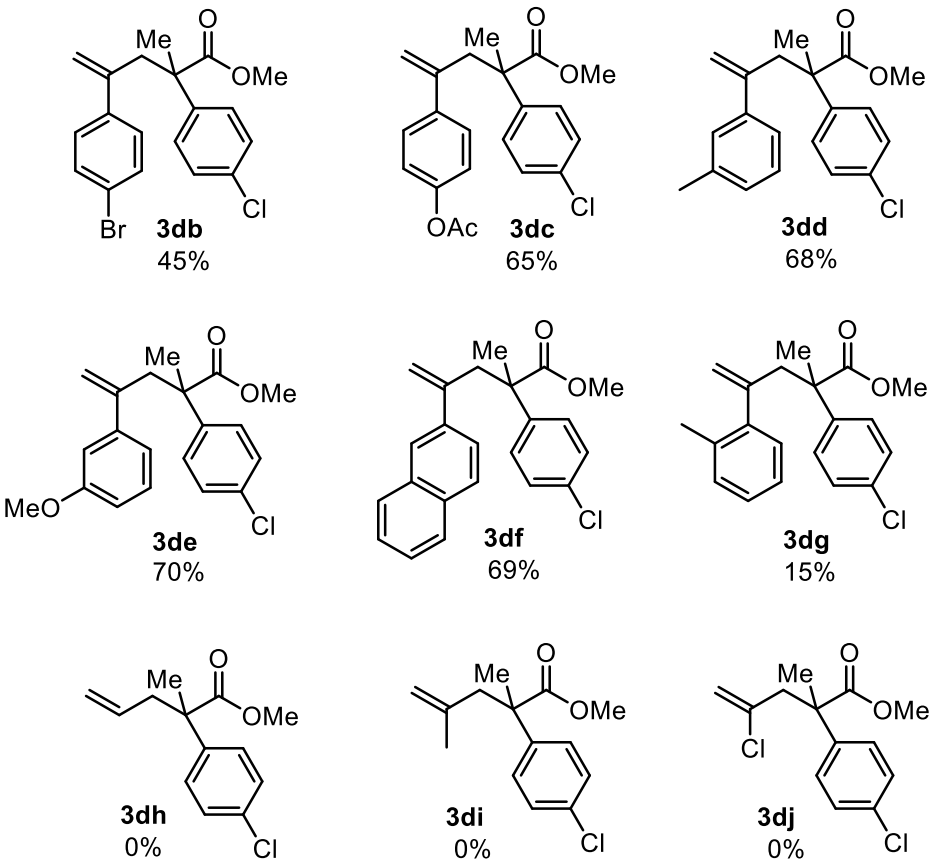

Fig 1.13 Sulfone scope
isolated yield is shown

1.5 Mechanistic investigation

1.5.1 control experiments

To probe the reaction mechanism, control experiments were performed to check the necessity of every component. Entry 2, 4 and 5 suggest that boron and ligand were both crucial in the postulated enolate intermediate that can be activated by photoexcitation. Entry 3 indicates light is essential in this reaction, where a radical pathway may be involved.

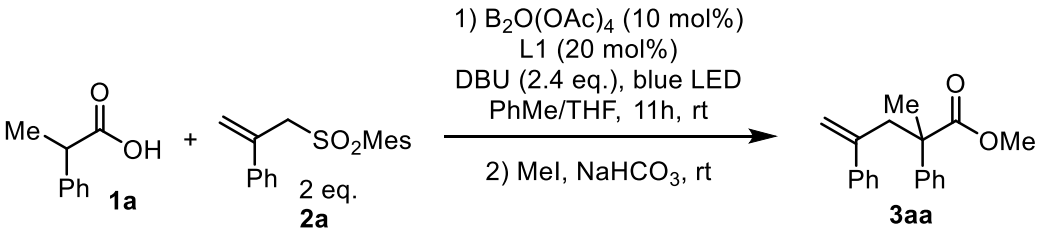

entry	deviation	yield / %
1	none	69
2	w/o L1•2H	7
3	w/o LED	0
4	w/o B2O(OAc)4	0
5	w/o DBU	0

Fig 1.14 Control experiments

1.5.2 addition of radical inhibitor

To further support a scenario of radical process, radical inhibitors were added to the reaction. It was found that the addition of radical inhibitors completely impeded the reaction, which strongly suggests a radical mechanism.

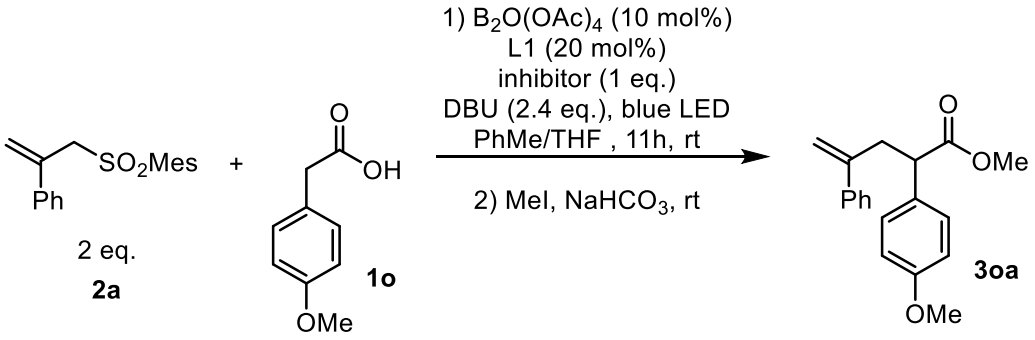

entry	inhibitor	yield / %
1	none	69
2	TEMPO	0
3	BHT	0

Fig 1.15 Radical inhibitors completely stopped the reaction

1.5.3 competition reaction

A ketene silyl acetal (**4j**) was added to the normal reaction, which provided the corresponding product (**3ja**). Meanwhile the same product was not found without the carboxylic acid substrate coexisting in the reaction. This proved the contribution of the allyl radical in the formation of the product. The results also indicate that the anion of the ligand was not likely to be able to reduce the sulfone by themselves. At the same time, the pathway of a single electron transfer from enolate to the sulfone became more plausible.

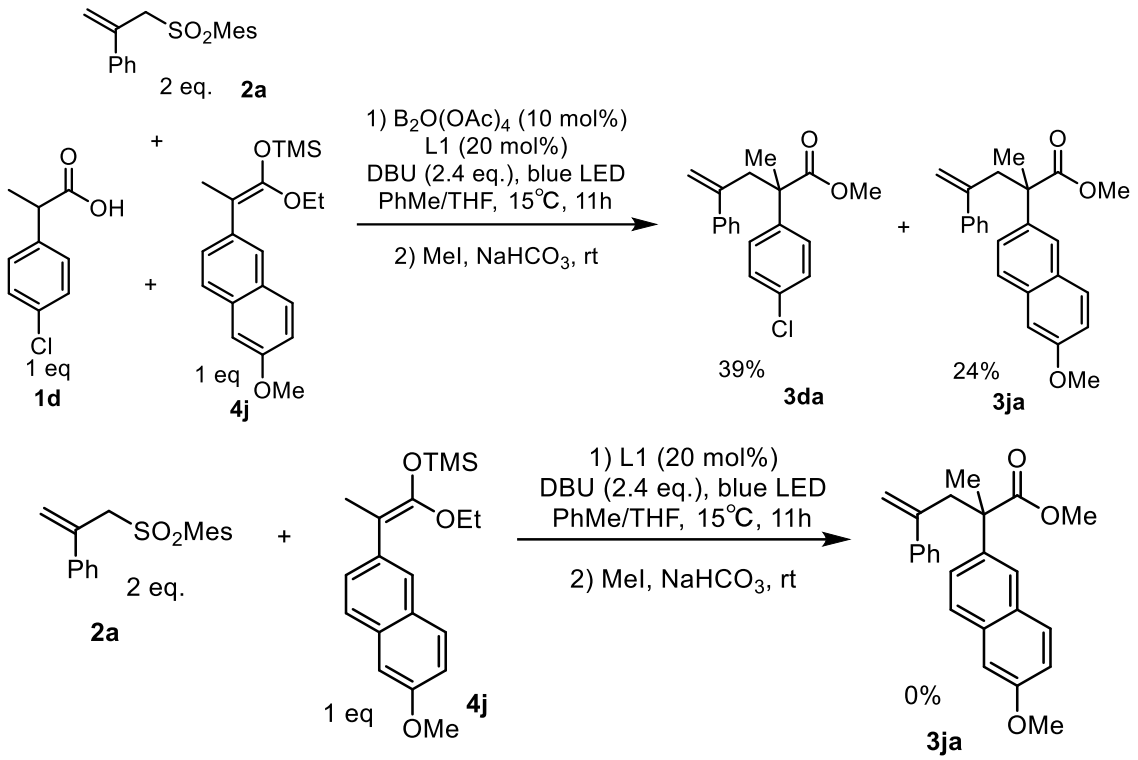

Fig 1.16 Competitive reaction proved the participation of an allyl radical

1.5.4 radical clock experiment

A substrate bearing a dangling double bond (**1r**) was synthesized. As the substrate, this carboxylic acid gave 7% α-allylated product (**3ra**) along with 25% cyclized product (**5ra**). This reaction verified the generation of the α-radical on carboxylic acid.

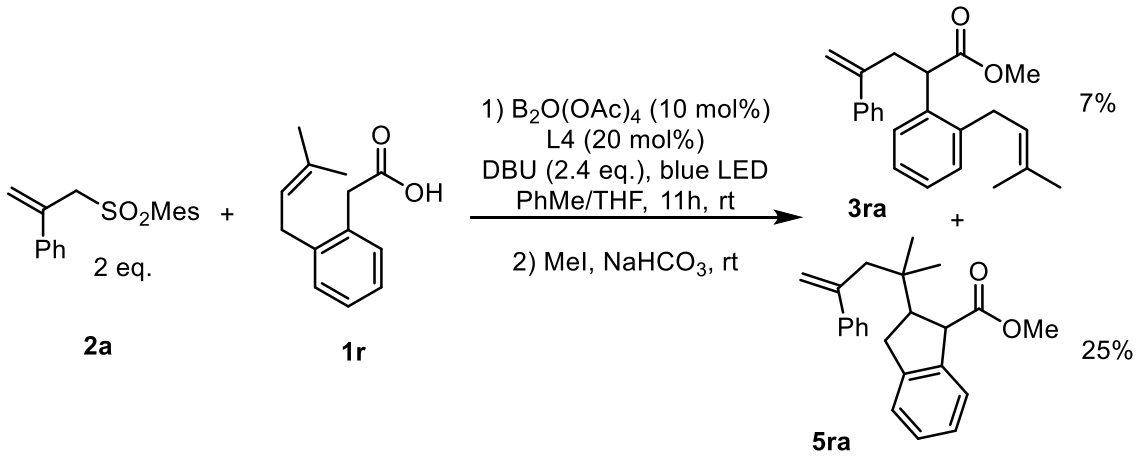

Fig 1.17 Radical clock experiment

1.5.5 effect of LED irradiation

Light on-off experiments were conducted to check the role of blue LED light. The reaction was found to only proceed under light irradiation. This indicates the reaction requires the activation of the intermediate by light energy. Moreover, the rate of product generation dropped below the rate of substrate consumption, which suggests for decomposition side pathways. Finally, the carboxylic acid substrate was fully consumed while the yield did not reach 80%. The deactivation of the catalyst likely occurred during the reaction.

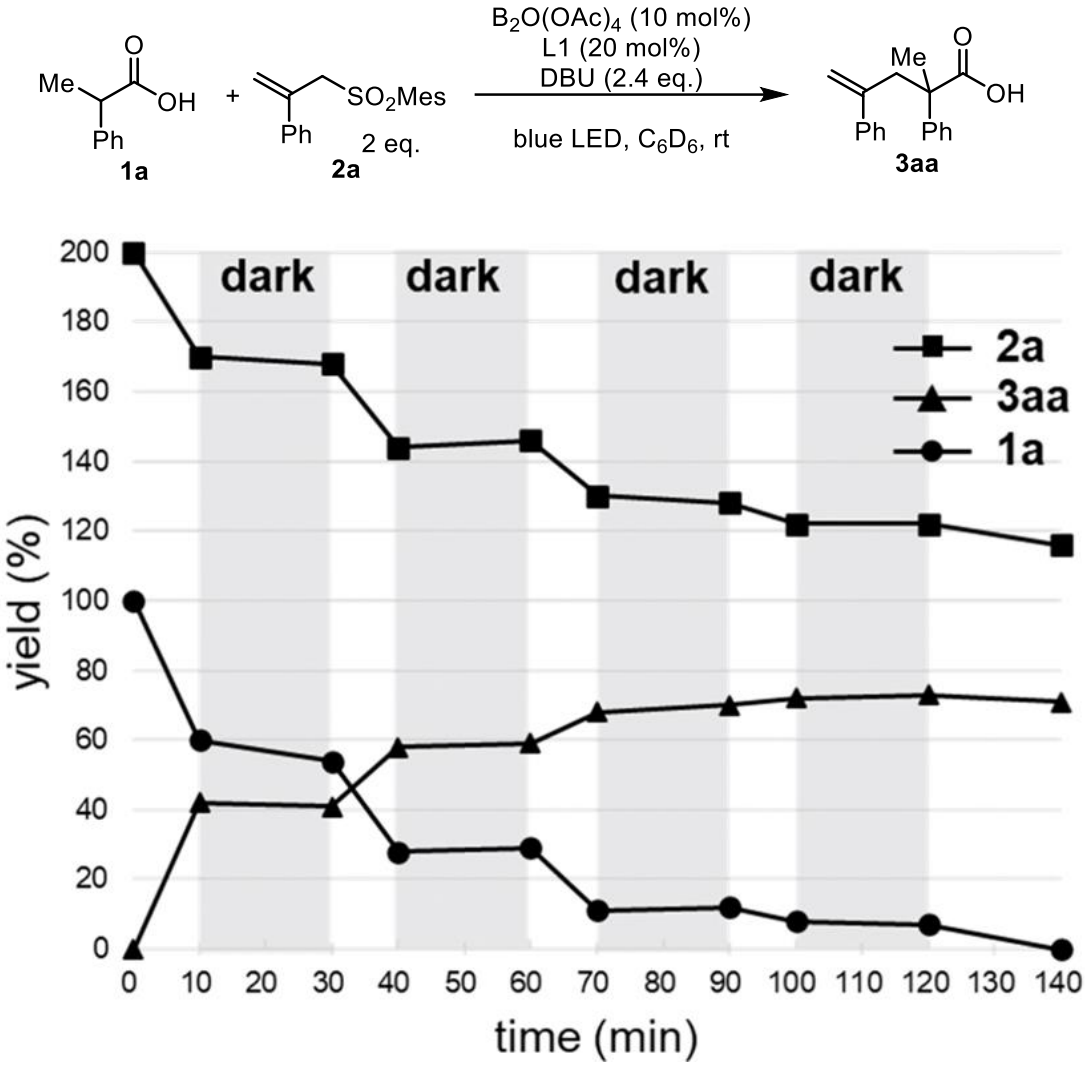

Fig 1.18 Light on-off experiments

1.5.6 quantum yield measurement

It is possible that allyl radical can react with enolate to generate the product, followed by single electron transfer to sulfone to produce allyl radical again. To check the existence of this radical chain pathway, quantum yield was measured. The reaction was performed

with standard condition except for the usage of deuterated solvent. The blue light source was equipped with a 460 nm bandpass filter for the exact measurement of the quantum yield of the reaction. The light intensity was measured to be 29.6 mW/cm^2, and the transmittance of the reaction sample at the same wavelength was 22.3%. After 0.5 hours photoirradiation, yield of this reaction was directly determined to be 14.8 % by ^{1}H NMR measurement using $SiMe_4$ as the internal standard. Thus, the quantum yield of the reaction was calculated to be Φ = 9.3%. As a conclusion, the proof for a radical chain mechanism was not obtained.

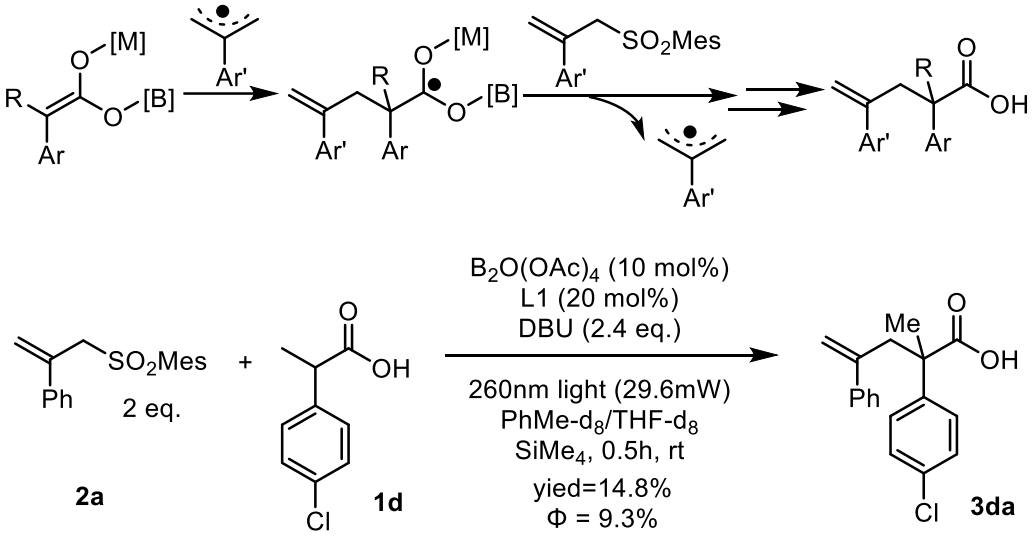

Fig 1.19 Quantum yield of the reaction was measurement

1.5.7 UV-vis measurement

From the quantum yield measurement, 460nm light was proved to be suitable for the absorption by active species that promote the reaction. Some UV-vis measurement was performed to gain further insight into the reaction.

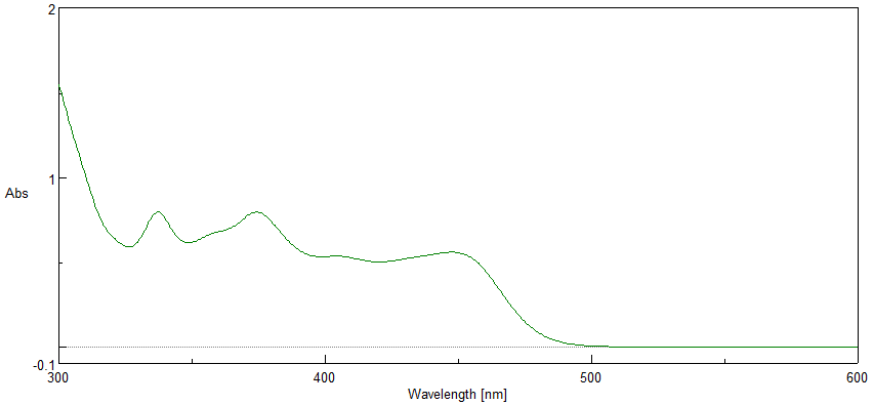

Fig 1.20 L1 (0.03 mM) and DBU (0.72 mM)

The ligand in basic solution showed absorption up to around 500 nm. This indicates that anion of the ligand can be photoexcited under the reaction condition.

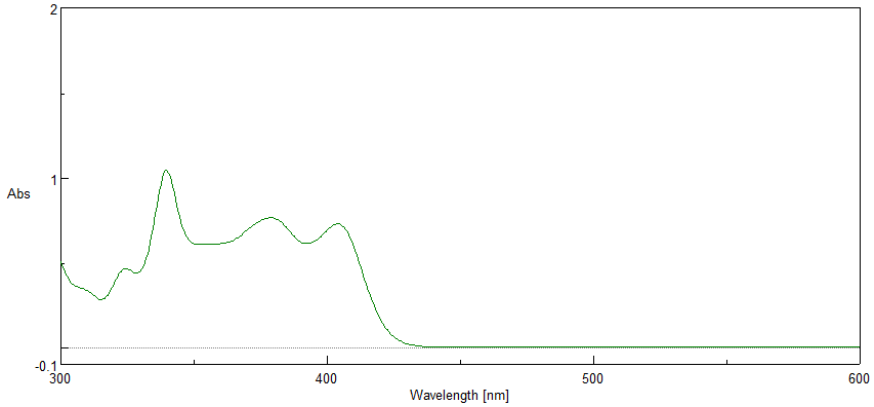

Fig 1.21 L1 (0.02 mM), [B] cat. (0.01 mM), and DBU (0.24mM)

However, if the boron catalyst is also added to the solution, the critical absorption above 430nm disappeared. This indicates that the free anion of the ligand was all coordinated to the boron atom to give different species.

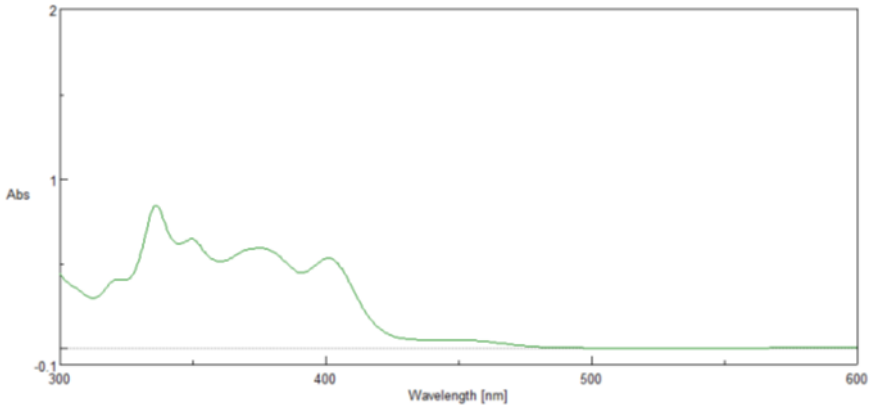

Fig 1.22 L1 (0.02 mM), [B] cat. (0.01 mM), DBU (0.24 mM), and carboxylic acid substrate (0.04 mM)

When carboxylic acid substrate was also added. The absorbance at 460 nm can be seen at a low level. The reappearance of the absorption can be explained by the generation of new species or the dissociation of ligand from boron.

NMR of the same combination was checked. Unfortunately, it showed that there are multiple unidentified species in the solution. Thus, the source of this absorption cannot be clarified.

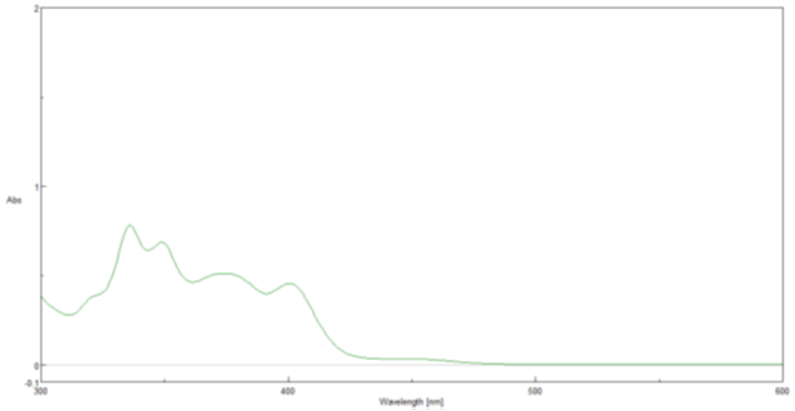

Fig 1.23 L1 (0.02 mM), [B] cat.(0.01 mM), DBU (0.24 mM), carboxylic acid substrate (0.04mM), and sulfone (0.04 mM)

Further addition of sulfone did not give apparent change of the spectrum. Thus, the formation of EDA complex is not likely.

1.5.8 fluorescence quenching experiment

The fluorescence intensity was measured with a solution of **L1** and DBU in MeCN with different concentration of sulfone 2a added. It can be clearly seen that sulfone cannot quench the fluorescence of excited ligand anion. This further indicates the existence of low concentration of the truly active intermediate, which was supposed to be boron enediolate.

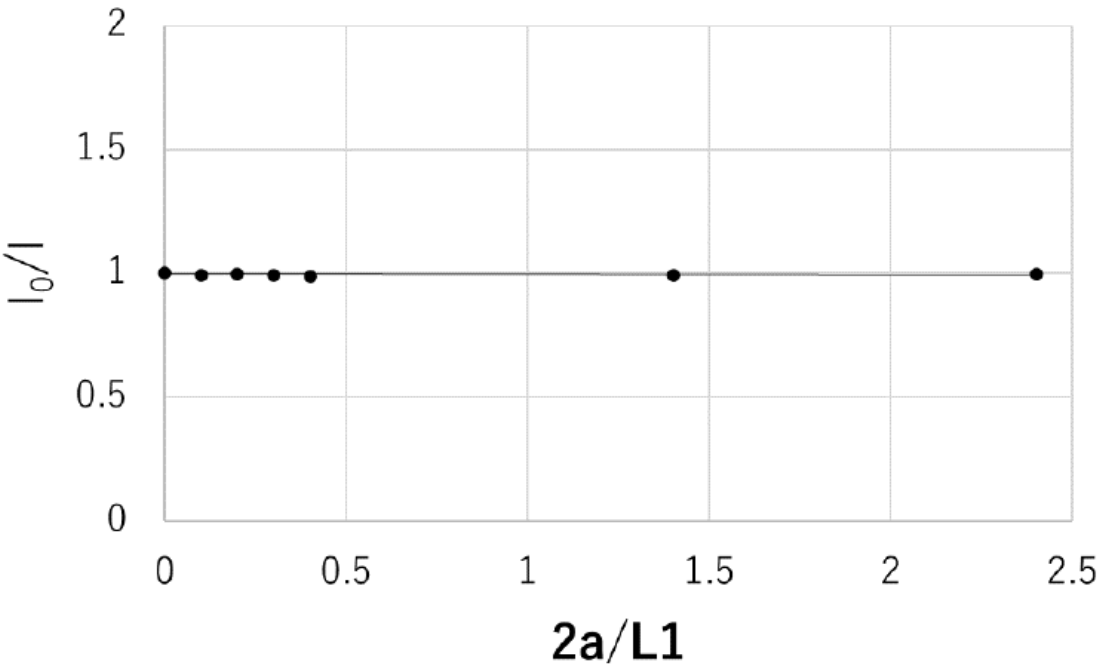

Fig 1.24 Fluorescence quenching was not related to the sulfone

1.5.9 proposed mechanism

Based on the experimental observations, the catalytic mechanism was proposed as below. Energetically unfavorable α-deprotonation of the boron carboxylate with DBU forms a small amount of electron-rich boron enediolate, and this species is photoexcited by blue LED irradiation. Single-electron transfer from the excited boron enediolate to allylsulfone followed by elimination of the sulfinate anion from the resulting anion radical generates a radical pair consisting of the cation radical of the boron enediolate and the allyl radical. The generated allyl radical may react with either the cation radical or the closed-shell species. In the former case, immediate radical−radical coupling of the radical pair affords the α-allylation product. Finally, the exchange of the carboxylate groups produces the α-allylated carboxylic acid as a DBU salt with regeneration of the boron carboxylate to close the catalytic cycle. Alternatively, the allyl radical may react with the closed shell enolate intermediate to propagate a radical chain process, while it can exist in only a very low concentration as discussed before. If this is the case, a highly electron-rich α,α-dioxycarbon radical would form and undergo single-electron reduction of allylsulfone to produce the boron carboxylate and the allyl radical.

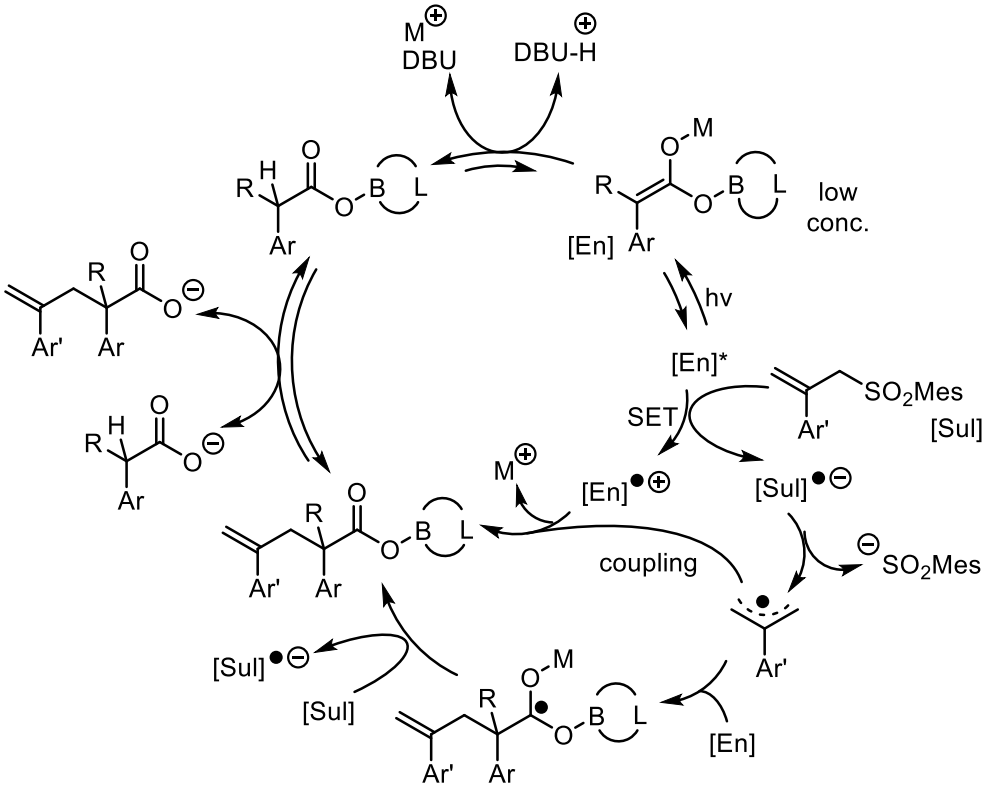

Fig 1.25 Proposed mechanism

1.6 Summary

The methodology of photocatalysis and boron-catalyzed functionalization of carboxylic acid was studied. As a result, blue-light-driven α-allylation of carboxylic acid with allyl sulfone was successfully developed. It was proposed that the catalytically formed boron enediolate performs single electron transfer to sulfone after photoexcitation. C-C bond was formed subsequently via a radical pathway. Sterically demanding quaternary α-carbon was constructed by this transformation. The ligand bearing large π-system is likely to increase the efficiency of photoexcitation.

1.7 General procedure

The procedure of this reaction is described here as, in a glovebox, DBU was added to a solution of $(AcO)_4B_2O$ and the carboxylic acid substrate in anhydrous toluene/THF. After stirring for 5 minutes at room temperature, L1 and the sulfone were added to the reaction mixture. The resulting solution was removed from the glovebox, cooled to 15 °C, and stirred for 11 h under the irradiation of blue LED (Kessil A 160WE Tuna Blue 40 W, λmax = 465 nm). To the mixture were added MeI (37.4 μL, 0.6 mmol) and $NaHCO_3$ (50.4 mg, 0.6 mmol). After stirring for an additional 2 hours at room temperature, 1 M HCl (aq.) and EtOAc were added to the mixture. The organic layer was extracted with EtOAc, and washed with 1 M NaOH (aq.), followed by brine and dried over $MgSO_4$. After filtration and evaporation, the residue was purified by silica gel chromatography to give the desired product.

1.8 Preparation of the ligand and substrates

1.8.1 synthesis of **L1**

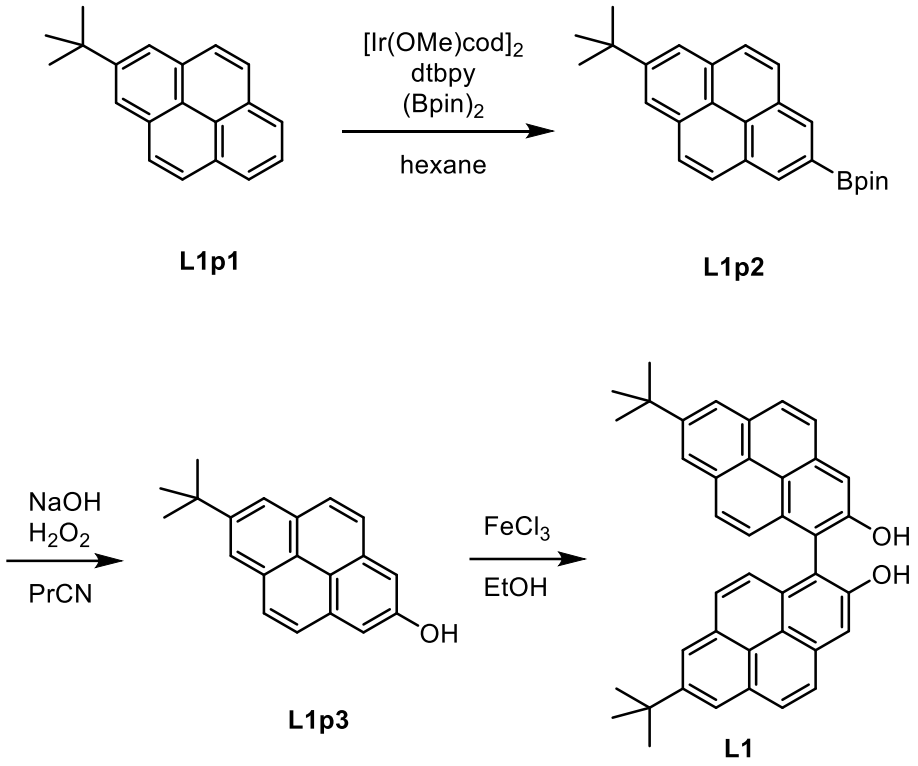

Fig 1.26 Scheme of the synthesis of **L1**

2-(7-(*tert*-Butyl)pyren-2-yl)-4,4,5,5-tetramethyl-1,3,2-dioxaborolane (L1p2)

To a 50 mL two-necked flask equipped with a stirring bar were added $[Ir(\mu\text{-OMe})cod]_2Cl_2$ (43.6 mg, 65.8 μmol, 1.3 mol%), 4,4'-di-tert-butylbipyridine (34.6 mg, 129 μmol, 2.6 mol%), B_2pin_2 (1.70 g, 6.71 mmol, 1.3 equiv) and hexane (12 mL, 0.42 M) sequentially. After fully dissolving the solid materials, **L1p1** (1.3 g, 5.03 mmol, 1 equiv) were added and the mixture was stirred at 80 °C for 16 h. The reaction mixture was passed through a plug of silica gel with a mixture eluent of toluene/CH_2Cl_2/EtOAc (10:50:0.6), after which the solvent was evaporated. Further purification was performed by silica gel column chromatography (toluene/hexane/CH_2Cl_2 from 30:10:0.4 to 50:10:1.8), giving **L1p2** (1.82 g, 94%) as white solid. R_f = 0.43 (DCM/hexane 1:2).

IR (ATR) 2966, 1384, 1360, 1234, 1143, 718 cm^{-1}.

^1H NMR (400 MHz, $CDCl_3$) δ 8.59 (s, 2H), 8.20 (s, 2H), 8.07 (d, *J* = 9.0 Hz, 2H), 8.03 (d, *J* = 9.0 Hz, 2H), 1.58 (s, 9H), 1.44 (s, 12H).

^{13}C NMR (100.5 MHz, $CDCl_3$) δ 149.5, 131.4, 131.1, 130.2, 127.6, 127.4, 126.3, 125.6, 122.8, 122.1, 84.1, 35.2, 31.9, 25.0.

HRMS–FD (m/z): $[M]^+$ calcd for $C_{26}H_{29}BO_2$, 384.2261; found, 384.2266.

7-(*tert*-Butyl)pyren-2-ol (L1p3)

In a 50 mL two-necked flask equipped with a stirring bar, **L1p2** (1.48 g, 3.85 mmol, 1 equiv) was dissolved in n-butyronitrile (148 mL, 26 mM). Then NaOH pellet (924 mg, 23.1 mmol, 6 equiv) and 30% H_2O_2 aq. (5.9 mL, ca. 57.8 mmol, 15 equiv) were added sequentially at 0 ℃. After stirring for 30 min at room temperature using water bath, 70 mL water was added and stirred for another 1 h. Resulting solution was diluted with chloroform and washed with water. The organic layer was dried over $MgSO_4$ and evaporated to give crude mixture. Recrystallization from chloroform/hexane afforded pure **L1p3** (875 mg, 83%) as pale yellow solid.

IR (ATR) 3322, 2952, 1600, 1447, 1419, 1289, 1226, 1159, 1139, 978, 877, 858, 711 cm^{-1}.

^1H NMR (400 MHz, $CDCl_3$) δ 8.17 (s, 2H), 8.00 (d, J = 12.4 Hz, 2H), 7.86 (d, J = 9.2 Hz, 2H), 7.54 (s, 2H), 5.25 (brs, 1H), 1.56 (s, 9H).

^{13}C NMR (100.5 MHz, $CDCl_3$) δ 153.3, 148.1, 132.6, 129.9, 128.4, 126.4, 122.8, 122.7, 120.0, 111.3, 35.1, 31.9

HRMS–FD (m/z): $[M]^+$ calcd for $C_{20}H_{18}O$, 274.1358; found, 274.1353.

7,7'-Di-*tert*-butyl-[1,1'-bipyrene]-2,2'-diol (L1)

To a 20 mL two-necked flask equipped with a stirring bar were added **L1p3** (250 mg, 911 μmol, 1 equiv), $FeCl_3$ (591 mg, 3.64 mmol, 4.0 equiv), and EtOH (5 mL, 0.2 M) sequentially. The resulting mixture was stirred at room temperature for 12 h. Then the reaction mixture was passed through a plug of silica gel with the eluent of chloroform followed by mixture eluent of toluene/EtOAc (2:1). The eluted mixture was washed with half saturated Na_2CO_3 aq., followed by 1:1 mixture solution of saturated Na_2CO_3 aq. and brine. The organic layer was dried over $MgSO_4$ and evaporated to give crude material including **L1** as well as unreacted **L1p3**. The mixture was purified by silica gel column chromatography (toluene/hexane/EtOAc from 1:1:0.02 to 2:1:0.18), R_f = 0.13 (EtOAc/hexane 1:5). Finally, recrystallization from chloroform/hexane was performed to give pure **L1** (149 mg, 60%) as colorless crystals.

IR (ATR) 3536, 2962, 1709, 1596, 1442, 1306, 1258, 1226, 1173, 1143, 879 cm^{-1}.

^1H NMR (400 MHz, $CDCl_3$) δ 8.27 (d, J = 1.6 Hz, 2H), 8.18 (s, 2H), 8.15 (d, J = 9.2Hz, 2H), 8.08 (d, J = 9.2Hz, 2H), 7.98 (s, 2H), 7.89 (d, J = 9.2Hz, 2H), 7.36 (d, J = 9.2Hz, 2H), 5.26 (s, 2H), 1.57 (s, 18H).

^{13}C NMR (100.5 MHz, $CDCl_3$) δ 152.6, 148.6, 133.7, 131.8, 130.1, 129.7, 129.5, 129.2, 126.6, 123.9, 123.3, 123.1, 122.8, 120.5, 113.4, 111.9, 35.2, 31.9.

HRMS–FD (m/z): $[M]^+$ calcd for $C_{40}H_{34}O2$, 546.2559; found, 546.2548.

1.8.2 synthesis of allyl sulfones

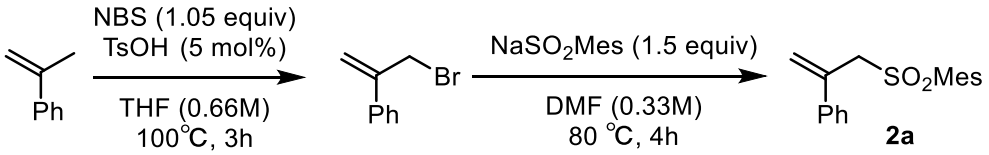

Fig 1.27 Synthesis route to **2a**

preparation of allylbromide

To a solution of α-methylstyrene (7.80 mL, 60 mmol, 1 equiv) in THF (90 mL, 0.66 M) in 200 mL two-necked flask were added NBS (11.21 g, 63 mmol, 1.05 equiv) and p-toluenesulfonic acid monohydrate (571 mg, 3 mmol, 0.05 equiv). The resulting solution was heated at 100 ℃ for 3 h. After cooling to room temperature, water and EtOAc were added and organic phase was separated. The water layer was extracted once with EtOAc. The combined organic layer was washed with brine, dried over $MgSO_4$. After filtration and evaporation, the residue was purified by silica gel chromatography (hexane) to give pure product as pale yellow liquid (6.63 g, 56%).

preparation of sodium 2,4,6-trimethylbenzenesulfinate

To a 30 mL two-necked flask were added 2-mesitylenesulfonyl chloride (1.75 g, 8 mmol, 1 equiv), sodium bicarbonate (1.34 g, 16 mmol, 2 equiv), sodium sulfite (2.02 g, 16 mmol, 2 equiv) and water (8 mL, 1 M) sequentially. The resulting mixture was heated at 80 ℃ for 4h. After evaporation of the solvent, 30 mL 70 ℃ ethanol was added. The suspension was filtered through celite and filter cake was washed with 30 mL of 70 ℃ ethanol twice. The solvent was evaporated to give titled product as white solid quantitatively, which was used for next step without further purification.

preparation of allylsulfone

To a solution of the sodium 2,4,6-trimethylbenzenesulfinate (1.86 g, 9 mmol) in dry DMF (18 mL, 0.33 M) was added allylbromide (857 μl, 6 mmol) at room temperature. The mixture was warmed to 80 ℃ and stirred for 4 h. The solution was added ethyl acetate and washed with water, brine and dried over $MgSO_4$. After filtration and evaporation, the residue was purified by silica gel chromatography. (hexane/EtOAc from 100:1 to 20:1) to give **2a** as off white solid. Further purification was carried out by recrystallization from chloroform/hexane to give pure **2a** (1.02 g, 3.38 mmol, 56%) as colorless crystals.

1,3,5-Trimethyl-2-((2-phenylallyl)sulfonyl)benzene (2a)

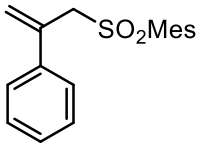

IR (ATR) 2937, 1602, 1444, 1311, 1135, 911, 886, 776, 701, 674 cm^{-1}.
^{1}H NMR (400 MHz, $CDCl_3$) δ 7.26-7.30 (m, 2H), 7.20-7.25 (m, 3H), 6.82 (s, 2H), 5.59 (s, 1H), 5.22 (s, 1H), 4.27 (s, 2H), 2.57 (s, 6H), 2.24 (s, 3H).
^{13}C NMR (100.5 MHz, $CDCl_3$) δ 143.28, 140.28, 138.91, 136.33, 132.38, 131.97, 128.24, 127.82, 126.03, 121.60, 61.58, 23.08, 20.92.
HRMS–FD (m/z): $[M]^+$ calcd for $C_{18}H_{20}O_2S$, 300.1184; found, 300.1194.

2-((2-(4-Bromophenyl)allyl)sulfonyl)-1,3,5-trimethylbenzene (2b)

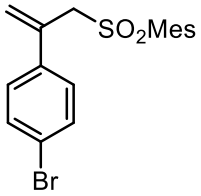

IR (ATR) 2938, 1602, 1489, 1396, 1313, 1135, 1008, 832, 680 cm^{-1}.
^{1}H NMR (400 MHz, $CDCl_3$) δ 7.35 (dt, J = 8.4, 2.2 Hz, 2H), 7.15 (dt, J = 8.4, 2.2 Hz, 2H), 6.83 (s, 2H), 5.59 (s, 1H), 5.24 (s, 1H), 4.22 (s, 2H), 2.56 (s, 6H), 2.26 (s, 3H).
^{13}C NMR (100.5 MHz, $CDCl_3$) δ 143.64, 140.23, 137.79, 135.49, 132.24, 132.05, 131.34, 127.68, 122.21, 122.01, 61.45, 23.10, 20.96.
HRMS–FD (m/z): $[M]^+$ calcd for $C_{18}H_{19}BrO_2S$, 378.0289; found, 378.0291.

4-(3-(Mesitylsulfonyl)prop-1-en-2-yl)phenyl acetate (2c)

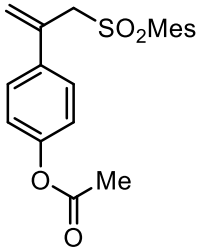

IR (ATR) 2939, 1758, 1603, 1509, 1370, 1311, 1198, 1171, 1133, 1016, 912, 852, 681 cm^{-1}.
^{1}H NMR (400 MHz, $CDCl_3$) δ 7.30 (dt, J = 8.8, 2.2 Hz, 2H), 6.95 (dt, J = 8.8, 2.2 Hz, 2H), 6.84 (s, 2H), 5.57 (s, 1H), 5.21 (s, 1H), 4.24 (s, 2H), 2.57 (s, 6H), 2.30 (s, 3H), 2.25 (s, 3H).

^{13}C NMR (100.5 MHz, $CDCl_3$) δ 169.30, 150.32, 143.51, 140.26, 136.71, 135.54, 132.27, 132.06, 127.20, 121.88, 121.36, 61.63, 23.10, 21.14, 20.93.
HRMS–FD (m/z): $[M]^+$ calcd for $C_{20}H_{22}O_4S$, 358.1239; found, 358.1244.

1,3,5-Trimethyl-2-((2-(*m*-tolyl)allyl)sulfonyl)benzene (2d)

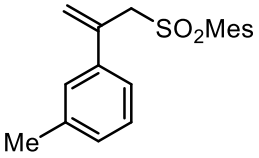

IR (ATR) 2938, 1603, 1454, 1402, 1312, 1151, 1133, 908, 792, 722, 672 cm^{-1}.
^{1}H NMR (400 MHz, $CDCl_3$) δ 7.06-7.13 (m, 2H), 6.99-7.03 (m, 1H), 6.96-6.98 (m, 1H), 6.81 (s, 2H), 5.57 (s, 1H), 5.23 (s, 1H), 4.26 (s, 2H), 2.57 (s, 6H), 2.25 (s, 3H), 2.23 (s, 3H).
^{13}C NMR (100.5 MHz, $CDCl_3$) δ 143.18, 140.30, 138.83, 137.72, 136.45, 132.51, 131.91, 128.52, 128.12, 126.77, 123.16, 121.36, 61.70, 23.08, 21.34, 20.91.
HRMS–FD (m/z): $[M]^+$ calcd for $C_{19}H_{22}O_2S$, 314.1341; found, 314.1352.

2-((2-(3-Methoxyphenyl)allyl)sulfonyl)-1,3,5-trimethylbenzene (2e)

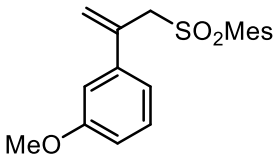

IR (ATR) 2939, 1601, 1577, 1490, 1453, 1311, 1227, 1150, 1133, 1048, 859, 784, 723, 673 cm^{-1}.
^{1}H NMR (400 MHz, $CDCl_3$) δ 7.14 (ddd, J = 8.0, 8.0, 0.8 Hz, 1H), 6.87 (ddd, J = 8.0, 1.6, 1.2 Hz, 1H), 6.82 (s, 2H), 6.74-6.79 (m, 2H), 5.59 (s, 1H), 5.24 (s, 1H), 4.25 (s, 2H), 3.77 (s, 3H), 2.58 (s, 6H), 2.24 (s, 3H).
^{13}C NMR (100.5 MHz, $CDCl_3$) δ 159.35, 143.30, 140.48, 140.29, 136.25, 132.40, 131.98, 129.22, 121.80, 118.53, 113.35, 111.77, 61.69, 55.12, 23.11, 20.91.
HRMS–FD (m/z): $[M]^+$ calcd for $C_{19}H_{22}O_3S$, 330.1290; found, 330.1302.

2-(3-(Mesitylsulfonyl)prop-1-en-2-yl)naphthalene (2f)

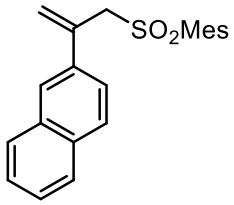

IR (ATR) 2937, 1603, 1403, 1313, 1135, 895, 859, 820, 753 cm^{-1}.
^{1}H NMR (400 MHz, $CDCl_3$) δ 7.73-7.80 (m, 1H), 7.65-7.72 (m, 2H), 7.59 (s, 1H), 7.40-7.49 (m, 3H), 6.69 (s, 2H), 5.74 (s, 1H), 5.36 (s, 1H), 4.38 (s, 2H), 2.57 (s, 6H), 2.04 (s, 3H).
^{13}C NMR (100.5 MHz, $CDCl_3$) δ 143.41, 140.21, 136.30, 135.87, 132.93, 132.71, 132.34, 131.94, 128.19, 127.91, 127.39, 126.22, 126.18, 125.15, 123.92, 122.00, 61.68, 23.12, 20.71.
HRMS–FD (m/z): $[M]^+$ calcd for $C_{22}H_{22}O_2S$, 350.1341; found, 350.1347.

1,3,5-Trimethyl-2-((2-(*o*-tolyl)allyl)sulfonyl)benzene (2g)

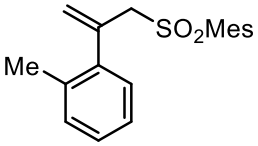

IR (ATR) 2937, 1603, 1403, 1313, 1135, 895, 859, 820, 753 cm^{-1}.
^{1}H NMR (400 MHz, $CDCl_3$) δ 7.08-7.17 (m, 2H), 6.99 (ddd, J = 7.6, 6.4, 2.0 Hz), 6.87 (s, 2H), 6.83 (d, J = 7.6 Hz, 1H), 5.62 (s, 1H), 5.32 (d, J = 0.8 Hz, 1H), 4.16 (s, 2H), 2.55 (s, 6H), 2.28 (s, 3H), 2.24 (s, 3H).
^{13}C NMR (100.5 MHz, $CDCl_3$) δ 143.21, 140.31, 140.04, 136.56, 134.48, 133.29, 132.07, 130.14, 128.50, 127.51, 125.54, 123.82, 62.77, 22.81, 20.95, 20.03.
HRMS–FD (m/z): $[M]^+$ calcd for $C_{19}H_{22}O_2S$, 314.1341; found, 314.1344.

1-Methyl-4-((2-phenylallyl)sulfonyl)benzene (2a')

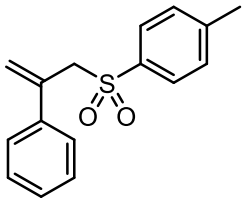

IR (ATR) 2980, 1598, 1447, 1400, 1314, 1298, 1245, 1175, 1137, 1087, 915, 900, 810, 781, 773, 709, 699 cm^{-1}.

^{1}H NMR (400 MHz, $CDCl_3$) δ 7.62-7.68 (m, 2H), 7.18-7.30 (m, 7H), 5.59 (s, 1H), 5.21 (s, 1H), 4.25 (s, 2H), 2.39 (s, 3H).
^{13}C NMR (100.5 MHz, $CDCl_3$) δ 144.6, 138.9, 136.5, 135.3, 129.5, 128.6, 128.3, 127.9, 126.2, 62.1, 21.6.
HRMS–FD (m/z): $[M]^+$ calcd for $C_{16}H_{16}O_2S$, 272.0871; found, 272.0862.

(3-(Methylsulfonyl)prop-1-en-2-yl)benzene (2a")

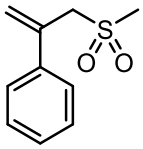

IR (ATR) 3024, 2931, 1680, 1625, 1496, 1447, 1410, 1297, 1246, 1169, 1127, 969, 916, 896, 780, 716, 700 cm^{-1}.
^{1}H NMR (400 MHz, $CDCl_3$) δ 7.45-7.51 (m, 2H), 7.30-7.42 (m, 3H), 5.77 (s, 1H), 5.57 (s, 1H), 4.20 (s, 2H), 2.72 (s, 3H).
^{13}C NMR (100.5 MHz, $CDCl_3$) δ 138.6, 136.6, 128.8, 128.6, 126.3, 122.1, 60.7, 40.2.
HRMS–FD (m/z): $[M]^+$ calcd for $C_{10}H_{12}O_2S$, 196.0558; found, 196.0553.

1.9 Characterization of Products

Methyl 2-methyl-2,4-diphenylpent-4-enoate (3aa)

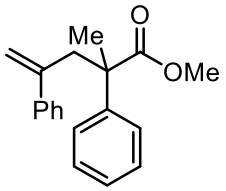

18.3 mg, 65% yield, Colorless oil.
R$_f$: 0.55 (EtOAc/Hex 5:1)
IR (ATR) 2949, 1731, 1496, 1446, 1206, 1122, 905, 778, 697 cm^{-1}.
^{1}H NMR (400 MHz, $CDCl_3$) δ 7.16-7.29 (m, 10H), 5.20 (d, *J* = 1.6 Hz, 1H), 4.97(t, *J* = 1.2 Hz, 1H),3.47 (d, *J* = 13.6 Hz, 1H), 3.35 (s, 3H), 3.09 (d, *J* = 14.4 Hz, 1H), 1.41 (s, 3H).
^{13}C NMR (100.5 MHz, $CDCl_3$) δ 175.98, 145.63, 143.88, 142.52, 128.26, 127.97, 127.08, 126.77, 126.69, 125.99, 118.04, 51.71, 50.48, 43.98, 23.31.
HRMS–FD (m/z): [M]+ calcd for $C_{19}H_{20}O_2$, 280.1463; found, 280.1455.

Methyl 2-(4-(*tert*-Butyl)phenyl)-2-methyl-4-phenylpent-4-enoate (3ba)

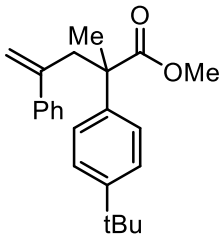

12.4 mg, 37% yield, Colorless oil.

R_f : 0.6 (EtOAc/Hex 5:1)

IR (ATR) 2927, 1733, 1461, 1270, 1202, 1119, 778 cm^{-1}.

^{1}H NMR (400 MHz, $CDCl_3$) δ 7.14-7.26 (m, 9H), 5.21 (d, *J* = 2 Hz, 1H), 5.01(d, *J* = 1.2 Hz, 1H), 3.44 (d, *J* = 13.6 Hz, 1H), 3.35 (s, 3H), 3.08 (d, *J* = 13.2 Hz, 1H), 1.42 (s, 3H), 1.26 (s, 9H).

^{13}C NMR (100.5 MHz, $CDCl_3$) δ 176.11, 149.35, 145.84, 142.47, 140.74, 127.90, 126.99, 126.78, 125.58, 125.12, 117.92, 51.67, 49.97, 44.15, 34.29, 31.27, 23.20.

HRMS–FD (m/z): [M]+ calcd for $C_{23}H_{28}O_2$, 336.2089; found, 336.2100.

Methyl 2-(4-methoxyphenyl)-2-methyl-4-phenylpent-4-enoate (3ca)

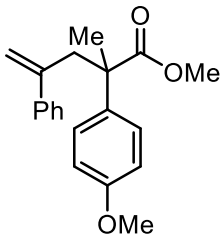

13.4 mg, 43% yield, Colorless oil.

R_f : 0.55 (EtOAc/Hex 5:1)

IR (ATR) 2949, 1729, 1513, 1458, 1251, 1184, 1122, 1032, 902, 829, 777, 698 cm–1.

^{1}H NMR (400 MHz, $CDCl_3$) δ 7.17-7.26 (m, 7H), 6.79 (ddd, *J* = 9.2, 2.8, 2.8 Hz, 2H), 5.20 (d, *J* = 2.0 Hz, 1H), 4.95 (d, *J* = 1.2 Hz, 1H), 3.78 (s, 3H), 3.44 (d, *J* = 13.2 Hz, 1H), 3.36 (s, 3H), 3.05 (d, *J*= 12.8 Hz, 1H), 1.40 (s, 3H).

^{13}C NMR (100.5 MHz, $CDCl_3$) δ 176.20, 158.16, 145.67, 142.51, 135.87, 127.95, 127.10, 127.04, 126.76, 118.00, 113.55, 55.21, 51.75, 49.67, 44.17, 23.24.

HRMS–FD (m/z): [M]+ calcd for $C_{20}H_{22}O_3$, 310.1569; found, 310.1576.

Methyl 2-(4-chlorophenyl)-2-methyl-4-phenylpent-4-enoate (3da)

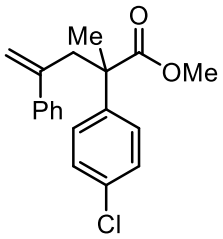

15.9 mg, 51% yield, Colorless oil.

R_f : 0.55 (EtOAc/Hex 5:1)

IR (ATR) 2925, 1732, 1493, 1238, 1096, 1013, 903, 777, 699 cm^{-1}.

^{1}H NMR (400 MHz, $CDCl_3$) δ 7.16-7.26 (m, 9H), 5.20 (d, *J* = 2.8 Hz, 1H), 4.96 (d, J = 0.8 Hz, 1H), 3.40 (d, *J* = 11.6 Hz, 1H), 3.39 (s, 3H), 3.08 (d, *J* = 14.0 Hz, 1H), 1.41 (s, 3H).

^{13}C NMR (100.5 MHz, $CDCl_3$) δ 175.69, 145.35, 142.30, 142.08, 132.59, 128.29, 128.01, 127.61, 127.12, 126.74, 118.26, 51.92, 50.06, 44.20, 23.00.

HRMS–FD (m/z): [M]+ calcd for $C_{19}H_{19}ClO_2$, 314.1074; found, 314.1074.

Methyl 2-(3-bromophenyl)-2-methyl-4-phenylpent-4-enoate (3ea)

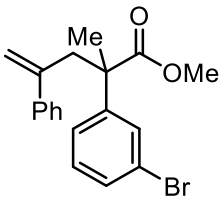

24.7 mg, 69% yield, Colorless oil.

R_f : 0.55 (EtOAc/Hex 5:1)

IR (ATR) 2949, 1733, 1566, 1458, 1205, 1123, 906, 778, 695 cm^{-1}.

^{1}H NMR (400 MHz, $CDCl_3$) δ 7.38 (t, *J* = 1.8 Hz, 1H), 7.28 (dq, *J* = 7.8, 0.9 Hz, 1H), 7.15-7.23 (m, 6H), 7.09 (t, *J* = 7.6 Hz, 1H), 5.21 (d, *J* = 1.2 Hz, 1H), 4.98 (t, *J* = 1.0 Hz, 1H), 3.39 (s, 3H), 3.38 (d, *J* = 14.0 Hz, 1H), 3.09 (d, *J* = 13.6 Hz, 1H), 1.41 (s, 3H).

^{13}C NMR (100.5 MHz, $CDCl_3$) δ 175.45, 145.85, 145.29, 142.20, 129.82, 129.70, 129.38, 127.97, 127.17, 126.72, 124.91, 122.47, 118.35, 51.95, 50.28, 44.10, 22.93.

HRMS–FD (m/z): [M]+ calcd for $C_{19}H_{19}BrO_2$, 358.0568; found, 358.0559.

Methyl 2-methyl-4-phenyl-2-(thiophen-3-yl)pent-4-enoate (3fa)

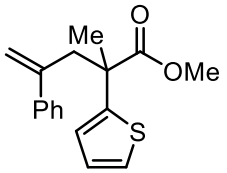

13.7 mg, 48% yield, Colorless oil.

R_f : 0.6 (EtOAc/Hex 5:1)

IR (ATR) 2983, 1733, 1372, 1237, 1045, 907, 778, 698 cm^{-1}.

^{1}H NMR (400 MHz, $CDCl_3$) δ 7.19-7.27 (m, 6H), 7.04-7.07 (m, 2H), 5.22 (d, *J* = 1.6 Hz, 1H), 5.00 (d, *J* = 0.8 Hz, 1H), 3.47 (d, *J* = 12.8 Hz, 1H), 3.36 (s, 3H), 2.99 (dd, J = 13.6, 1.6 Hz, 1H), 1.44 (s, 3H).

^{13}C NMR (100.5 MHz, $CDCl_3$) δ 175.27, 145.51, 144.88, 142.27, 127.99, 127.13, 126.74, 125.23, 120.43, 117.81, 51.77, 48.23, 44.94, 22.87.

HRMS–FD (m/z): [M]+ calcd for $C_{17}H_{18}O_2S$, 286.1028; found, 286.1021.

Methyl 2-(benzo[*d*][1,3]dioxol-5-yl)-2-methyl-4-phenylpent-4-enoate (3ga)

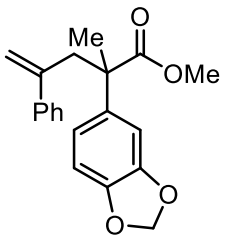

14.0 mg, 43% yield, Colorless oil.

R_f : 0.5 (EtOAc/Hex 5:1)

IR (ATR) 2949, 1728, 1505, 1489, 1434, 1236, 1122, 1038, 935, 908, 778, 700 cm^{-1}.

^{1}H NMR (400 MHz, $CDCl_3$) δ 7.16-7.24 (m, 5H), 6.75 (d, *J* = 1.6 Hz, 1H), 6.71 (dd, *J* = 8.4, 1.6 Hz, 1H), 6.67 (d, *J* = 8.4 Hz, 1H), 5.90 (d, *J* = 1.2 Hz, 1H), 5.89 (d, *J* = 1.2 Hz, 1H), 5.20 (d, *J* = 1.2 Hz, 1H), 4.97 (d, *J* = 1.2 Hz, 1H), 3.39 (s, 3H), 3.36 (d, *J* = 13.2 Hz, 1H), 3.06 (d, *J* = 15.4 Hz, 1H), 1.39
(s, 3H).

^{13}C NMR (100.5 MHz, $CDCl_3$) δ 176.05, 147.50, 146.14, 145.55, 142.46, 137.50, 127.92, 126.98, 126.74, 119.12, 118.10, 107.81, 107.08, 100.97, 51.88, 50.03, 44.31, 23.16.

HRMS–FD (m/z): [M]+ calcd for $C_{20}H_{20}O_4$, 324.1362; found, 324.1366.

Methyl 2-ethyl-2,4-diphenylpent-4-enoate (3ha)

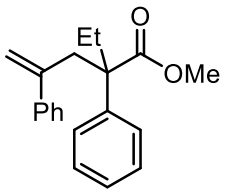

19.7 mg, 67% yield, Colorless oil.

R_f : 0.6 (EtOAc/Hex 5:1)

IR (ATR) 2948, 1731, 1496, 1446, 1223, 1117, 1026, 904, 776, 697 cm^{-1}.

^{1}H NMR (400 MHz, $CDCl_3$) δ 7.13-7.19 (m, 4H), 7.19-7.25 (m, 6H), 5.14 (d, *J* = 2.0 Hz, 1H), 4.91(s, 1H), 3.35 (d, *J* = 13.6 Hz, 1H), 3.32 (s, 3H), 3.18 (d, *J* = 14 Hz, 1H), 1.94 (q, *J* = 7.2 Hz, 2H), 0.61 (t, *J* = 7.2 Hz, 3H).

^{13}C NMR (100.5 MHz, $CDCl_3$) δ 175.87, 145.60, 142.58, 142.46, 128.09, 127.85, 126.97, 126.78, 126.53, 118.07, 54.65, 51.55, 39.22, 26.91, 8.49.

HRMS–FD (m/z): [M]+ calcd for $C_{20}H_{22}O_2$, 294.1620; found, 294.1630.

Methyl 2-methyl-4-phenyl-2-(m-tolyl)pent-4-enoate (3ia)

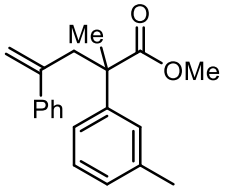

13.9 mg, 47% yield, Colorless oil.

R_f : 0.6 (EtOAc/Hex 5:1)

IR (ATR) 2949, 1732, 1457, 1205, 1122, 905, 777, 698 cm^{-1}.

^{1}H NMR (400 MHz, $CDCl_3$) δ 7.13-7.28 (m, 6H), 7.05-7.10 (m, 2H), 6.99 (d, *J* = 7.2 Hz, 1H), 5.21 (d, *J* = 2.0 Hz, 1H), 4.99 (d, *J* = 1.2 Hz, 1H), 3.45 (d, *J* = 13.2 Hz, 1H), 3.34 (s, 3H), 3.08 (d, *J* = 12.8 Hz, 1H), 2.29 (s, 3H), 1.40 (s, 3H).

^{13}C NMR (100.5 MHz, $CDCl_3$) δ 176.07, 145.72, 143.83, 142.52, 137.78, 128.16, 127.92, 127.47, 127.06, 126.77, 126.69, 122.95, 118.04, 51.72, 50.32, 43.90, 23.42, 21.59.

HRMS–FD (m/z): [M]+ calcd for $C_{20}H_{22}O_2$, 294.1620; found, 294.1631.

Methyl 2-(6-methoxynaphthalen-2-yl)-2-methyl-4-phenylpent-4-enoate (3ja)

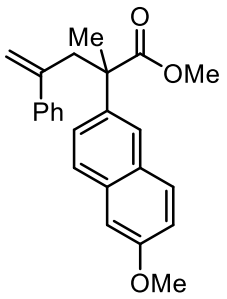

18.6 mg, 52% yield, White solid.

R_f : 0.55 (EtOAc/Hex 5:1)

IR (ATR) 2949, 1730, 1606, 1459, 1393, 1268, 1225, 1123, 1031, 904, 853, 812, 778 cm^{-1}.

^{1}H NMR (400 MHz, $CDCl_3$) δ 7.68 (d, *J* = 9.2 Hz, 1H), 7.64 (d, *J* = 5.2 Hz, 1H), 7.62 (s, 1H), 7.35 (dd, *J* = 9.0, 1.8 Hz, 1H), 7.25-7.28 (m, 2H), 7.19-7.24 (m, 2H), 7.14-7.18 (m, 1H), 7.12 (dd, *J* = 9.0, 2.8 Hz, 1H), 7.07 (d, *J* = 2.8 Hz, 1H), 5.20 (d, *J* = 2.0 Hz, 1H), 4.97 (dd, *J* = 1.0, 1.0 Hz, 1H), 3.91
(s, 3H), 3.56 (d, *J* = 13.6 Hz, 1H), 3.36 (s, 3H), 3.19 (d, *J* = 13.2 Hz, 1H), 1.50 (s, 3H).

^{13}C NMR (100.5 MHz, $CDCl_3$) δ 176.12, 157.66, 145.60, 142.47, 138.90, 133.24, 129.55, 128.57, 127.93, 127.05, 126.76, 125.24, 124.18, 118.81, 118.08, 105.32, 55.30, 51.79, 50.36, 43.84, 23.32.

HRMS–FD (m/z): [M]+ calcd for $C_{24}H_{24}O_3$, 360.1725; found, 360.1714.

Methyl 2-methyl-2-(4-((2-oxocyclopentyl)methyl)phenyl)-4-phenylpent-4-enoate (3ka)

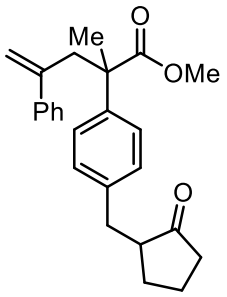

20.5 mg, 54% yield, Colorless oil.

R_f : 0.23 (EtOAc/Hex 5:1)

IR (ATR) 2949, 1734, 1513, 1457, 1207, 1153, 1123, 904, 779, 699 cm^{-1}.

^{1}H NMR (400 MHz, $CDCl_3$) δ 7.14-7.27 (m, 7H), 7.04 (d, *J* = 8.4 Hz, 2H), 5.20 (d, *J* = 1.6 Hz, 1H), 4.98 (s, 1H), 3.42 (d, *J* = 14.0 Hz, 1H), 3.367 (s, 1.7H), 3.363 (s, 1.3H),

3.05-3.12 (m, 2H), 2.46 (dd, *J* = 13.6, 9.6 Hz, 1H), 2.25-2.39 (m, 2H), 2.02-2.16 (m, 2H), 1.91-2.01 (m, 1H), 1.67-1.79 (m, 1H), 1.47-1.58 (m, 1H), 1.41 (s, 3H).
^{13}C NMR (100.5 MHz, $CDCl_3$) δ 220.20, 176.05, 145.64, 142.48, 141.64, 138.39, 128.72, 127.92, 127.01, 126.76, 126.07, 118.04, 51.74, 50.94, 50.11, 44.09, 38.17, 35.04, 29.25, 23.19, 20.53.
HRMS–FD (m/z): [M]+ calcd for $C_{25}H_{28}O_3$, 376.2038; found, 376.2038.

Methyl 2-(4-(*tert*-butyl)phenyl)-4-phenylpent-4-enoate (3na)

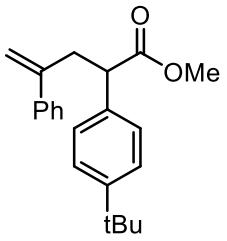

16.9 mg, 52% yield, Colorless oil.
R_f : 0.55 (EtOAc/Hex 5:1)
IR (ATR) 2959, 1737, 1435, 1269, 1220, 1159, 1027, 900, 830, 778, 706 cm^{-1}.
^{1}H NMR (400 MHz, $CDCl_3$) δ 7.25-7.37 (m, 7H), 7.19 (dt, *J* = 8.6, 2.6 Hz, 2H), 5.25 (d, *J* = 1.2 Hz, 1H), 5.05 (d, *J* = 0.8 Hz, 1H), 3.71 (dd, *J* = 9.2, 6.0 Hz,, 1H), 3.60 (s, 3H), 3.31 (ddd, *J* = 14.4, 9.2, 1.1 Hz, 1H), 2.89 (ddd, *J* = 14.4, 6.0, 1.1 Hz, 1H), 1.30 (s, 9H).
^{13}C NMR (100.5 MHz, $CDCl_3$) δ 174.05, 150.11, 145.69, 140.61, 135.59, 128.34, 127.54, 127.42, 126.28, 125.49, 114.52, 51.88, 49.76, 39.35, 34.43, 31.30.
HRMS–FD (m/z): [M]+ calcd for $C_{22}H_{26}O_2$, 322.1933; found, 322.1946.

Methyl 2-(4-methoxyphenyl)-4-phenylpent-4-enoate (3oa)

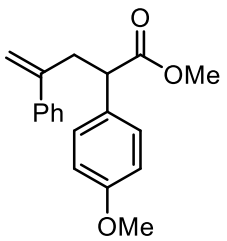

16.0 mg, 54% yield, Colorless oil.
R_f : 0.5 (EtOAc/Hex 5:1)
IR (ATR) 2952, 1735, 1611, 1512, 1436, 1250, 1179, 1160, 1034, 780, 707 cm^{-1}.

^{1}H NMR (400 MHz, $CDCl_3$) δ 7.33 (dd, *J* = 4.4, 2.4 Hz, 4H), 7.25-7.30 (m, 1H), 7.15 (dt, *J* = 8.8, 2.5 Hz, 2H), 6.82 (dt, *J* = 8.8, 2.5 Hz, 2H), 5.20 (d, *J* = 0.8 Hz, 1H), 4.99 (d, *J* = 1.2 Hz, 1H), 3.78 (s, 3H), 3.66 (dd, *J* = 8.4, 6.8 Hz, 1H), 3.59 (s, 3H), 3.30 (ddd, *J* = 14.7, 8.4, 0.9 Hz, 1H), 2.87 (ddd, *J* =
14.4, 6.8, 1.2 Hz, 1H).
^{13}C NMR (100.5 MHz, $CDCl_3$) δ 174.30, 158.86, 145.61, 140.64, 130.75, 129.04, 128.48, 127.67, 126.39, 114.85, 114.02, 55.32, 52.03, 49.31, 39.48.
HRMS–FD (m/z): [M]+ calcd for $C_{19}H_{20}O_3$, 296.1412; found, 296.1420.

Methyl 2-(4-chlorophenyl)-4-phenylpent-4-enoate (3pa)

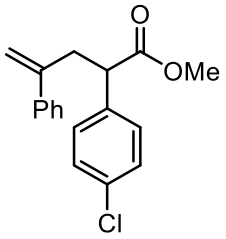

15.8 mg, 53% yield, Colorless oil.
R_f : 0.5 (EtOAc/Hex 5:1)
IR (ATR) 2926, 1736, 1492, 1436, 1161, 1092, 1015, 903, 779, 707 cm^{-1}.
^{1}H NMR (400 MHz, $CDCl_3$) δ 7.24-7.37 (m, 7H), 7.15 (dt, *J* = 8.4, 2.4 Hz, 2H), 5.20 (d, *J* = 1.6 Hz, 1H), 4.98 (d, *J* = 1.2 Hz, 1H), 3.68 (dd, *J* = 8.0, 8.0 Hz, 1H), 3.62 (s, 3H), 3.31 (ddd, *J* = 14.5, 8.0, 0.8 Hz, 1H), 2.87 (ddd, *J* = 14.5, 8.0, 0.8 Hz, 1H).
^{13}C NMR (100.5 MHz, $CDCl_3$) δ 173.60, 145.09, 140.24, 136.91, 133.16, 129.35, 128.70, 128.45, 127.70, 126.28, 115.14, 52.11, 49.40, 39.28.
HRMS–FD (m/z): [M]+ calcd for $C_{18}H_{17}ClO_2$, 300.0917; found, 300.0904.

Methyl 2-(4-bromophenyl)-4-phenylpent-4-enoate (3qa)

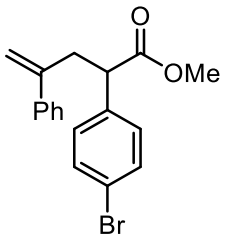

16.9 mg, 49% yield, Colorless oil.
R_f : 0.55 (EtOAc/Hex 5:1)
IR (ATR) 2924, 1735, 1489, 1435, 1160, 1074, 1012, 903, 823, 779, 758, 706 cm^{-1}.

^{1}H NMR (400 MHz, CDCl3) δ 7.41 (dt, *J* = 8.8, 2.4 Hz, 2H), 7.26-7.35 (m, 5H), 7.08 (dt, *J* = 8.0, 2.2 Hz, 2H), 5.20 (d, *J* = 0.8 Hz, 1H), 4.97 (d, *J* = 1.2 Hz, 1H), 3.66 (dd, J = 8.0, 7.6 Hz, 1H), 3.61 (s, 3H), 3.31 (ddd, *J* = 14.6, 8.0, 1.2 Hz, 1H), 2.87 (ddd, *J* = 14.6, 7.6, 1.0 Hz, 1H).
^{13}C NMR (100.5 MHz, $CDCl_3$) δ 173.49, 145.03, 140.21, 137.40, 131.63, 129.71, 128.44, 127.69, 126.26, 121.28, 115.14, 52.10, 49.45, 39.21.
HRMS–FD (m/z): [M]+ calcd for $C_{18}H_{17}BrO_2$, 344.0412; found, 344.0423.

Methyl 2-(4-chlorophenyl)-4-(3-methoxyphenyl)-2-methylpent-4-enoate (3db)

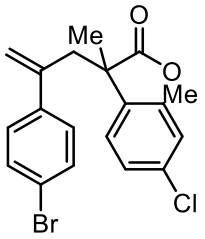

17.5 mg, 45% yield, Colorless oil.
R_f : 0.53 (EtOAc/Hex 5:1)
IR (ATR) 2949, 1732, 1491, 1238, 1122, 1097, 1012, 907, 830, 757 cm^{-1}.
^{1}H NMR (400 MHz, $CDCl_3$) δ 7.35 (dt, *J* = 8.8, 2.1 Hz, 2H), 7.20 (dt, *J* = 8.4, 2.1 Hz, 2H), 7.15 (dt, *J* = 8.8, 2.1 Hz, 2H), 7.07 (dt, *J* = 8.8, 2.1 Hz, 2H), 5.19 (d, *J* = 1.6 Hz, 1H), 4.97 (d, *J* = 1.2 Hz, 1H),
3.43 (s, 3H), 3.33 (d, *J* = 13.6 Hz, 1H), 3.05 (d, *J* = 13.6 Hz, 1H), 1.40 (s, 3H).
^{13}C NMR (100.5 MHz, $CDCl_3$) δ 175.60, 144.31, 141.74, 141.22, 132.76, 131.09, 128.37, 128.33, 127.55, 121.11, 118.84, 52.01, 50.02, 44.16, 22.86.
HRMS–FD (m/z): [M]+ calcd for $C_{19}H_{18}BrClO_2$, 392.0179; found, 392.0164.

Methyl 4-(4-acetoxyphenyl)-2-(4-chlorophenyl)-2-methylpent-4-enoate (3dc)

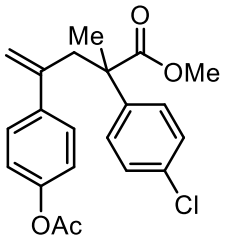

24.3 mg, 65% yield, Colorless oil.
R_f : 0.33 (EtOAc/Hex 5:1)

IR (ATR) 2951, 1760, 1731, 1507, 1494, 1370, 1197, 1122, 1096, 1013, 909, 851, 828, 758 cm^{-1}.

^{1}H NMR (400 MHz, $CDCl_3$) δ 7.19-7.24 (m, 4H), 7.18 (dt, *J* = 8.8, 2.4 Hz, 2H), 6.95 (dt, *J* = 8.8, 2.4 Hz, 2H), 5.19 (d, *J* = 1.6 Hz, 1H), 4.97 (s, 1H), 3.37 (d, *J* = 13.6 Hz, 1H), 3.38 (s, 3H), 3.05 (d, *J* = 13.6 Hz, 1H), 2.29 (s, 3H), 1.42 (s, 3H).

^{13}C NMR (100.5 MHz, $CDCl_3$) δ 175.61, 169.41, 149.78, 141.99, 139.85, 132.62, 128.33, 127.79, 127.53, 121.08, 118.60, 52.00, 49.87, 44.24, 22.99, 21.12.

HRMS–FD (m/z): [M]+ calcd for $C_{21}H_{21}ClO_4$, 372.1128; found, 372.1134.

Methyl 2-(4-chlorophenyl)-2-methyl-4-(*m*-tolyl)pent-4-enoate (3dd)

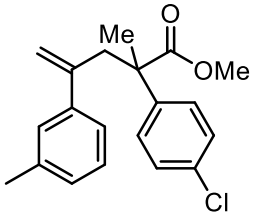

22.4 mg, 68% yield, Colorless oil.

R$_f$: 0.59 (EtOAc/Hex 5:1)

IR (ATR) 2985, 1737, 1447, 1373, 1236, 1096, 1045, 847, 792 cm^{-1}.

^{1}H NMR (400 MHz, $CDCl_3$) δ 7.14-7.20 (m, 4H), 7.11 (t, *J* = 7.6 Hz, 1H), 6.99-7.03 (m, 2H), 6.95(s, 1H), 5.18 (d, *J* = 1.6 Hz, 1H), 4.93 (d, *J* = 1.2 Hz, 1H), 3.41 (s, 3H), 3.36 (d, *J* = 14.0 Hz, 1H), 3.08 (d, *J* = 14.0 Hz, 1H), 2.28 (s, 3H), 1.41 (s, 3H).

^{13}C NMR (100.5 MHz, $CDCl_3$) δ 175.78, 145.45, 142.20, 142.01, 137.43, 132.53, 128.18, 127.90, 127.81, 127.62, 127.45, 123.83, 117.91, 51.91, 50.02, 44.24, 22.85, 21.33.

HRMS–FD (m/z): [M]+ calcd for $C_{20}H_{21}ClO_2$, 328.1230; found, 328.1222.

Methyl 2-(4-chlorophenyl)-4-(3-methoxyphenyl)-2-methylpent-4-enoate (3de)

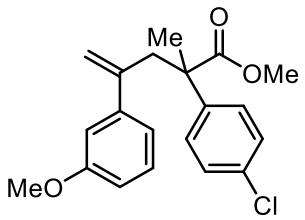

24.0 mg, 70% yield, Colorless oil.

R$_f$: 0.6 (EtOAc/Hex 5:1)

IR (ATR) 2950, 1731, 1598, 1576, 1491, 1457, 1432, 1286, 1232, 1118, 1096, 1048, 1013, 908, 827, 785, 727 cm^{-1}.

^{1}H NMR (400 MHz, $CDCl_3$) δ 7.12-7.22 (m, 5H), 6.80 (dt, *J* = 9.2, 1.1 Hz, 1H), 6.74 (ddd, *J* = 8.4, 2.8, 0.8 Hz, 1H), 6.70 (t, *J* = 2.2 Hz, 1H), 5.20 (d, *J* = 2.0 Hz, 1H), 4.93 (dd, *J* = 0.8, 0.8 Hz, 1H), 3.79 (s, 3H), 3.45 (s, 3H), 3.35 (d, *J* = 14.0 Hz, 1H), 3.07 (d, *J* = 14.0 Hz, 1H), 1.41 (s, 3H).
^{13}C NMR (100.5 MHz, $CDCl_3$) δ 175.76, 159.25, 145.20, 143.83, 141.91, 132.57, 128.97, 128.22, 127.63, 119.28, 118.21, 112.73, 112.30, 55.19, 51.96, 50.10, 44.27, 22.78.
HRMS–FD (m/z): [M]+ calcd for $C_{20}H_{21}ClO_3$, 344.1179; found, 344.1165.

Methyl 2-(4-chlorophenyl)-2-methyl-4-(naphthalen-2-yl)pent-4-enoate (3df)

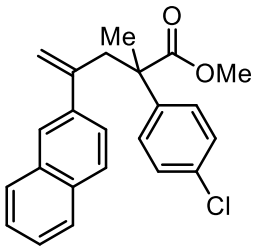

25.0 mg, 69% yield, Colorless oil.
R_f : 0.53 (EtOAc/Hex 5:1)
IR (ATR) 2949, 1730, 1493, 1458, 1433, 1239, 1205, 1111, 1097, 1013, 896, 859, 822, 753 cm^{-1}.
^{1}H NMR (400 MHz, $CDCl_3$) δ 7.75-7.79 (m, 2H), 7.71 (d, *J* = 8.8 Hz, 1H), 7.64 (d, *J* =1.2 Hz, 1H), 7.41-7.48 (m, 2H), 7.38 (dd, *J* = 8.4, 2.0 Hz, 1H), 7.16-7.21 (m, 4H), 5.33 (d, *J* = 2.0 Hz, 1H), 5.04 (dd, *J* = 1.2, 1.2 Hz, 1H), 3.51 (d, *J* = 13.6 Hz, 1H), 3.33 (s, 3H), 3.17 (d, J = 14.0 Hz, 1H), 1.42 (s,
3H).
^{13}C NMR (100.5 MHz, $CDCl_3$) δ 175.75, 145.15, 142.03, 139.57, 133.06, 132.62, 132.52, 128.27, 127.96, 127.59, 127.47, 126.11, 125.79, 125.30, 125.18, 118.78, 51.97, 50.16, 44.12, 23.01.
HRMS–FD (m/z): [M]+ calcd for $C_{23}H_{21}ClO_2$, 364.1230; found, 364.1217.

Methyl 2-(4-chlorophenyl)-2-methyl-4-(*o*-tolyl)pent-4-enoate (S23)

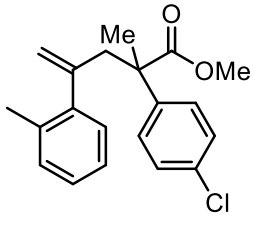

4.8 mg, 15% yield, Colorless oil.

R_f : 0.55 (EtOAc/Hex 5:1)

IR (ATR) 2950, 1733, 1627, 1492, 1457, 1209, 1097, 1013, 907, 828, 770, 732 cm^{-1}.

^{1}H NMR (400 MHz, $CDCl_3$) δ 7.20 (s, 4H), 7.04-7.12 (m, 3H), 6.99 (dd, *J* = 6.8, 1.6 Hz, 1H), 5.17 (dd, *J* = 0.8, 0.8 Hz, 1H), 5.01 (d, *J* = 2.0 Hz, 1H), 3.35 (d, *J* = 13.6 Hz, 1H), 3.24 (s, 3H), 2.95 (d, *J* = 14.0 Hz, 1H), 2.30 (s, 3H), 1.50 (s, 3H).

^{13}C NMR (100.5 MHz, $CDCl_3$) δ 175.34, 145.63, 142.25, 142.13, 134.81, 132.59, 130.08, 128.75, 128.33, 127.40, 126.86, 125.29, 119.85, 51.78, 49.40, 46.00, 23.25, 20.11.

HRMS–FD (m/z): [M]+ calcd for $C_{20}H_{21}ClO_2$, 328.1230; found, 328.1232.

1.10 References

[17] Sun, K.; Ueno, M.; Imaeda, K.; Ueno, K.; Sawamura, M. ;Shimizu, Y. *ACS Catal.* **2021**, *11*, 9722−9728.

[18] Shih, H. W. ; Wal, M. N. V.; Grange, R. L.; MacMillan, D. W. C., *J. Am. Chem. Soc*. **2010**, *132*, 13600–13603

[19] Arceo, E.; Jurberg, I. D.; Álvarez-Fernández, A.; Melchiorre, P., *Nat. Chem*. **2013**, *5*, 750−756.

[20] Nappi, M.; Bergonzini, G.; Melchiorre, *Angew. Chem. Int. Ed*. **2014**, *53*, 4921 –4925.

[21] Chen, T. Q.; MacMillan, D. W. C., *Angew.Chem. Int. Ed*. **2019**, *58*, 14584–14588.

[22] Lipshutz, B. H.; Sengupta, S. *Organic Reactions*, **1992**, *41*, 135– 631.

[23] Xu, Y.; Zhang, M.; Oestreich, M., *ACS Catal*. **2022**, *12*, 10546-10550.

[24] Yang, X.-H.; Davison, R. T.; Nie, S.-Z.; Cruz, F. A.; McGinnis, T. M.; Dong, V. M., *J. Am. Chem. Soc*. **2019**, *141*, 3006-1013.

Chapter 2
Light-driven β-Allylation of Carboxylic Acids

2.1 Introduction

2.1.1 direct β-functionalization of free carboxylic acid

As described in previous chapters, the α-functionalization of free carboxylic acid was highlighted in past decades. On the other hand, the β-functionalization is comparatively more challenging due to the inertness of the β-H.

The early research dates back to 2007, when the Yu lab[25] reported a palladium catalyzed β-arylation of pivalic acid derivatives. However, the selectivity of mono-arylation against di-arylation was mediocre.

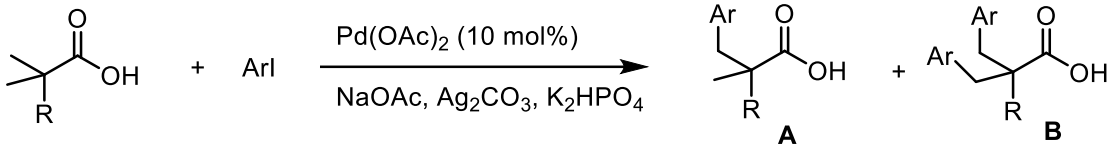

entry	R	Ar	yield / %	**A : B**
1	Me	Ph	70	5 : 2
2	nPr	pMePh	60	3 : 1
3	Et	Ph	72	4 : 1

Fig 2.1 Palladium catalyzed β-arylation

Yingsheng Zhao and coworkers[26] reported a β-arylation in 2017. By applying a ligand, Ac-Gly-OH, palladium catalyzed β-arylation of carboxylic acid was largely improved in terms of selectivity and scope. This reaction requires no directing group on the substrate. Also, a 10-gram scale reaction was successfully conducted.

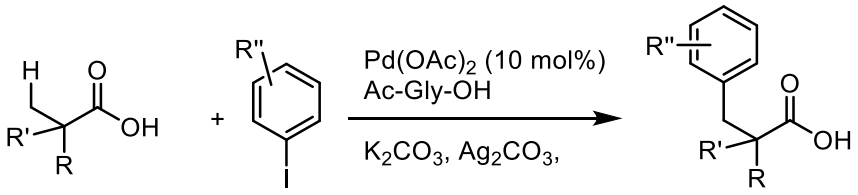

Fig 2.2 β-Arylation applying a ligand

Manuel van Gemmeren and coworkers[27] reported a direct β-alkynylation of carboxylic acids enabled by palladium catalyst. A ligand derived from ethylenediamine was applied. Interestingly, α-non-quaternary carboxylic acids gave lower yields as compared to the more sterically demanding standard substrates.

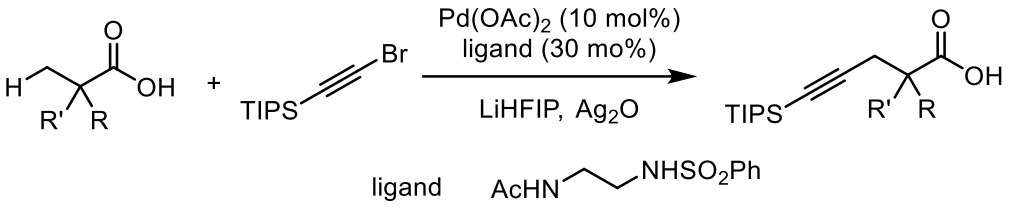

Fig 2.3 Pd catalyzed β-alkynylation of carboxylic acids

Jin-Quan Yu and coworkers[28] reported a β-acyloxylation using tert-butyl hydrogen peroxide as the only oxidant. The reaction was enabled by a cyclopentane-based mono-N-protected β-amino acid ligand. The selectivity for mono-functionalization of substrates bearing two α-methyl groups was excellent. α-Non-quaternary aliphatic carboxylic acids were well tolerated.

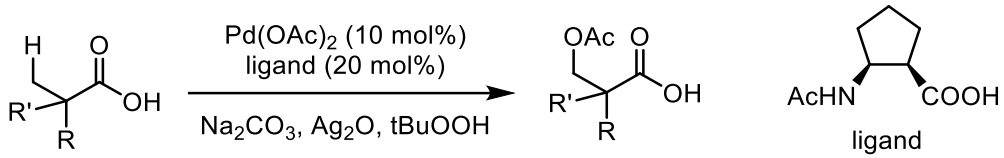

Fig 2.4 β-Acyloxylation with tert-butyl peroxide as the oxidant

Rodolphe Jazzar, Guy Bertrand, K. N. Houk, Jin-Quan Yu and coworkers[29] reported a β-bromination via C(sp^3)-H activation using Pd catalyst. The carboxylic acid-metal catalyst affinity was enhanced by hydrogen bonding. This reaction showed excellent mono-selectivity. They found the geometric relationship between carboxylic acid substrate and the ligand in the complex intermediate plays very important roles.

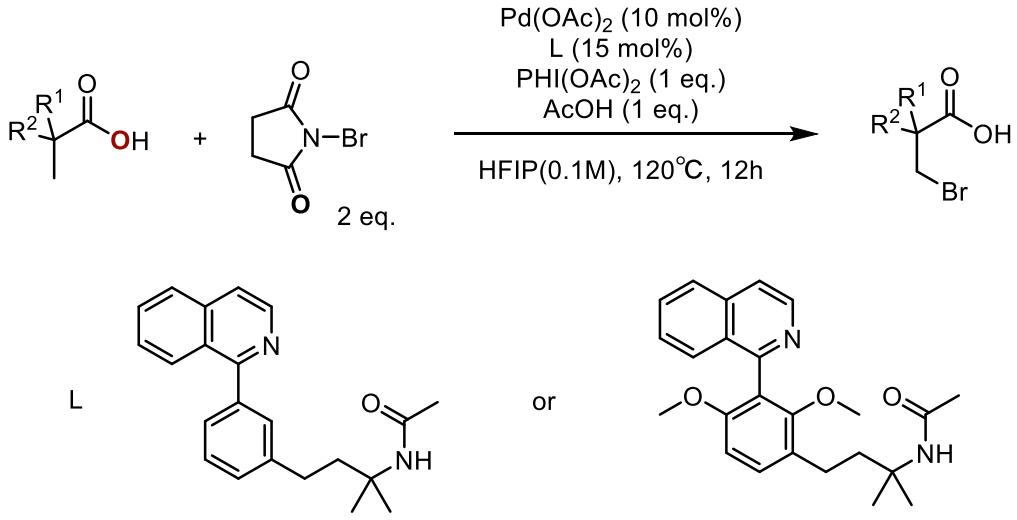

Fig 2.5 β-Bromination via C(sp^3)-H activation

Jin-Quan Yu and coworkers[30] reported a β-arylation of free carboxylic acids enabled by β-methylene C(sp^3)−H activation. By applying a unique bidentate pyridine-pyridone ligand, β-methylene C-H activation of free carboxylic acid can be achieved for the first time.

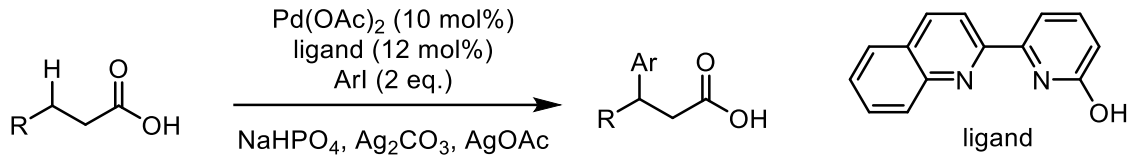

Fig 2.6 β-Arylation by β-methylene C(sp3)−H activation

These reactions feature direct β-functionalization of free carboxylic acid by palladium catalysis. They serve as brand new synthetic methods capable of constructing complicated carboxylic acid structures conveniently. In most cases, unique ligands were used in these reactions to activate the β-C-H by distal interactions.

Notwithstanding the great improvement these reactions brought to organic chemistry, there are still many challenging tasks remained to be tackled. For example, robust methods of the β-alkylation have not been reported yet. In addition, β-functionalization of α-aryl carboxylic acid is rarely reported in the literature. Furthermore, present methods require expensive palladium catalyst and silver reagents in most cases, which increase the cost of the approach.

2.1.2 β-alkylation functionalization of carbonyl compounds

Among β-functionalization of free carboxylic acids, arylation, bromination, acyloxylation etc. are all well documented, while alkylation was rarely reported. On the other hand, methods for β-alkylation of other carbonyl compounds have been published.

Wei Wang and coworkers[31] reported an enantioselective β-alkylation of aldehydes. Amine catalyst reacts with the aldehyde substrate to form the enamine intermediate. The enamine is then oxidated to generate an iminium species, which further reacts with a special nucleophile in a manner of cascade reactions. A non-toxic reagent, IBX (o-iodoxybenzoic acid), was used as the oxidant. Also, a one-pot construction of complex molecular architectures was showcased.

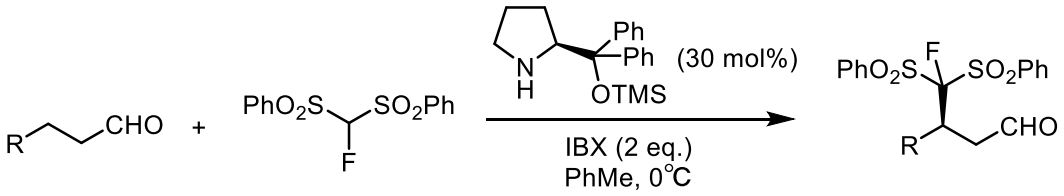

Fig 2.7 Enantioselective β-alkylation of aldehydes

The MacMillan group[32] reported a β-coupling of cyclic ketones with aryl ketones. Synergistic combination of photoredox catalysis and organocatalysis enabled this transformation. The ketone precursors were turned into diaryl oxymethyl or aryl−alkyl oxymethyl radicals via single-electron reduction. These intermediates were further merged with β-enaminyl radical generated by photon-induced enamine oxidation to afford the product. The nature of ketyl radical precursor and the photocatalyst was proved to be crucial in this reaction.

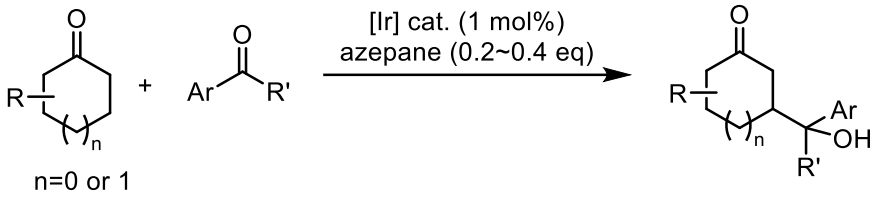

Fig 2.8 β-Coupling of cyclic ketones with aryl ketones

The MacMillan group[33] then reported a β-Mannich reaction of cyclic ketones. This reaction was also enabled by a synergistic combination of photoredox catalysis and organocatalysis as the reaction above. DABCO (1,4-Diazabicyclo[2.2.2]octane) was utilized as both a base and an electron transfer agent in this reaction.

Fig 2.9 β-Mannich reaction of cyclic ketones

These reactions feature oxidation of the intermediate generated from carbonyl substrates and organocatalyst. Among them, the single electron transfer strategy was intriguing, because they showed the application of photochemistry in these transformations, which may also be combined with boron-catalyzed photochemistry.

Tomislav Rovis and coworkers[34] reported a C–H alkylation of ketones or carboxylic acids by coupling them with electron deficient olefins. Cuprate catalyst generates a chlorine radical by ligand-to-metal charge transfer. The chlorine radical abstracts the electron-rich C(sp^3)−H bonds to generate radical intermediates from substrates. However,

the reaction requires β-C–H bond having low BDE. The existence of other ow BDE bonds induce mediocre regioselectivity.

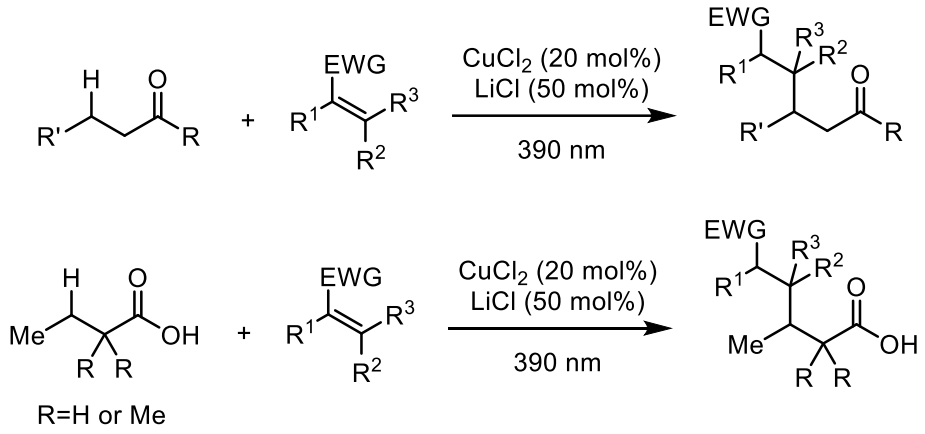

Fig 2.10 Copper catalyzed C(sp^3)–H bond alkylation

From the above examples, it can be seen that β-alkylation of carbonyl compounds are typically difficult to achieve. Protocol for β-alkylation of carboxylic acids via catalytically generated β-radicals remains a challenge to tackle.

2.2 Hypothesis and initial screening

In the previous paragraph, the boron catalysis system has been introduced, in which carboxylic acid enolates generate facilely. Single electron transfer between photoexcited enolates and allyl sulfones generate two radical species. Following radical-radical coupling furnishes C-C bond formation. It was conceived that a similar mechanism would allow for the catalytic β-allylation of carboxylic acids if the coupling can occur selectively with the radical intermediate that has been transposed to β-position.

It was envisioned that by using two ligands playing different roles, deprotonation of β-H can be promoted to yield the β-radical. The following radical-radical coupling will accomplish the β-allylation. One ligand should be responsible for the photoinduction, and the BINOL-type ligands have been shown to be suitable candidates. Another co-ligand should assist β-H deprotonation with either electronic effect or distal interactions.

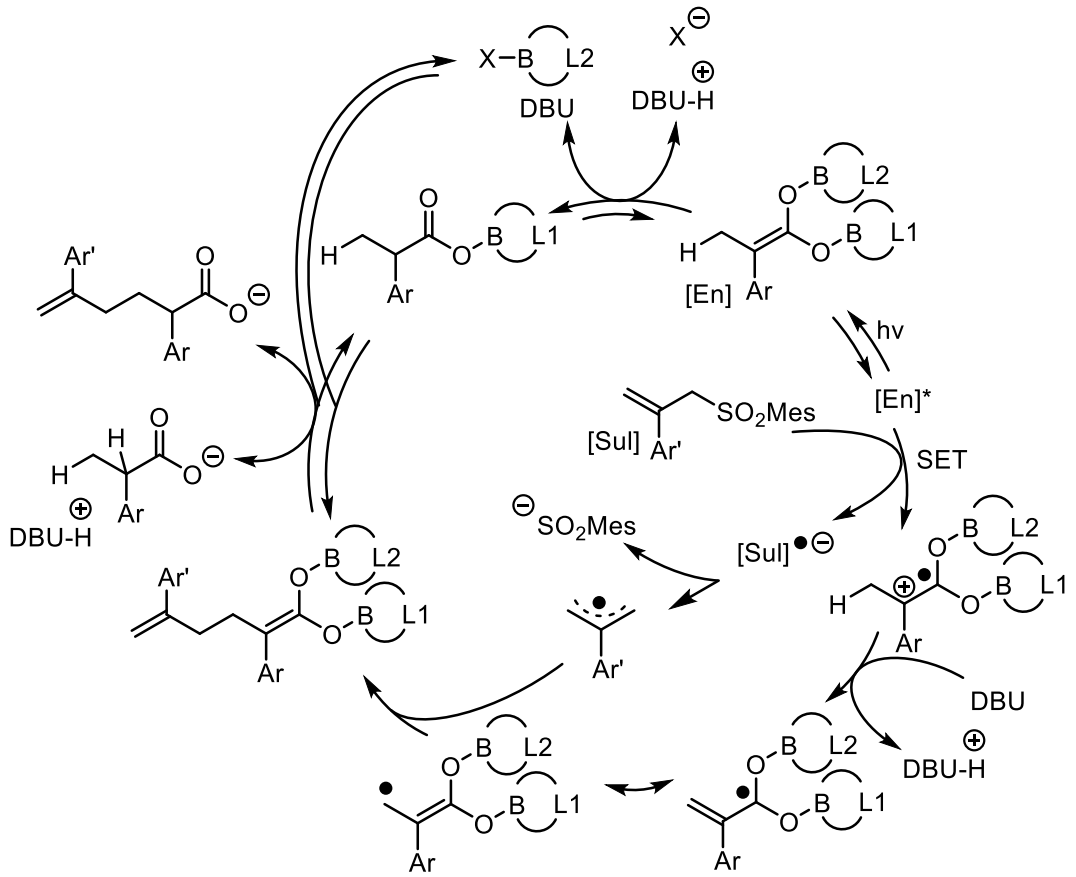

Fig 2.11 Conceived mechanism for β-allylation

Upon careful analysis of the reaction with bipyrenol ligand **L1**, the optimal ligand for α-allylation, a small amount of β-allylation product **9aa** (7% yield) was detected along with α-product **8aa** as shown below.

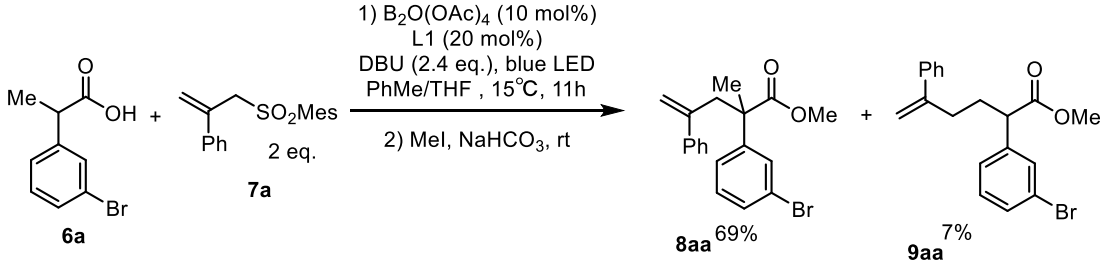

Fig 2.12 The detection of β-allylation product

The screening with various combinations of different ligands was conducted at the beginning of the optimization. Since the reaction probably goes through a diboron enediolate intermediate, two ligands on two boron atoms can play distinct roles. It was

gladly found that by combing (L)-FOS-Val and L7, β-allylation product could be obtained with 20% yield, albeit with low selectivity against α-allylation.

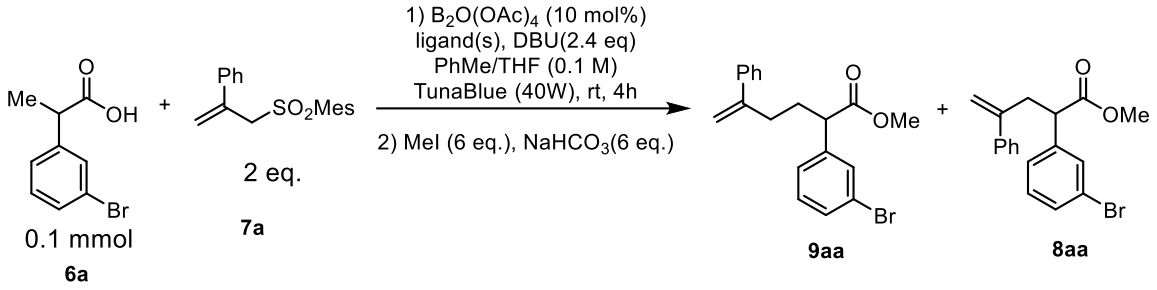

entry	ligand(s)	**9aa** / %	**8aa** / %
1	L7 (20 mol%)	0	18
2	L7 (10 mol%)	3	43
3	L7 (10 mol%) + (L)FOS-Val (10 mol%)	20	12
4	L1 (10 mol%) + (L)FOS-Val (10 mol%)	11	17
5	L4 (10 mol%) + (L)FOS-Val (10 mol%)	7	11

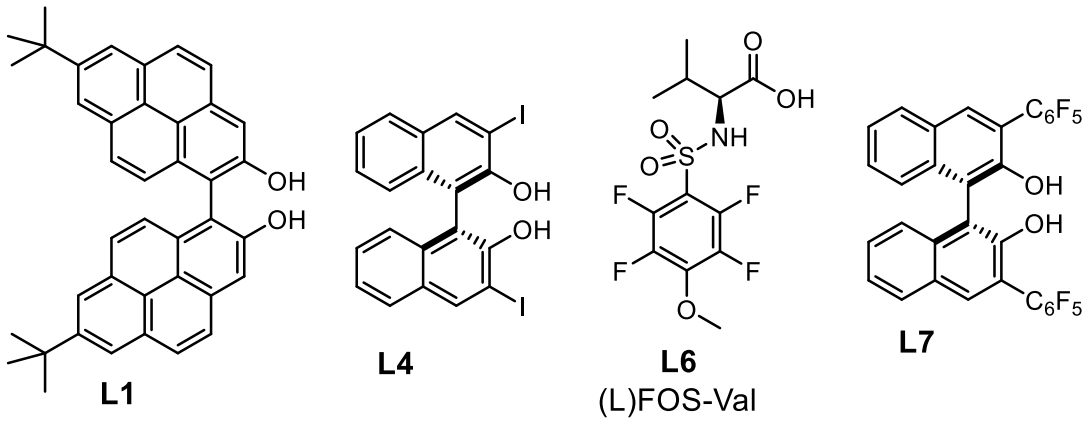

Fig 2.13 Screening with some combinations of different ligands

2.3 BINOL screening with ML (machine learning)

The screening of BINOL-type ligand was carried out at first. Various molecules of this type were synthesized to create a real library. Ligands in this library were tested in the β-allylation with the same reaction conditions. By doing so, experimental data was obtained, which was used to train the ML models.

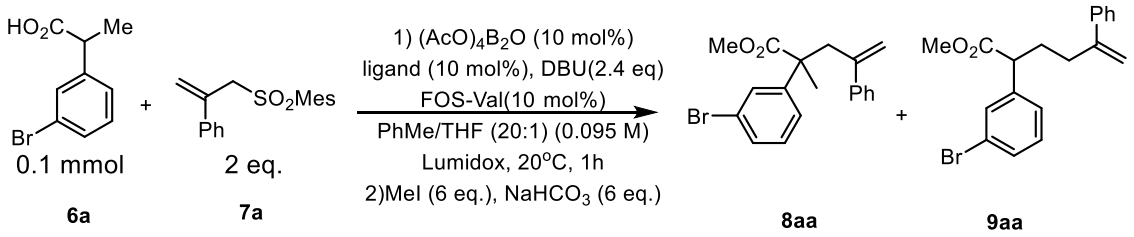

entry	ligand	**9aa / %**	**8aa** / %
1	L3	2	1
2	L4	19	10
3	L7	16	3
4	L8	5	0
5	L9	15	3
6	L10	4	4
7	L11	28	6
8	L12	19	4
9	L13	27	0
10	L14	23	10
11	L15	7	5
12	L16	19	9
13	L17	4	1
14	L18	2	7
15	L19	13	2
16	L20	4	2
17	L21	15	3

entry	ligand	**9aa / %**	**8aa** / %
18	L22	7	5
19	L23	23	3
20	L24	17	9
21	L25	1	1
22	L26	2	4
23	L27	22	2
24	L28	13	16
25	L29	29	4
26	L30	4	3
27	L31	14	2
28	L32	5	2
29	L33	12	4
30	L34	8	5
31	L35	10	2
32	L36	23	3
33	L37	9	3

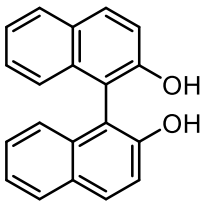

L3

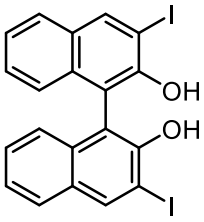

L4

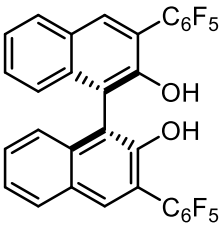

L7

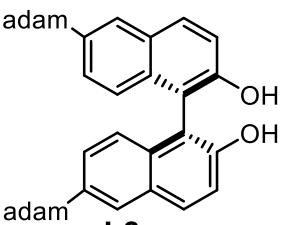

L8

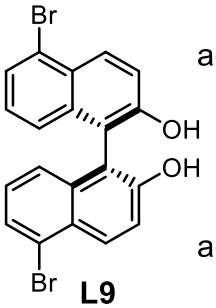

L9

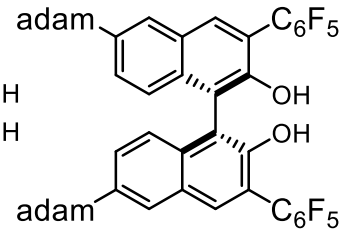

L10

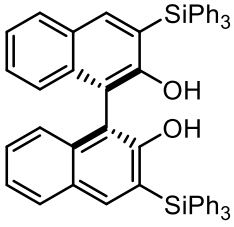

L11

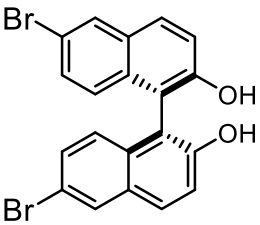

L12

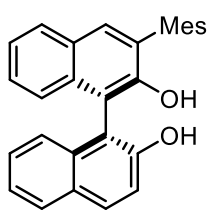

L13
(R)Mes-BINOL

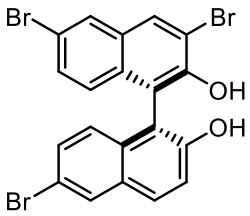

L14

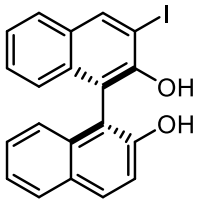

L15

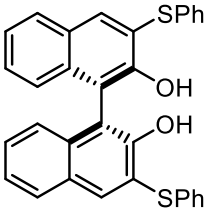

L16

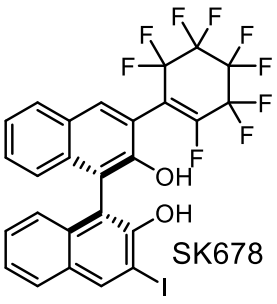

L17

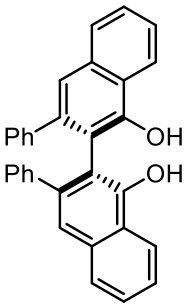

L18

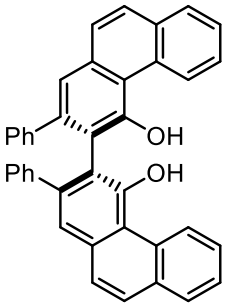

L19

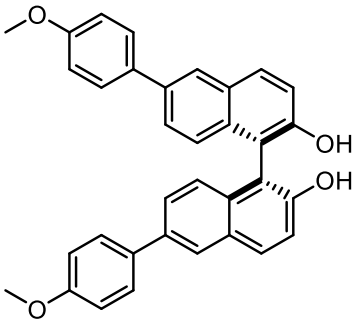

L20

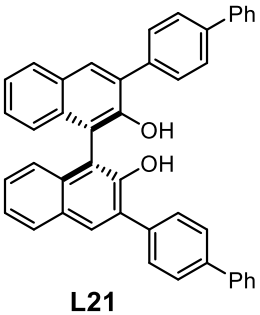

L21

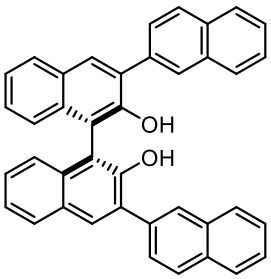

L22

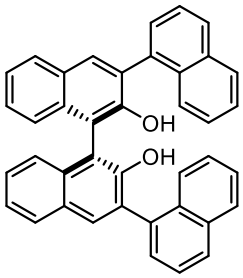

L23

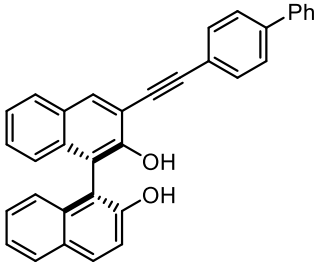

L24

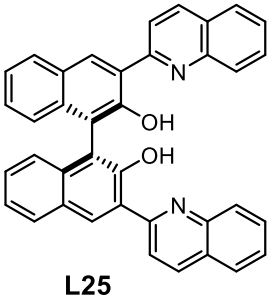

L25

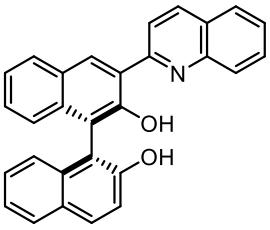

L26

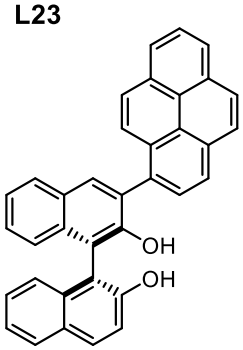

L27

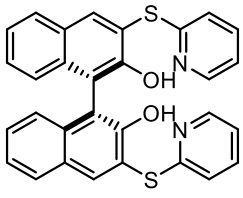

L28

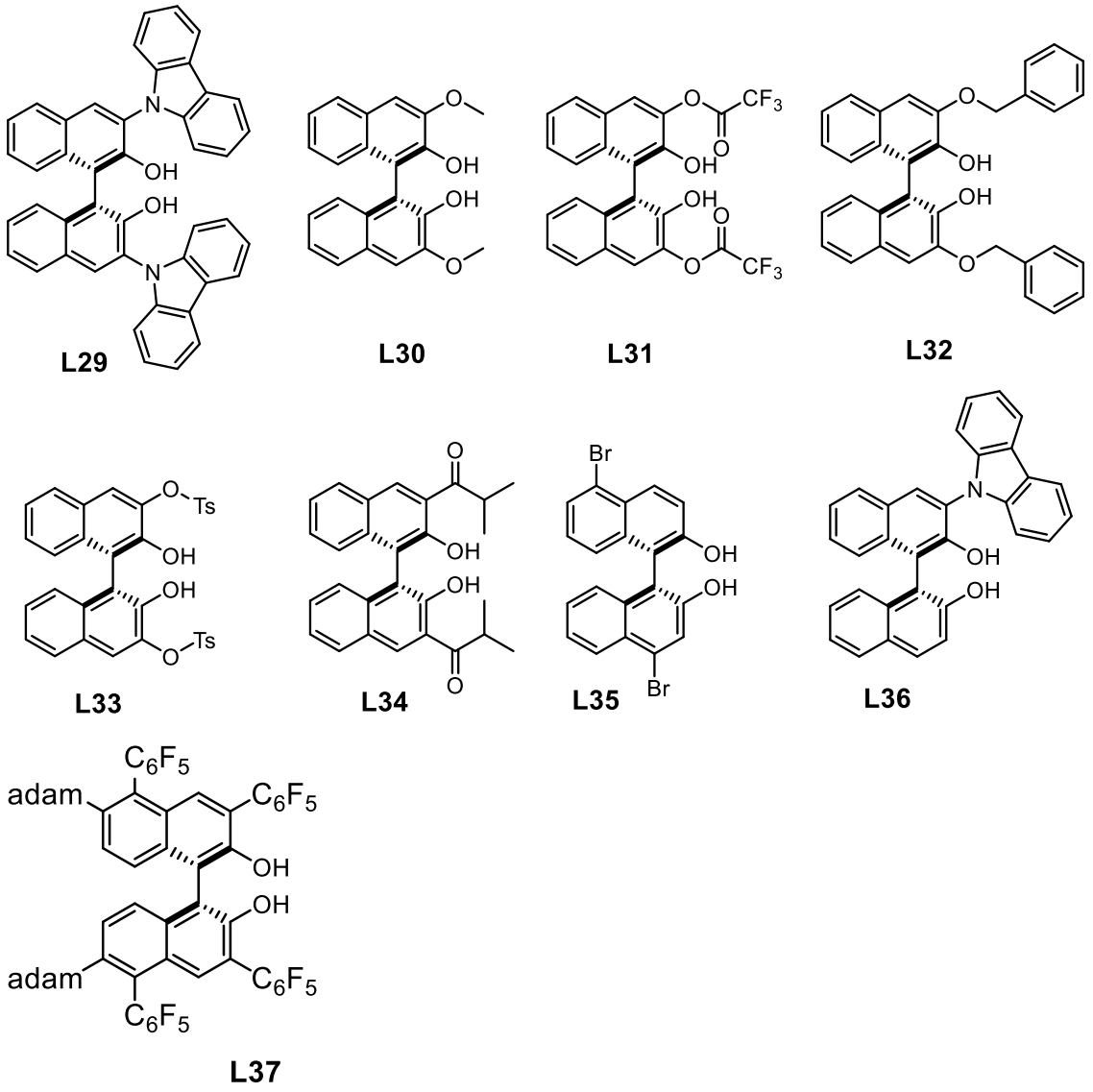

Fig 2.14 BINOL screening

Parameterization was then implemented to acquire descriptors for model construction. DFT calculation was performed with structures as below.

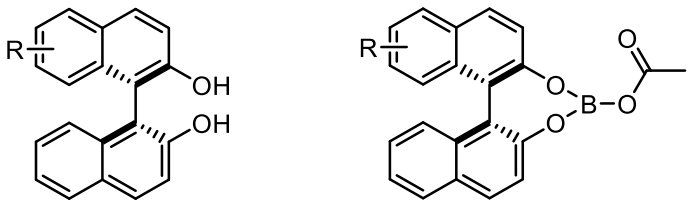

Fig 2.15 BINOL structures used for DFT calculation

First, a "core" of BINOLs as drawn below was defined. This biphenyl motif is divided to an upper part and a lower part. They were named as PhHigh/PhLow

respectively, according to the NBO charge on C3. This nomenclature is actually arbitrary, i.e. any division is acceptable. Besides, the oxygen is considered separately and named CoreO. C1/C2/C3s on the core are also specially considered.

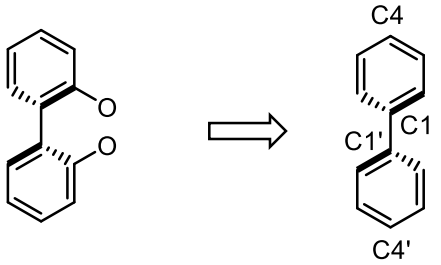

Fig 2.16 BINOL "core"

Conjugated fused ring for each BINOL was then located, named "CFR", and was also divided into two parts, CFRHigh/CFRLow.

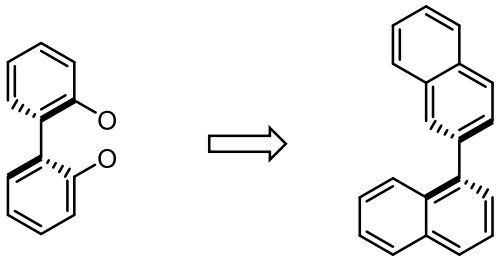

Fig 2.17 BINOL "CFR"

The substitution groups on the C3s are also considered, named "sub3".

Finally, properties for each part was calculated. This includes the total charge, total electron population, total local and delocalized electron, total σ/π electron population, total bond length, total valence L shell/M+ shell lone pair electron population, total σ/π bond energy and stabilization energy, distribution to HOMO/LUMO orbitals, distribution to IR energy, total valence/Rydberg electron etc.

"sub3" is specially considered because it was known that they have important effect on yield of the reaction. Additional descriptors including the volume corresponding to van der Waals radius/ion radius, lone pair/charge/π electron in shells with different size, electron potential etc.

Beside these descriptors, parameters unrelative to these moieties are also calculated. Such as HOMO/LUMO energy, dihedral angle of the upper and lower parts of BINOL, typical IR vibration, total electron energy, molecular weight, degree of freedom of the molecule, total bond stabilization energy, total occupied orbital energy etc.

Over 1000 descriptors were created in this way. With these data, models were built with feedforward neuro network algorithm. Their structures were depicted as bellow. Experimental result was separated to training set and validation set by choosing 3 data

randomly as validation data, and the remaining as training set. Input descriptors were also randomly chosen from over 100 models was then found to describe experimental data well, giving coefficient of determination, r^2, from 0.5 ~ 1.0. The prediction yield was finally calculated from an ensemble model combining all models as the weighted average of all these models according to their r^2.

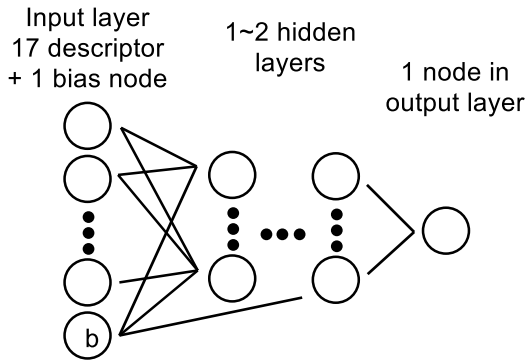

Fig 2.18 Neural network models

It was expected that the ensemble model can be used to predict the yield using other BINOL-type ligands that are out of the real library containing synthesized molecules. When a ligand is predicted to give better yield, it can then be synthesized and tested to improve the performance of β-allylation.

Sequentially, a virtual library consisting of around 600 BINOL-type ligands with diverse structures was designed. Their structures were calculated with DFT to extract descriptors. As a result, their performance was predicted with the ensemble model. Despite the significant variance of predicted yield between models in the ensemble, the prediction of the ensemble model was taken and sorted. Disappointingly, it was found that none of the ligands was predicted to outperform the best ligand in the real library, i.e. (R)-Mes-BINOL. However, considering the variance of the prediction, it is still possible to find better ligands by trying more promising ones. BINOL-type ligands were then ranked according to their predicted yield. The one with a higher upper bound of predicted performance was considered to be more promising.

A closer examination of the data revealed that: (1) heavy atom is effective for promoting the reaction, (2) steric hindrance is good for yield, (3) π-electron system at 3-position may promote the reaction, which may also be related to photoelectronic effect, and (4) it seems that electronic effect of substituents is not obvious in the reaction outcome.

Four promising ligands were synthesized and tested. Unfortunately, none of them outperform (R)-Mes-BINOL (**L13**), as predicted by the ensemble model.

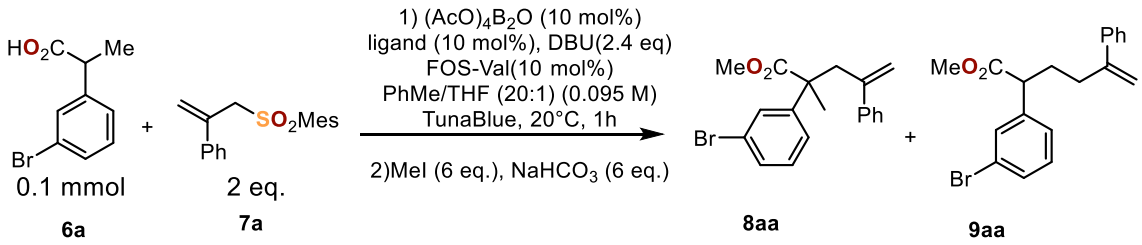

entry	ligand	**9aa** / %	**8aa** / %
1	(R)Mes-BINOL	27	0
2	**L38**	26	7
3	**L39**	22	8
4	**L40**	27	5
5	**L41**	25	4

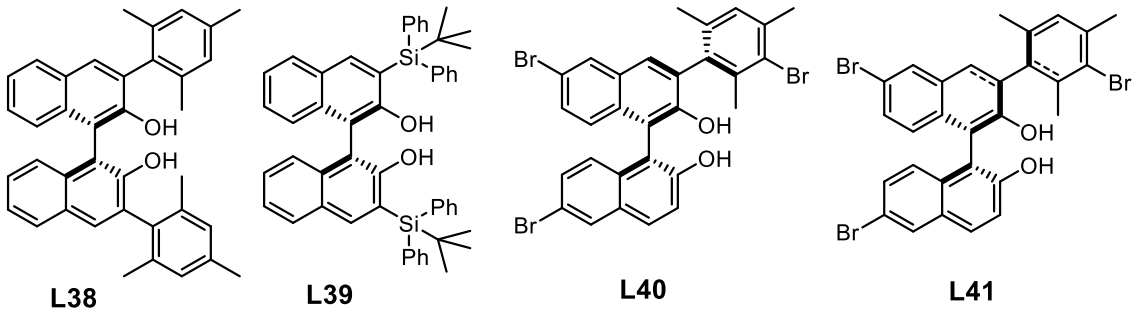

Fig 2.19 Results of the further screening

In summary, it was found that the yield of β-allylation product could not be improved by applying the new ligands within the ligand library.

2.4 Additional screenings of rection conditions

2.4.1 base screening

It has been known that basicity of DBU is crucial to deprotonate α-H, while for β-H, the requirement was unknown. Considering less bulky base may more efficiently deprotonate β-H, several variants of bases, such as DMAP (4-dimethylaminopyridine) or DMAN (1,8-Bis(dimethylamino)naphthalene), in combination with different amount of DBU was tested. However, no meaningful improvement was obtained.

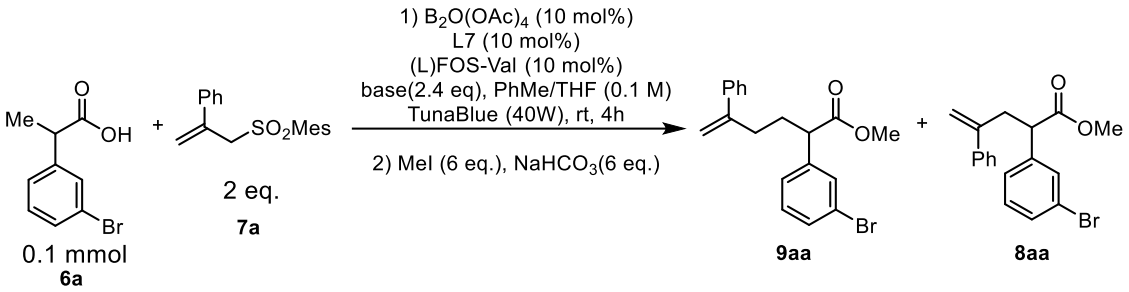

entry	base	**9aa** / %	**8aa** / %
1	DBU (2.4 eq)	20	12
2	DBU (2.8 eq)	22	6
3	DBU (2.4 eq) + DMAP (0.4 eq)	12	4
4	DBU (2.4 eq) + Et_3N (0.4 eq)	17	8
5	DBU (2.4 eq) + DABCO (0.4 eq)	16	9
6	DBU (2.4 eq) + DMAN (0.4 eq)	22	4
7	DBU (2.4 eq) + CsF (0.4 eq)	7	6
8	DBU (2.4 eq) + tBuOK (0.4 eq)	0	0

Fig 2.20 Base screening

2.4.2 sulfone screening

Leaving group on the sulfone was screened during the development of direct α-allylation of carboxylic acid. A brief screening was also performed with condition for β-allylation. However, the mesityl group remained the most suitable.

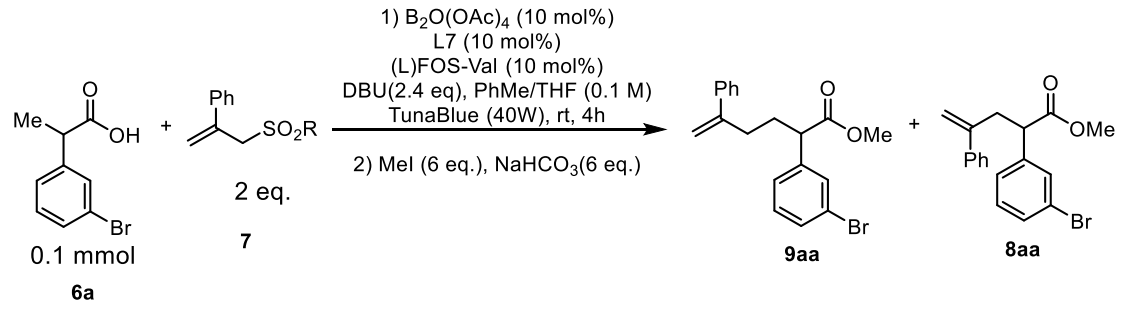

entry	sulfone	**9aa** / %	**8aa** / %
1	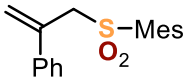	20	12
2	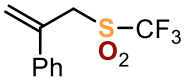	0	0
3	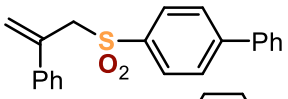	20	10
4	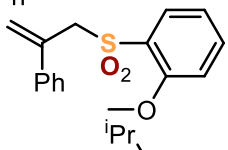	18	10
5	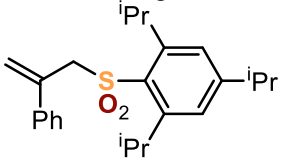	0	2
6	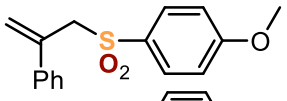	8	1
7	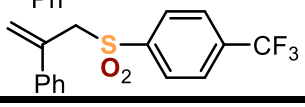	13	9

Fig 2.21 Sulfone screening

2.4.3 co-ligand screening

The other ligand used along with BINOL-type ligand was also screened. (L)FOS-Val was identified to be the best co-ligand with respect to yield and selectivity. The electronic effect, steric effect, and other aspects may all influence the performance of the co-ligand.

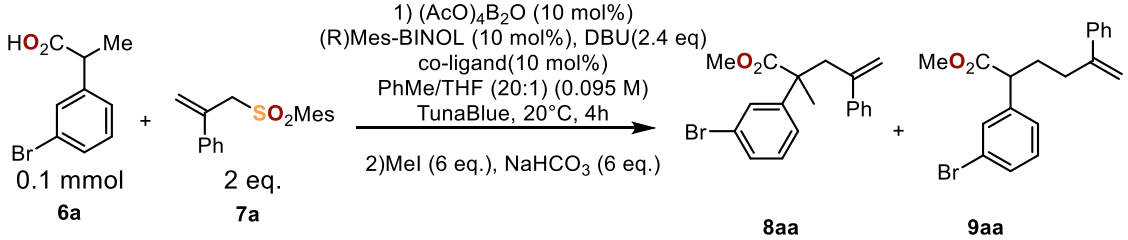

entry	co-ligand	**9aa** / %	**8aa** / %
1	(L)FOS-Val	37	4
2	**L42**	19	7
3	**L43**	23	2
4	**L44**	27	8
5	**L45**	13	18
6	**L46**	9	34
7	**L47**	1	0
8	**L48**	1	9
9	**L49**	8	27
10	**L50**	2	24
11	**L51**	3	24
12	**L52**	3	23

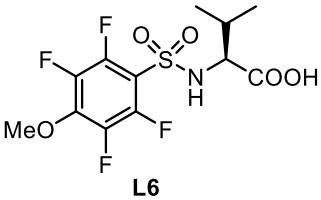

L6
(L)FOS-Val

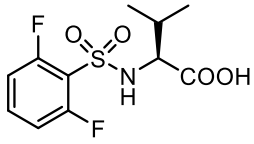

L42

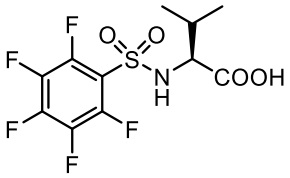

L43

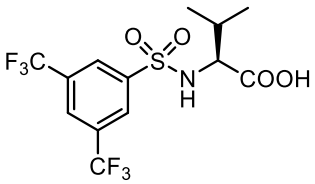

L44

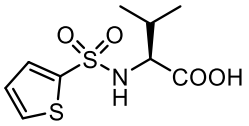

L45

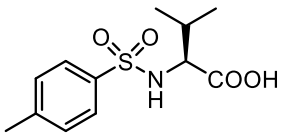

L46

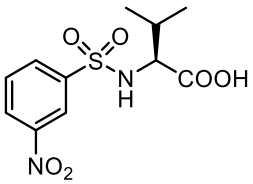

L47

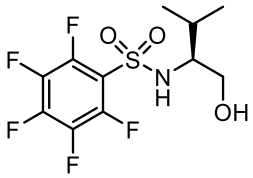

L48

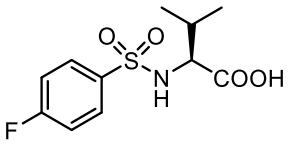

L49

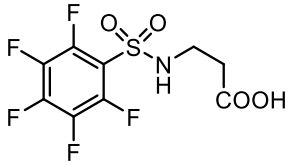

L50

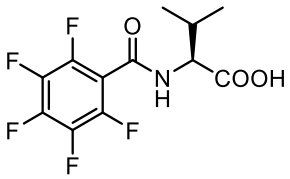

L51

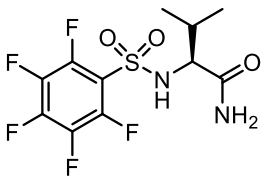

L52

Fig 2.22 Co-ligand screening

2.4.4 reaction time screening

The reaction time was screened. It was found that the best reaction time is 4h. Longer reaction time caused a reduction of the yield, which indicates a product decomposition.

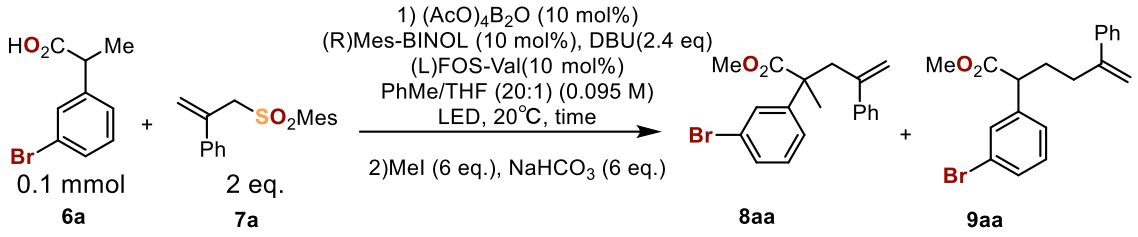

entry	reaction time / h	**9aa** / %	**8aa** / %
1	1	27	0
2	4	37	4
3	12	31	13

Fig 2.23 Reaction time screening

2.4.5 solvent screening

Solvent screening was conducted, and the result showed that the optimized solvent is o-xylene or m-xylene. THF, used previously as co-solvent, was found to inhibit the reaction.

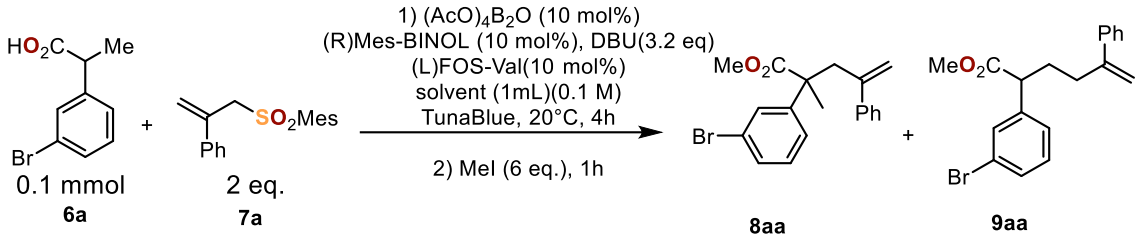

entry	solvent	**9aa** / %	**8aa** / %
1	PhMe (+50μL THF)	40	6
2	PhMe	48	4
3	THF	8	4
4	DCM	10	1
5	DMF	32	2
6	o-xylene	50	3
7	PhH	37	3
8	m-xylene	51	3

Fig 2.24 Solvent screening

2.4.6 concentration screening

The concentration of 100 mM was found to be the optimal concentration, which was the concentration used initially before the screening.

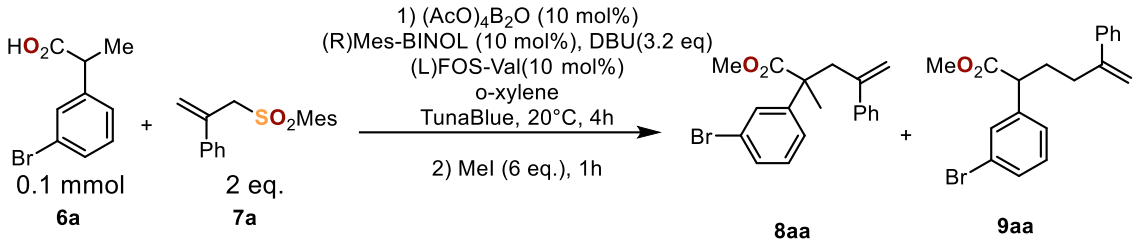

entry	concentration/mM	**9aa** / %	**8aa** / %
1	81	47	6
2	100	50	3
3	129	49	4
4	180	37	3
5	300	27	2

Fig 2.25 Concentration screening

2.5 Scope

The scope of this reaction was explored. For the carboxylic acid scope, meta-methyl substituent (**9hb**) instead of bromo substituent (**9ab**) on the phenyl ring of 2-arylpropanoic acid as well as non-substituted 2-phenylpropanoic acid (**9bb**) afforded the corresponding products in moderate yields. 2-Arylpropanoic acid with electron-withdrawing trifluoromethyl group at the para-position (**9cb**) was a competent substrate, providing β-allylation products in 65% yield. The reactions of and bearing a para-chloro (**9db**) or bromo substituent (**9eb**) also proceeded in good yields. Weakly coordinative para-cyano substituent (**9fb**) and electron-donating tert-butyl substituent (**9gb**), however, decreased the yields. The tolerance of halide substituents thus opens the possibility for subsequent derivatization. For the sulfone scope, methoxy (**9ac**) or methyl (**9ad**) substituent at the meta-position was tolerated.

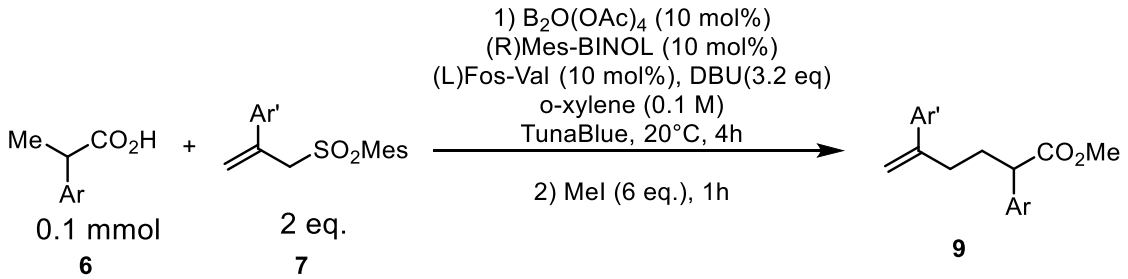

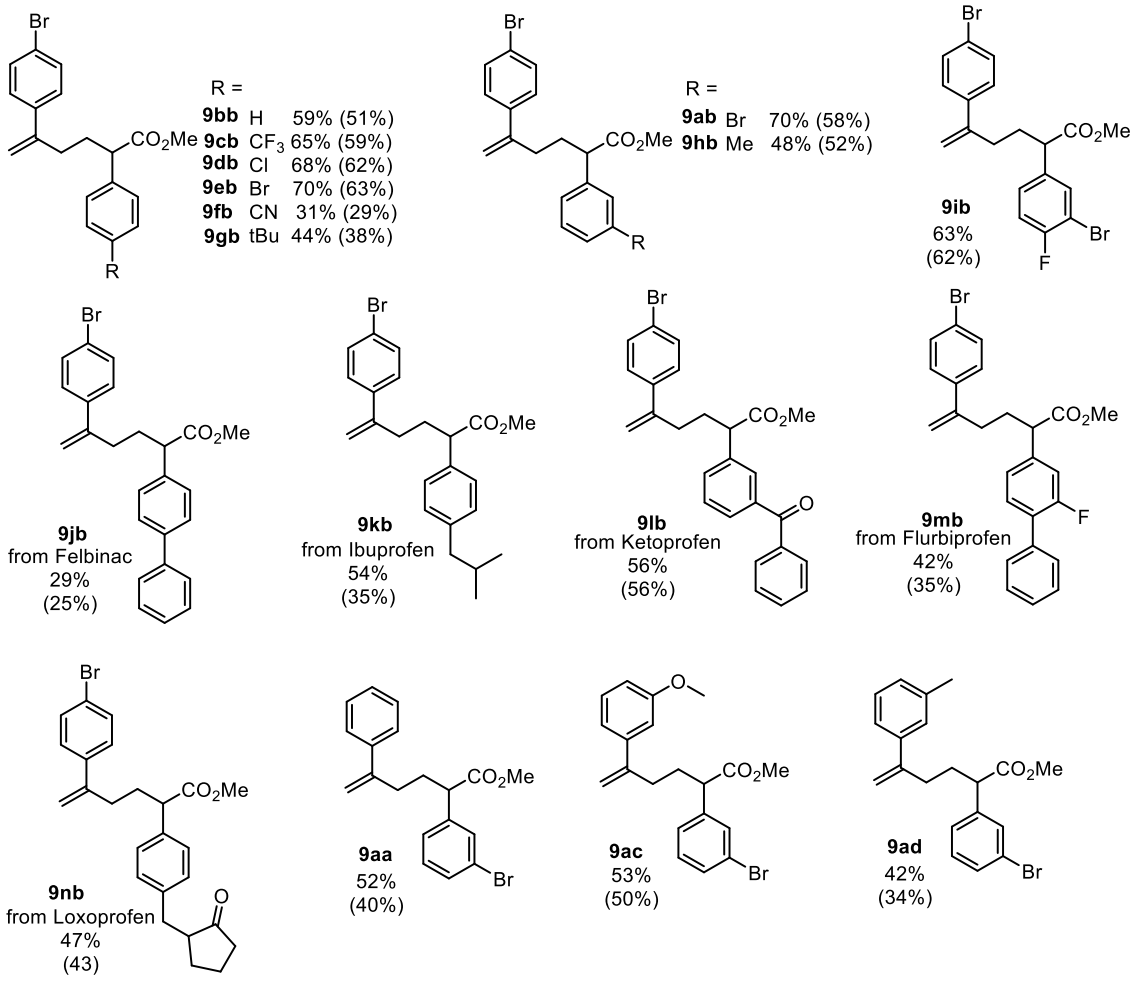

Fig 2.26 Reaction scope

number inside the parenthesis is isolated yield, number outside is NMR yield

2.6 Mechanistic investigation

To probe the mechanism of this reaction, several mechanistic experiments were performed.

2.6.1 control experiments:

It was found that the combination of two different ligands is crucial for the reaction. (L)FOS-Val greatly improves the reaction performance, while it alone cannot catalyze the reaction.

Thus, it is most probable that the reaction proceeds through a diboron enediolate intermediate, where each boron bears one of each ligand.

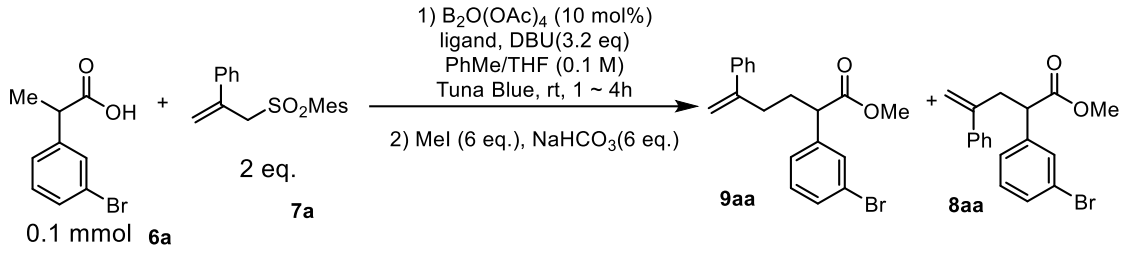

entry	ligand	βpro / %	αpro / %	time / h
1	(R)Mes-BINOL (10 mol%) + (L)Fos-Val (10 mol%)	27	1	1
2	(R)Mes-BINOL (20 mol%)	5	5	2
3	(L)Fos-Val (20 mol%)	0	2	12

Fig 2.27 Control experiments

2.6.2 comparison between (L)FOS-Val and (D)FOS-Val ligands:

It was observed that using different chirality of FOS-Val ligand gave different yield. (D)FOS-Val gave slightly lower yield than (L)FOS-Val no matter how long the reaction time was. This further proves the role of diboron enediolate intermediate, where different enantiomers of FOS-Val create diastereomer of intermediates that results in different reaction yields.

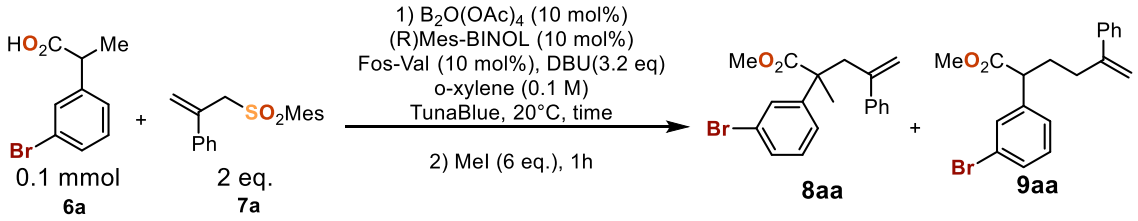

entry	FOS-Val	βpro/%	time
1	L	51	4h
2	D	47	4h
3	L	8.5	7 min
4	D	7.4	7 min

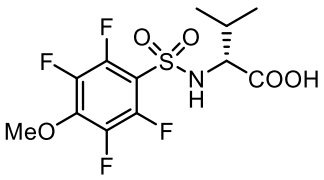

Fig 2.28 Comparison of (L)FOS-Val and (D)FOS-Val ligands

2.6.3 investigation of α,β-unsaturated carboxylic acid as a possible intermediate

During the study of this reaction, a side product was observed, hereby named **1ene**, which is the α,β-unsaturated version of the carboxylic acid. It can potentially act as an intermediate of the generation of β-allylation product as drawn bellow.

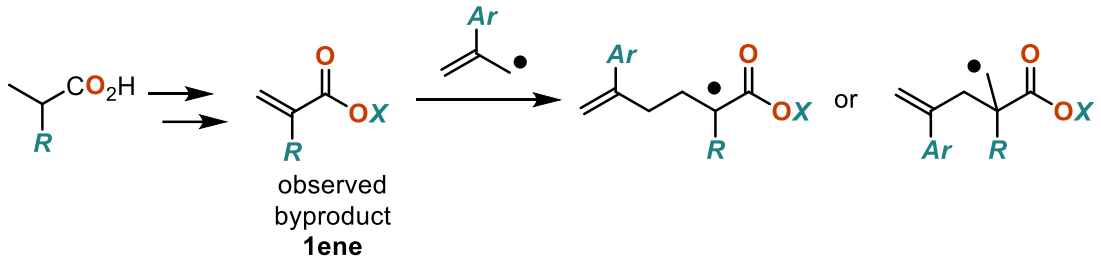

Fig 2.29 Possible mechanism

To probe this possibility, a set of competition reactions was conducted. As can be seen in the figure below, the β-allylation product (**9bb**) of α,β-unsaturated carboxylic acid (**6b'**) was not observed. This result thus excludes α,β-unsaturated carboxylic acid as the intermediate of the β-allylation.

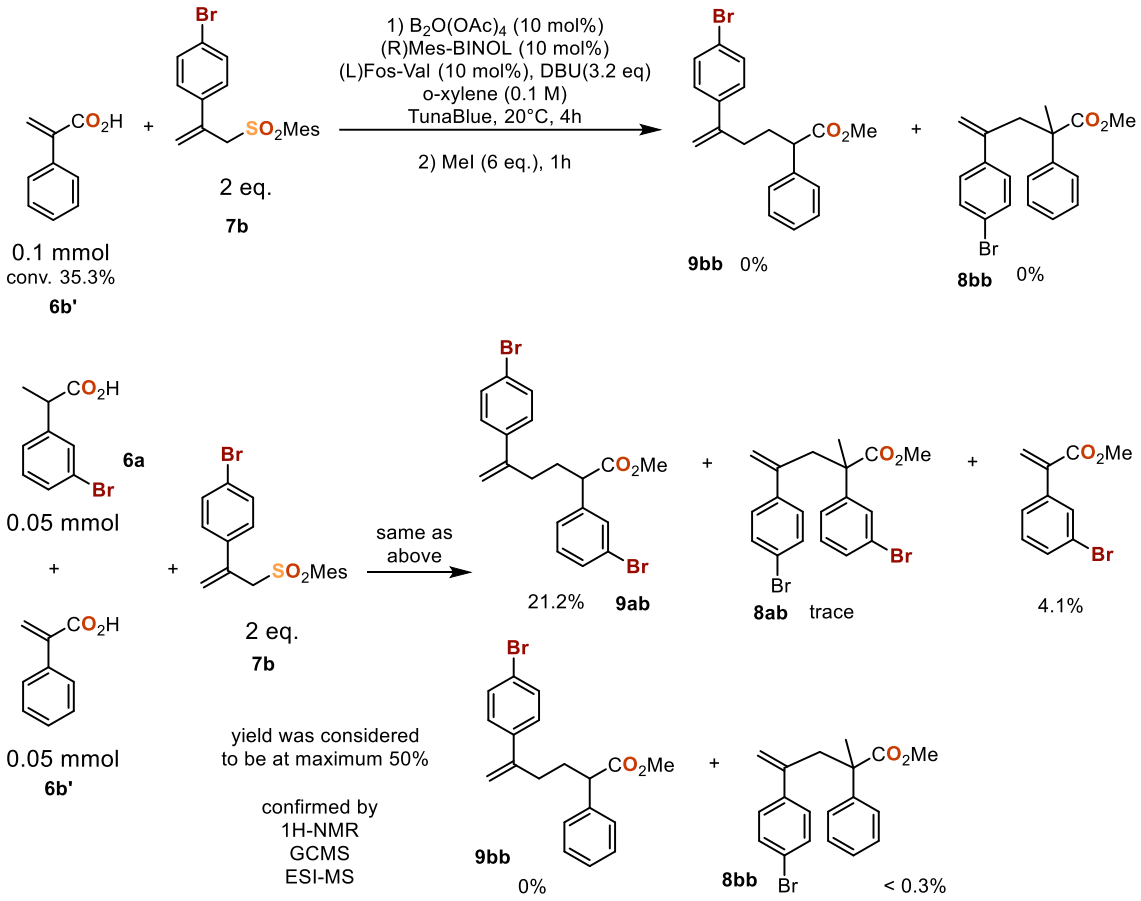

Fig 2.30 Competition reaction

2.6.4 investigation of energy transfer as a possible mechanism:

The possibility of an energy transfer mechanism was also checked.

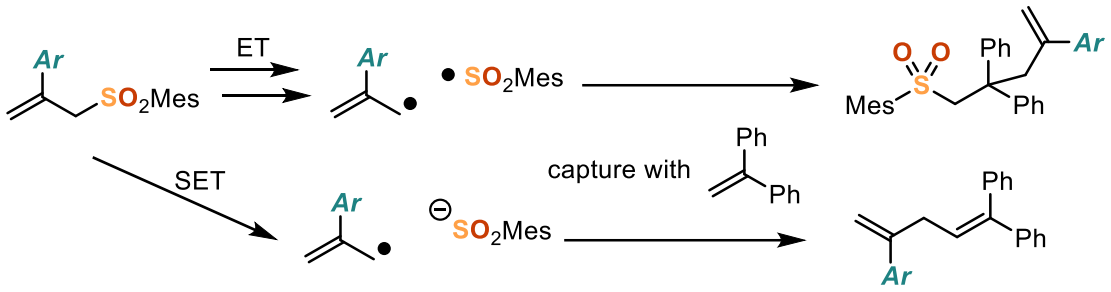

Fig 2.31 Possible mechanism

UV light or photocatalysts was used to activate the sulfone substrate, and an alkene was introduced to capture the possible radical generated. In either case, no A or B was detected (checked by NMR and GCMS). Although some conversion of sulfone was detected, mostly isomerization from terminal alkene to internal alkene was responsible. The result indicates that an energy transfer scenario is not likely to be operative.

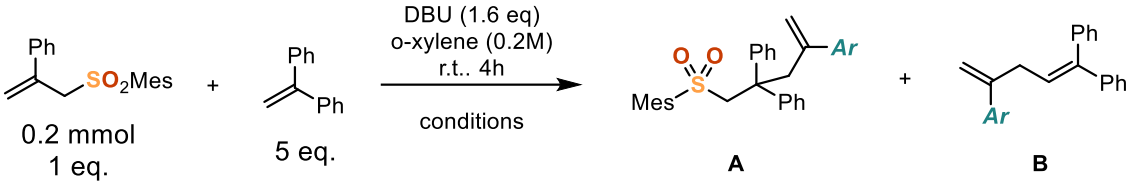

entry	conditions	**A**/%	**B**/%
1	UV light	0	0
2	Tuna Blue, Ir(ppy)3	0	0
3	Tuna Blue, 1,10-phenyl+phenothiazine	0	0
4	Tuna Blue, eosin Y	0	0

Fig 2.32 Energy transfer possibility investigation

2.6.5 kinetic study

A series of reactions was conducted to obtain some information of the rate determining step of this reaction.

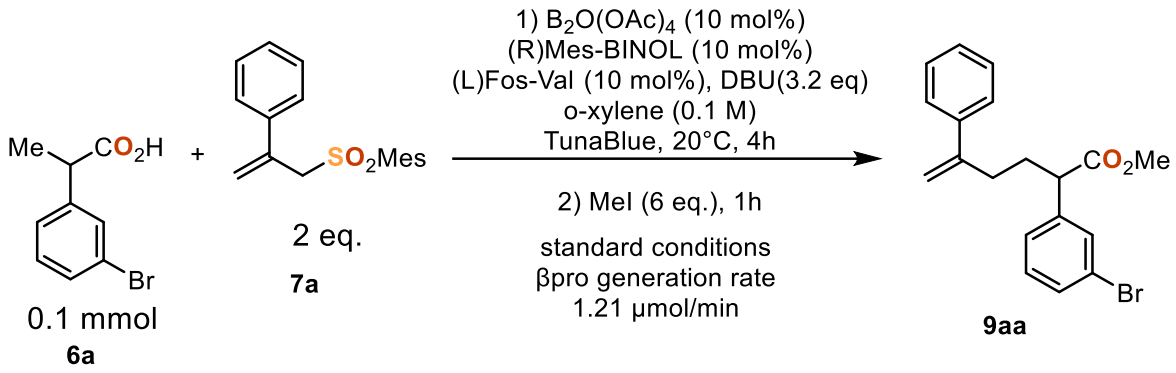

Fig **2.33** Standard conditions of the kinetic study

a. amount/conc. of DBU

entry	DBU/eq	rate(μM/min)	relative rate
1	2.3	1.28	1.06
2	3.2(std)	1.21	1.00
3	3.8	1.13	0.93
4	4.4	1.07	0.88

Fig 2.34 Effect of the amount/conc. of DBU

It is difficult to explain the results, where increased DBU concentration seems to slow down the reaction. All the equilibriums involving DBU such as step generating enolate with different boron species may influence the result.

b. amount/conc. of sulfone

entry	sulfone/eq	rate(μM/min)	relative rate
1	1.0	0.78	0.64
2	2.0(std)	1.21	1.00
3	2.4	1.31	1.08

Fig 2.35 Effect of the amount/conc. of sulfone

The step involving sulfone or the step behind may be rate-determining step. The step of SET between sulfone and activated enolate is the most possible, but a definite proof cannot be obtained at this point.

c. amount of carboxylic acid substrate:

entry	carboxylic acid/eq	DBU/eq	rate(μM/min)	relative rate
1	0.6	2.8	1.18	0.98
2	1.0(std)	3.2(std)	1.21	1.00
3	1.3	3.5	1.22	1.01

Fig 2.36 Effect of the amount of carboxylic acid substrate

The difference between data is too low to analyze. It was found that the carboxylic acid substrate, ligand and boron catalyst form multiple species in the solution. A complicated equilibrium exists among these species. Thus, it is considered that such equilibrium influences this result, which makes the result difficult to explain.

d. amount of boron catalyst:

entry	[B]cat/mol%	rate(μM/min)	relative rate
1	10(std)	1.21	1.00
2	20	0.60	0.50

Fig 2.37 Effect of the amount of boron catalyst

The equilibrium mentioned above also influences this result. It is considered that additional boron catalyst increases the concentration of acetate which forms inactive species. Additionally, boron atom bind to carboxylic acid substrate without ligand also results in inactive species. These processes decrease the concentration of the active intermediate.

As a summary, unfortunately, there was not any firm conclusion that can be drawn from these kinetic experiments. Although it had been known from the study of the α-allylation in the previous chapter, the only thing clear is that the equilibrium between carboxylic acids, ligands and boron is very complicated.

2.7 Summary

The first β-allylation was achieved by combining two different ligands with boron catalyst. Diboron enediolate is proposed to be the intermediate, which undergoes single electron transfer to allyl sulfone in the formation of allyl radical as the coupling partner.

Radical-radical coupling with α-radical is inhibited by a bulky BINOL-type ligand. At the same time, β-H is deprotonated to yield the key β-radical. Finally, radical-radical coupling furnishes the product.

2.8 General procedure

Carboxylic acid (0.1 mmol, 1.0 equiv) substrate, sulfone substrate (0.2 mmol, 2.0 equiv) and both ligands were added to a 4mL vial and then brought into the glovebox. $B_2O(OAc)_4$ (2.7 mg, 0.1 equiv), o-xylene (1 mL) and DBU (47.5 μL, 3.2 equiv) were sequentially added. The vial was sealed and removed from the glovebox, and the resulting solution was stirred for 4 h under the irradiation of blue LED (Kessil A 160WE Tuna Blue 40 W, λmax = 465 nm) in a 20℃ water bath. MeI (37.4 μL, 6 equiv) was consequently added, and the reaction mixture was left stirred for another 1 h. Then the reaction was worked up by adding 2 mL of 2:1:1 solution of brine, water and 4 M HCl, followed by extraction with EtOAc (3 times) in the vial. The combined organic layer was dried with Na_2SO_4 and evaporated on a rotavapor. To this crude product was added tetrabromoethane (11.6 μL, 0.1 mmol) as the NMR standards for the determination of NMR yield.

The residue was then purified by silica gel chromatography on a Biotage Isolera One using a dry-load method. Further purification was performed with GPC using chloroform as the eluent.

2.9 Characterization of products

The finally isolated products were collected as 2 samples separately each. Some samples contain inseparable impurities. They will be especially noted in detail bellow.

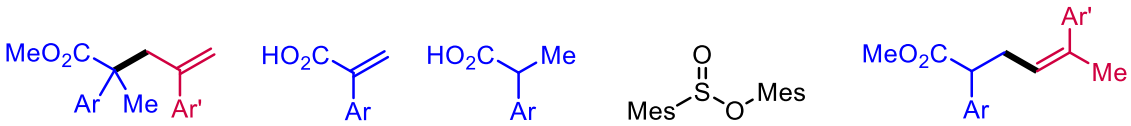

4xx **1E1x** **1E2x** **2B** **3Vxx**

Fig 2.38 Byproducts of the reaction

Methyl 2-(3-bromophenyl)-5-(4-bromophenyl)hex-5-enoate (9ab)

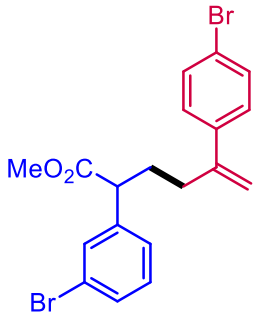

Silica gel chromatography was performed with EtOAc/hexane (0 ~ 2%).

Further purified with silica gel chromatography again instead of GPC using EtOAc/hexane (0 ~ 1%) as the eluent.

sample 1 : 14.7 mg, 34% yield, white solid.

sample 2 : 13.2 mg, containing 7 mol% **4aa**, 1 mol% **1E1a** and 31 mol% **1E2a**, 24% yield, colorless liquid.

Total yield of **9ab**: 58% yield.

R_f = 0.45 (EtOAc : hexane = 1 : 5)

^{1}H NMR (400 MHz, $CDCl_3$) δ (ppm) 7.44 (dt, J_1 = 8.9 Hz, J_2 = 2.3 Hz, 2H), 7.37~7.42 (m, 2H), 7.21 (dt, J_1 = 6.4 Hz, J_2 = 2.3 Hz, 2H), 7.18~7.19 (m, 2H), 5.29 (d, J = 0.4 Hz, 1H), 5.05 (d, J = 1.2 Hz, 1H), 3.66 (s, 3H), 3.53 (t, J = 7.6 Hz, 1H), 2.36~2.48 (m, 2H), 2.18 (dddd, J_1 = 14.3 Hz, J_2 = 8.8 Hz, J_3 = 7.9 Hz, J_4 = 6.6 Hz, 1H), 1.86 (dddd, J_1 = 13.8 Hz, J_2 = 9.0 Hz, J_3 = 7.5 Hz, J_4 = 6.3 Hz, 1H).

^{13}C NMR (100.5 MHz, $CDCl_3$) δ (ppm) 173.54, 146.15, 140.84, 139.42, 131.48, 131.03, 130.55, 130.21, 127.72, 126.65, 122.70, 121.50, 113.78, 52.19, 50.45, 32.87, 31.72.

Methyl 5-(4-bromophenyl)-2-phenylhex-5-enoate (9bb)

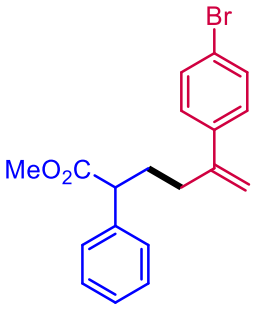

Silica gel chromatography was performed with EA/hexane (0 ~ 2%).

Further purified with silica gel chromatography again instead of GPC using the same eluent as above.

sample 1 : 7.2 mg, containing 5 mol% **4ba**, 19% yield, colorless liquid.

sample 2 : 13.7 mg, containing 18 mol% **4ba**, 2 mol% **1E1b** and 3 mol% **1E2b**, 32%

yield, colorless liquid.
Total yield of **9bb**: 51% yield.
R_f = 0.45 (EtOAc : hexane = 1 : 5)
^{1}H NMR (400 MHz, $CDCl_3$) δ (ppm) 7.43 (dt, J_1 = 9.1 Hz, J_2 = 2.4 Hz, 2H), 7.26~7.34 (m, 4H), 7.24~7.25 (m, 1H), 7.21 (dt, J_1 = 8.9 Hz, J_2 = 2.3 Hz, 2H), 5.28 (d, J = 0.8 Hz, 1H), 5.06 (d, J = 1.6 Hz, 1H), 3.65 (s, 3H), 3.57 (t, J = 7.6 Hz, 1H), 2.36~2.49 (m, 2H), 2.20 (dddd, J_1 = 14.0 Hz, J_2 = 8.8 Hz, J_3 = 7.7 Hz, J_4 = 6.3 Hz, 1H), 1.89 (dddd, J_1 = 13.7 Hz, J_2 = 9.3 Hz, J_3 = 7.5 Hz, J_4 = 6.2 Hz, 1H).
^{13}C NMR (100.5 MHz, $CDCl_3$) δ (ppm) 174.17, 146.39, 139.60, 138.70, 131.42, 128.68, 127.94, 127.74, 127.37, 121.40, 113.57, 52.02, 50.85, 32.94, 31.84.

Methyl 5-(4-bromophenyl)-2-(4-(trifluoromethyl)phenyl)hex-5-enoate (9cb)

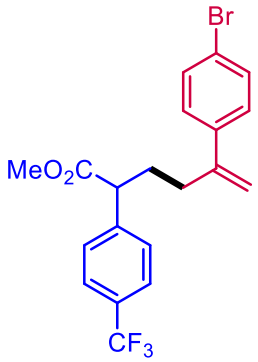

Silica gel chromatography was performed with EA/hexane (0 ~ 5%).
Further purification with GPC could not provide product with higher purity.
sample 1 : 18.6 mg, containing 2 mol% **4ca** and 5 mol% **3Vca**, 41% yield, colorless liquid.
sample 2 : 7.9 mg, containing 6 mol% **4ca** and 6 mol% **1E2c**, 17% yield, colorless liquid.
Total yield of **9cb**: 58% yield.
R_f = 0.44 (EtOAc : hexane = 1 : 5)
^{1}H NMR (400 MHz, $CDCl_3$) δ (ppm) 7.57 (d, J = 8.4 Hz, 2H), 7.44 (dt, J_1 = 9.1 Hz, J_2 = 2.4 Hz, 2H), 7.38 (d, J = 8.4 Hz, 2H), 7.21 (dt, J_1 = 8.9 Hz, J_2 = 2.4 Hz, 2H), 5.29 (d, J = 1.2 Hz, 1H), 5.05 (d, J = 1.2 Hz, 1H), 3.66 (s, 3H), 3.64 (t, J = 7.6 Hz, 1H), 2.37~2.50 (m, 2H), 2.23 (dddd, J_1 = 14.1 Hz, J_2 = 8.4 Hz, J_3 = 7.8 Hz, J_4 = 6.4 Hz, 1H), 1.89 (dddd, J_1 = 13.6 Hz, J_2 = 9.0 Hz, J_3 = 7.4 Hz, J_4 = 6.3 Hz, 1H).
^{19}F NMR (396 MHz, $CDCl_3$) δ (ppm) –62.45.
^{13}C NMR (100.5 MHz, $CDCl_3$) δ (ppm) 173.43, 146.08, 142.61 (q, J = 1.4 Hz), 139.39, 131.49, 129.69 (q, J = 32.6 Hz), 128.37, 127.71, 125.63 (q, J = 3.7 Hz), 124.03 (q, J = 272.2 Hz), 121.53, 113.85, 52.23, 50.62, 32.87, 31.71.

Methyl 5-(4-bromophenyl)-2-(4-chlorophenyl)hex-5-enoate (9db)

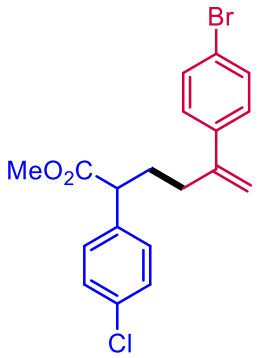

Silica gel chromatography was performed with Et_2O/pentane (0 ~ 5%).
sample 1 : 10.9 mg, containing 7 mol% **4da**, 26% yield, colorless liquid.
sample 2 : 19.3 mg, containing 12 mol% **4da**, 28 mol% **1E2d** and 9 mol% **2B**, 37% yield, colorless liquid.
Total yield of **9db**: 63% yield.
R_f = 0.45 (EtOAc : hexane = 1 : 5)
^{1}H NMR (400 MHz, $CDCl_3$) δ (ppm) 7.44 (dt, J_1 = 8.9 Hz, J_2 = 2.0 Hz, 2H), 7.28 (dt, J_1 = 8.8 Hz, J_2 = 2.4 Hz, 2H), 7.18~7.22 (m, 4H), 5.28 (s, 1H), 5.04 (d, J = 1.2 Hz, 1H), 3.64 (s, 3H), 3.54 (t, J = 7.8 Hz, 1H), 2.35~2.47 (m, 2H), 2.18 (dddd, J_1 = 14.1 Hz, J_2 = 8.4 Hz, J_3 = 7.6 Hz, J_4 = 6.6 Hz, 1H), 1.86 (dddd, J_1 = 13.8 Hz, J_2 = 8.7 Hz, J_3 = 7.5 Hz, J_4 = 6.4 Hz, 1H).
^{13}C NMR (100.5 MHz, $CDCl_3$) δ (ppm) 173.80, 146.19, 139.46, 137.08, 133.26, 131.46, 129.32, 128.84, 127.72, 121.48, 113.73, 52.14, 50.16, 32.85, 31.72.

Methyl 2,5-bis(4-bromophenyl)hex-5-enoate (9eb)

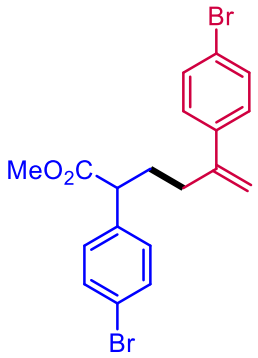

Silica gel chromatography was performed with Et_2O/pentane (0 ~ 5%).
sample 1 : 7.9 mg, 18% yield, white solid.
sample 2 : 23.6 mg, containing 7 mol% **4ea**, 1 mol% **1E1e** and 22 mol% **1E2e**, 45% yield, colorless liquid.

Total yield of **9eb**: 63% yield.

R_f = 0.43 (EtOAc : hexane = 1 : 5)

^{1}H NMR (400 MHz, $CDCl_3$) δ (ppm) 7.44 (dt, J_1 = 8.8 Hz, J_2 = 2.3 Hz, 4H), 7.20 (dt, J_1 = 9.1 Hz, J_2 = 2.2 Hz, 2H), 7.14 (dt, J_1 = 8.9 Hz, J_2 = 2.2 Hz, 2H), 5.28 (d, J = 1.2 Hz, 1H), 5.04 (dt, J_1 = J_2 = 1.2 Hz, 1H), 3.64 (s, 3H), 3.53 (t, J = 7.4 Hz, 1H), 2.35~2.47 (m, 2H), 2.18 (dddd, J_1 = 14.1 Hz, J_2 = 8.4 Hz, J_3 = 7.6 Hz, J_4 = 6.8 Hz, 1H), 1.86 (dddd, J_1 = 13.9 Hz, J_2 = 8.9 Hz, J_3 = 7.6 Hz, J_4 = 6.5 Hz, 1H).

^{13}C NMR (100.5 MHz, $CDCl_3$) δ (ppm) 173.70, 146.21, 139.49, 137.64, 131.80, 131.47, 129.70, 127.73, 121.49, 121.37, 113.73, 52.14, 50.26, 32.87, 31.68.

Methyl 5-(4-bromophenyl)-2-(4-cyanophenyl)hex-5-enoate (9fb)

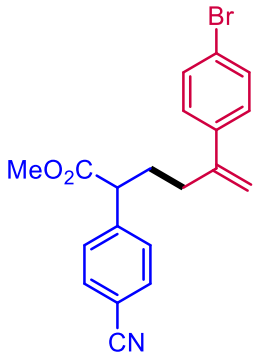

Silica gel chromatography was performed with Et_2O/pentane (3 ~ 33%).

Only one sample was obtained: 11.5 mg, containing 2 mol% **4fa**, 29% yield, colorless liquid.

R_f = 0.24 (EtOAc : hexane = 1 : 5)

^{1}H NMR (400 MHz, $CDCl_3$) δ (ppm) 7.61 (d, J = 8.4 Hz, 2H), 7.44 (dt, J_1 = 8.9 Hz, J_2 = 2.2 Hz, 2H), 7.37 (d, J = 8.4 Hz, 2H), 7.20 (dt, J_1 = 8.9 Hz, J_2 = 2.0 Hz, 2H), 5.29 (s, 1H), 5.04 (s, 1H), 3.66 (s, 3H), 3.63 (t, J = 7.4 Hz, 1H), 2.36~2.49 (m, 2H), 2.22 (dddd, J_1 = 14.4 Hz, J_2 = 8.4 Hz, J_3 = 7.6 Hz, J_4 = 6.8 Hz, 1H), 1.87 (dddd, J_1 = 13.6 Hz, J_2 = 9.1 Hz, J_3 = 7.2 Hz, J_4 = 6.8 Hz, 1H).

^{13}C NMR (100.5 MHz, $CDCl_3$) δ (ppm) 173.03, 145.95, 143.96, 139.31, 132.48, 131.54, 128.85, 127.70, 121.61, 118.58, 113.98, 111.45, 52.34, 50.84, 32.89, 31.67.

Methyl 5-(4-bromophenyl)-2-(4-(tert-butyl)phenyl)hex-5-enoate (9gb)

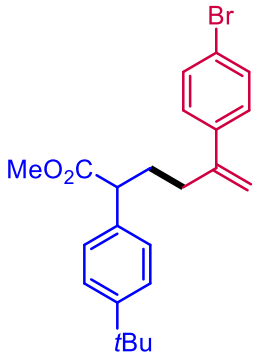

Silica gel chromatography was performed with Et_2O/pentane (0 ~ 5%).
sample 1 : 9.3 mg, 22% yield, colorless liquid.
sample 2 : 10.7 mg, containing 36 mol% **4ga** and 47 mol% **1E2g**, 16% yield, colorless liquid.
Total yield of **9fb**: 38% yield.
R_f = 0.48 (EtOAc : hexane = 1 : 5)
^{1}H NMR (400 MHz, $CDCl_3$) δ (ppm) 7.42 (dt, J_1 = 9.1 Hz, J_2 = 2.2 Hz, 2H), 7.32 (dt, J_1 = 8.5 Hz, J_2 = 2.2 Hz, 2H), 7.21 (dt, J_1 = 8.8 Hz, J_2 = 2.3 Hz, 2H), 7.18 (dt, J_1 = 8.4 Hz, J_2 = 2.0 Hz, 2H), 5.28 (d, J = 1.2 Hz, 1H), 5.06 (dt, J_1 = J_2 = 1.2 Hz, 1H), 3.65 (s, 3H), 3.55 (t, J = 7.6 Hz, 1H), 2.37~2.50 (m, 2H), 2.19 (dddd, J_1 = 13.6 Hz, J_2 = 8.8 Hz, J_3 = 8.4 Hz, J_4 = 6.2 Hz, 1H), 1.87 (dddd, J_1 = 13.6 Hz, J_2 = 9.4 Hz, J_3 = 7.3 Hz, J_4 = 6.3 Hz, 1H), 1.30 (s, 9H).
^{13}C NMR (100.5 MHz, $CDCl_3$) δ (ppm) 174.37, 150.19, 146.48, 139.67, 135.64, 131.40, 127.77, 127.50, 125.58, 121.37, 113.51, 51.96, 50.40, 34.46, 33.04, 31.95, 31.32.

Methyl 5-(4-bromophenyl)-2-(*m*-tolyl)hex-5-enoate (9hb)

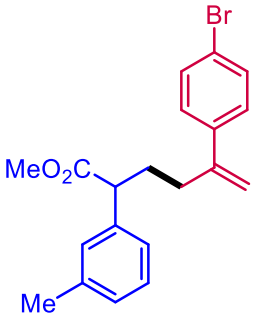

Silica gel chromatography was performed with EA/hexane (0 ~ 1%).
sample 1 : 8.1 mg, containing 1 mol% **4ha**, 21% yield, colorless liquid.
sample 2 : 14.3 mg, containing 26 mol% **4ha**, 30% yield, colorless liquid.
Total yield of **9hb**: 52% yield.
R_f = 0.49 (EtOAc : hexane = 1 : 5)

^{1}H NMR (400 MHz, $CDCl_3$) δ (ppm) 7.43 (dt, J_1 = 9.1 Hz, J_2 = 2.2 Hz, 2H), 7.21 (dt, J_1 = 8.7 Hz, J_2 = 2.0 Hz, 2H), 7.17~7.21 (m, 1H), 7.04~7.08 (m, 3H), 5.28 (d, J = 0.8 Hz, 1H), 5.06 (d, J = 0.8 Hz, 1H), 3.65 (s, 3H), 3.53 (t, J = 7.6 Hz, 1H), 2.35~2.49 (m, 2H), 2.33 (s, 3H), 2.19 (dddd, J_1 = 13.8 Hz, J_2 = 8.9 Hz, J_3 = 7.8 Hz, J_4 = 6.2 Hz, 1H), 1.87 (dddd, J_1 = 13.6 Hz, J_2 = 9.4 Hz, J_3 = 7.4 Hz, J_4 = 6.1 Hz, 1H).
^{13}C NMR (100.5 MHz, $CDCl_3$) δ (ppm) 174.26, 146.44, 139.62, 138.61, 138.35, 131.40, 128.57, 128.55, 128.13, 127.76, 124.96, 121.37, 113.52, 52.02, 50.77, 32.97, 31.85, 21.42.

Methyl 2-(3-bromo-4-fluorophenyl)-5-(4-bromophenyl)hex-5-enoate (9ib)

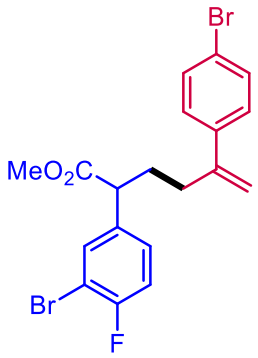

Silica gel chromatography was performed with EA/hexane (0 ~ 2%).
sample 1 : 7.1 mg, 16% yield, white solid.
sample 2 : 28.8 mg, containing 5 mol% **4ia**, 6 mol% **1E1i**, 44 mol% **1E2i** and 3 mol% **2B**, 46% yield, pale yellow solid.
Total yield of **9ib**: 62% yield.
R_f = 0.39 (EtOAc : hexane = 1 : 5)
^{1}H NMR (400 MHz, $CDCl_3$) δ (ppm) 7.45 (dt, J_1 = 8.8 Hz, J_2 = 2.2 Hz, 2H), 7.43~7.46 (m, 1H), 7.21 (dt, J_1 = 8.8 Hz, J_2 = 2.3 Hz, 2H), 7.18 (ddd, J_1 = 8.4 Hz, J_2 = 4.6 Hz, J_3 = 2.3 Hz, 1H), 7.06 (dd, J_1 = J_2 = 8.2 Hz, 1H), 5.29 (d, J = 0.8 Hz, 1H), 5.05 (d, J = 1.2 Hz, 1H), 3.66 (s, 3H), 3.52 (t, J = 7.6 Hz, 1H), 2.35~2.47 (m, 2H), 2.17 (dddd, J_1 = 14.0 Hz, J_2 = 8.0 Hz, J_3 = 7.0 Hz, J_4 = 6.2 Hz, 1H), 1.84 (dddd, J_1 = 13.8 Hz, J_2 = 8.9 Hz, J_3 = 7.6 Hz, J_4 = 6.3 Hz, 1H).
^{19}F NMR (396 MHz, $CDCl_3$) δ (ppm) –109.09 (ddd, J_1 = 9.0 Hz, J_2 = 6.8 Hz, J_3 = 4.9 Hz).
^{13}C NMR (100.5 MHz, $CDCl_3$) δ (ppm) 173.52, 158.38 (d, J = 247.5 Hz), 146.04, 139.36, 135.94 (d, J = 3.9 Hz), 132.93, 131.52, 128.52 (d, J = 7.2 Hz), 127.71, 121.56, 116.56 (d, J = 22.2 Hz), 113.88, 109.19 (d, J = 20.7 Hz), 52.25, 49.72, 32.82, 31.79.

Methyl 2-([1,1'-biphenyl]-4-yl)-5-(4-bromophenyl)hex-5-enoate (9jb)

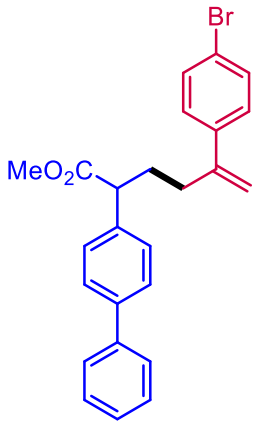

Silica gel chromatography was performed with EA/hexane (0 ~ 2%).

Only one sample was obtained before GPC purification.

18.1 mg, containing 36 mol% **4ja**, 13 mol% **1E1j** and 47 mol% **1E2j**, 25% yield, white solid.

The NMR spectra were obtained after GPC purification.

R_f = 0.45 (EtOAc : hexane = 1 : 5)

^{1}H NMR (400 MHz, $CDCl_3$) δ (ppm) 7.59-7.52 (m, 4H), 7.51-7.41 (m, 4H), 7.37-7.31 (m, 3H), 7.25-7.21 (m, 2H), 5.29 (d, *J* = 1.2 Hz, 1H), 5.07 (d, *J* = 1.2 Hz, 1H), 3.67 (s, 3H), 3.62 (t, *J* = 7.6 Hz, 1H), 2.53-2.40 (m, 2H), 2.30-2.19 (m, 1H), 1.98-1.88 (m, 1H).

^{13}C NMR (100.5 MHz, $CDCl_3$) δ (ppm) 174.2, 146.4, 140.6, 140.3, 139.6, 137.7, 131.4, 128.8, 128.4, 127.8, 127.4, 127.3, 127.0, 121.4, 113.6, 52.1, 50.5, 33.0, 31.9.

Methyl 5-(4-bromophenyl)-2-(4-isobutylphenyl)hex-5-enoate (9kb)

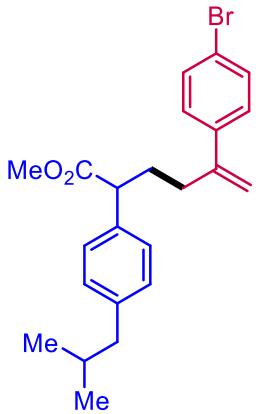

Silica gel chromatography was performed with Et_2O/pentane (0 ~ 3%).

sample 1 : 2.3 mg, 6% yield, white solid.

sample 2 : 23.1 mg, containing 35 mol% **4ka**, 7 mol% **1E1k**, and 95 mol% **1E2k**, 29% yield, white solid.

Total yield of **9kb**: 35% yield.

R_f = 0.49 (EtOAc : hexane = 1 : 5)

^{1}H NMR (400 MHz, $CDCl_3$) δ (ppm) 7.42 (d, *J* = 8.8 Hz, 2H), 7.20 (d, *J* = 8.8 Hz, 2H), 7.15 (d, *J* = 8.0 Hz, 2H), 7.07 (d, *J* = 8.0 Hz, 2H), 5.28 (s, 1H), 5.05 (d, *J* = 1.2 Hz, 1H), 3.65 (s, 3H), 3.54 (t, *J* = 7.6 Hz, 1H), 2.48-2.35 (m, 4H), 2.23-2.13 (m, 1H), 1.92-1.78 (m, 2H), 0.89 (d, *J* = 6.8 Hz, 6H).

^{13}C NMR (100.5 MHz, $CDCl_3$) δ (ppm) 174.4, 146.5, 140.8, 149.7, 135.9, 131.4, 129.4, 127.8, 127.6, 121.4, 113.5, 52.0, 50.5, 45.0, 33.0, 32.0, 30.2, 22.4.

Methyl 2-(3-benzoylphenyl)-5-(4-bromophenyl)hex-5-enoate (9lb)

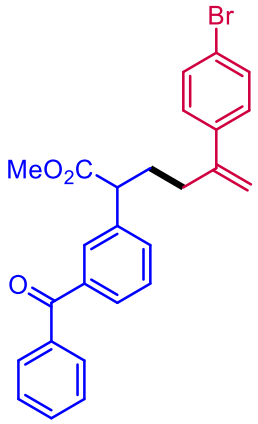

Silica gel chromatography was performed with EA/hexane (2 ~ 7%).

Further purified with silica gel chromatography again instead of GPC, EA/hexane (1 ~ 4%) was used as the eluent.

sample 1 : 14.8 mg, containing 2 mol% **4la**, 20 mol% **1E2l**, and 11 mol% sulfone substrate **2b**, 26% yield, white solid.

sample 2 : 22.6 mg, containing 2 mol% **4la**, 25 mol% **1E2l**, and 59 mol% sulfone substrate **2b**, 30% yield, white solid.

Total yield of **9lb**: 56% yield.

NMR spectra were obtained after GPC purification with sample 1.

R_f = 0.25 (EtOAc : hexane = 1 : 5)

^{1}H NMR (400 MHz, $CDCl_3$) δ (ppm) 7.80-7.76 (m, 2H), 7.71 (dd, $J_1 = J_2$ =1.6 Hz, 1H), 7.68 (ddd, J_1 = 7.6 Hz, $J_2 = J_3$ = 1.6 Hz, 1H), 7.60 (tt, J_1 = 6.8 Hz, J_2 = 1.2 Hz, 1H), 7.52-7.41 (m, 6H), 7.23-7.19 (m, 2H), 5.29 (d, *J* = 1.2 Hz, 1H), 5.06 (d, *J* = 1.2 Hz, 1H), 3.70-3.62 (m, 4H), 2.51- 2.38 (m, 2H), 2.30-2.17 (m, 2H), 1.97-1.87 (m, 2H).

^{13}C NMR (100.5 MHz, $CDCl_3$) δ (ppm) 196.4, 173.1, 146.2, 139.5, 139.0, 138.0, 137.4, 132.6, 131.8, 131.5, 130.1, 129.7, 129.2, 128.6, 128.3, 127.7, 121.5, 113.8, 52.2, 50.7, 33.0, 31.8.

Methyl 5-(4-bromophenyl)-2-(2-fluoro-[1,1'-biphenyl]-4-yl)hex-5-enoate (9mb)

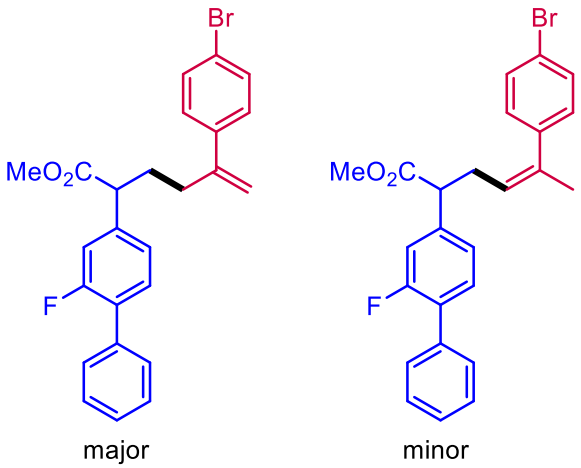

Silica gel chromatography was performed with Et_2O/pentane (0 ~ 33%).

sample 1 : 11.3 mg, containing 2 mol% **4ma** and 35 mol% **3Vma**, 18% yield, colorless liquid.

sample 2 : 11.7 mg, containing 4 mol% **4ma** and 49 mol% **3Vma**, 17% yield, colorless liquid.

Total yield of **9mb**: 35% yield.

R_f = 0.30 (EtOAc : hexane = 1 : 5)

^{1}H NMR (400 MHz, $CDCl_3$) δ (ppm) 7.60- 7.34 (m, 9H), 7.26-7.07 (m, 3H), 5.65 (t, *J* 6.2 Hz, 0.26H), 5.31 (s, 0.74H), 5.09 (s, 0.74H), 3.74-3.66 (m, 0.26x4H + 0.74x3H), 3.61 (t, *J* = 7.6 Hz, 0.74H), 2.98 (ddd, J_1 = 22.0 Hz, J_2 = 14.4 Hz, J_3 = 7.2 Hz, 0.26H), 2.70 (ddd, J_1 = 21.6 Hz, J_2 = 14.4 Hz, J_3 = 7.2 Hz, 0.26H), 2.54-2.41 (m, 0.74x2H), 2.28-2.17 (m, 0.74H), 2.02-1.87 (m, 0.26x3H + 0.74H).

^{19}F NMR (396 MHz, $CDCl_3$) δ (ppm) –117.3 (dd, J_1 = 28.9 Hz, J_2 = 9.1 Hz).

^{13}C NMR (100.5 MHz, $CDCl_3$) δ (ppm) 173.6, 173.5, 160.9, 158.4, 146.2, 142.4, 140.0, 139.93, 139.88, 139.81, 139.5, 136.6, 135.4, 131.5, 13.2, 130.9, 130.8, 128.93, 128.91, 128.4, 128.0, 127.75, 127.72, 127.4, 125.7, 124.6, 124.01, 123.98, 121.5, 120.8, 115.7, 115.5, 113.8, 52.3, 52.2, 50.9, 50.3, 32.9, 32.8, 31.7, 16.0.

Methyl 5-(4-bromophenyl)-2-(4-((2-oxocyclopentyl)methyl)phenyl)hex-5-enoate (9nb)

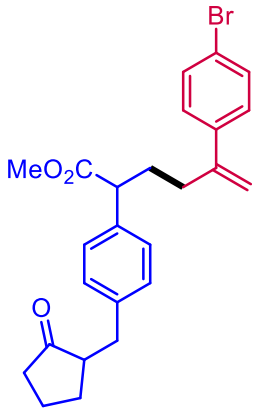

Silica gel chromatography was performed with Et_2O/pentane (3 ~ 20%).
sample 1 : 10.0 mg, containing 4 mol% **4na**, 21% yield, colorless liquid.
sample 2 : 12.5 mg, containing 26 mol% **4na**, 22% yield, white solid.
Total yield of **9nb**: 43% yield.
R_f = 0.18 (EtOAc : hexane = 1 : 5)
^{1}H NMR (400 MHz, $CDCl_3$) δ (ppm) 7.42 (d, *J* = 8.0 Hz, 2H), 7.21 (d, *J* = 8.0 Hz, 2H), 7.16 (d, *J* = 7.6 Hz, 2H), 7.10 (d, *J* = 7.6 Hz, 2H), 5.28 (s, 1H), 5.05 (s, 1H), 3.65 (s, 3H), 3.54 (t, *J* = 7.6 Hz, 1H), 3.12 (dd, J_1 = 15.6 Hz, J_2 = 3.6 Hz, 1H), 2.54~2.28 (m, 5H), 2.24-2.03 (m, 3H), 2.01-1.91(m, 1H), 1.91-1.80 (m, 1H), 1.80-1.66 (m, 1H), 1.60-1.48 (m, 1H).
^{13}C NMR (100.5 MHz, $CDCl_3$) δ (ppm) 220.1, 174.2, 146.4, 139.6, 139.2, 136.5, 131.4, 129.2, 128.0, 127.7, 121.4, 113.6, 52.0, 51.0, 50.5, 38.2, 35.2, 33.0, 31.9, 29.2, 20.5.

Methyl 2-(3-bromophenyl)-5-phenylhex-5-enoate (9aa)

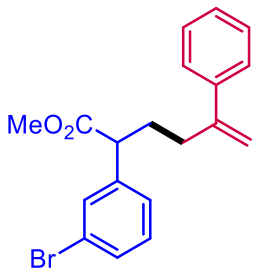

Silica gel chromatography was performed with EtOAc/hexane (0 ~ 3%).
Further purified with silica gel chromatography again instead of GPC using EtOAc/hexane (0 ~ 3%) as the eluent.
sample 1 : 12.5 mg, 35% yield, colorless liquid.
sample 2 : 1.9 mg, containing 7 mol% **4ab**, 5% yield, colorless liquid.
Total yield of **9aa**: 40% yield.
The ^{1}H-NMR spectrum was obtained after further purification with GPC.

R_f = 0.48 (EtOAc : hexane = 1 : 5)

^{1}H NMR (400 MHz, $CDCl_3$) δ (ppm) 7.42 (dd, $J_1 = J_2$ = 1.2 Hz, 1H), 7.39 (ddd, J_1 = 7.1 Hz, $J_2 = J_3$ = 1.9 Hz, 1H), 7.31~7.37 (m, 4H), 7.26~7.30 (m, 1H), 7.16~7.22 (m, 2H), 5.30 (d, J = 1.6 Hz, 1H), 5.04 (d, J = 0.8 Hz, 1H), 3.66 (s, 3H), 3.55 (t, J = 7.8 Hz, 1H), 2.40~2.52 (m, 2H), 2.21 (dddd, J_1 = 14.7 Hz, J_2 = 8.2 Hz, J_3 = 7.7 Hz, J_4 = 6.5 Hz, 1H), 1.89 (dddd, J_1 = 13.9 Hz, J_2 = 8.9 Hz, J_3 = 7.6 Hz, J_4 = 6.4 Hz, 1H).

^{13}C NMR (100.5 MHz, $CDCl_3$) δ (ppm) 173.66, 147.18, 140.98, 140.54, 131.05, 130.48, 130.16, 128.38, 127.54, 126.70, 126.06, 122.66, 113.19, 52.15, 50.49, 32.97, 31.78.

Methyl 2-(3-bromophenyl)-5-(3-methoxyphenyl)hex-5-enoate (9ac)

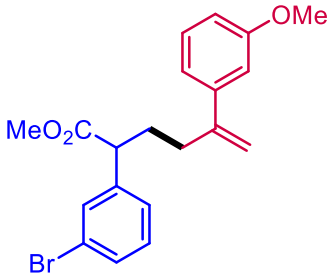

Silica gel chromatography was performed with Et_2O/pentane (0 ~ 25%).

sample 1 : 15.2 mg, containing 1 mol% **4ac**, 39% yield, colorless liquid.

sample 2 : 4.7 mg, containing 9 mol% **4ac**, 11% yield, colorless liquid.

Total yield of **9ac**: 50% yield.

R_f = 0.35 (EtOAc : hexane = 1 : 5)

^{1}H NMR (400 MHz, $CDCl_3$) δ (ppm) 7.42 (dd, $J_1 = J_2$ = 1.6 Hz, 1H), 7.39 (ddd, J_1 = 7.2 Hz, J_2 = 2.0 Hz, J_3 = 1.6 Hz, 1H), 7.15~7.24 (m, 3H), 6.94 (ddd, J_1 = 7.7 Hz, $J_2 = J_3$ = 0.8 Hz, 1H), 6.89 (dd, J_1 = 1.6 Hz, J_2 = 2.4 Hz, 1H), 6.82 (dd, J_1 = 8.2 Hz, J_2 = 2.6 Hz, 1H), 5.30 (d, J = 0.8 Hz, 1H), 5.03 (d, J = 0.8 Hz, 1H), 3.82 (s, 3H), 3.66 (s, 3H), 3.55 (t, J = 7.6 Hz, 1H), 2.38~2.50 (m, 2H), 2.21 (dddd, J_1 = 14.8 Hz, $J_2 = J_3$ = 8.0 Hz, J_4 = 6.8 Hz, 1H), 1.90 (dddd, J_1 = 13.9 Hz, J_2 = 8.8 Hz, J_3 = 7.3 Hz, J_4 = 6.7 Hz, 1H).

^{13}C NMR (100.5 MHz, $CDCl_3$) δ (ppm) 173.64, 159.60, 147.14, 142.16, 141.01, 131.07, 130.48, 130.16, 129.34, 126.70, 122.67, 118.61, 113.37, 112.76, 112.06, 55.22, 52.14, 50.51, 33.09, 31.83.

Methyl 2-(3-bromophenyl)-5-(*m*-tolyl)hex-5-enoate (9ad)

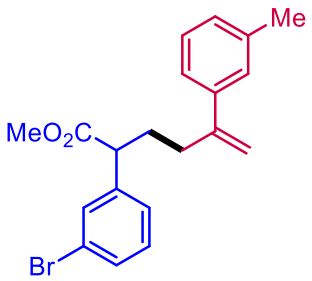

Silica gel chromatography was performed with Et_2O/pentane (0 ~ 7%).

Only one sample was obtained.

12.6 mg, 34% yield, colorless liquid.

R_f = 0.46 (EtOAc : hexane = 1 : 5)

^{1}H NMR (400 MHz, $CDCl_3$) δ (ppm) 7.42 (dd, J_1 = 2.0 Hz, J_2 = 1.6 Hz, 1H), 7.39 (ddd, J_1 = 7.2 Hz, J_2 = J_3 = 1.6 Hz, 1H), 7.18~7.23 (m, 3H), 7.13~7.16 (m, 2H), 7.09 (d, J = 7.2 Hz, 1H), 5.28 (d, J = 1.2 Hz, 1H), 5.01 (d, J = 0.8 Hz, 1H), 3.66 (s, 3H), 3.55 (t, J = 7.8 Hz, 1H), 2.38~2.51 (m, 2H), 2.35 (s, 3H), 2.20 (dddd, J_1 = 14.0 Hz, J_2 = 8.4 Hz, J_3 = 8.0 Hz, J_4 = 7.2 Hz, 1H), 1.90 (dddd, J_1 = 13.8 Hz, J_2 = 9.0 Hz, J_3 = 7.6 Hz, J_4 = 6.3 Hz, 1H).

^{13}C NMR (100.5 MHz, $CDCl_3$) δ (ppm) 173.67, 147.35, 141.03, 140.60, 137.90, 131.10, 130.47, 130.14, 128.30, 128.26, 126.83, 126.73, 123.18, 122.66, 112.99, 52.13, 50.52, 33.03, 31.82, 21.51.

2.10 References

[25] Giri, R.; Maugel, N.; Li, J. J.; Wang, D. H.; Breazzano, S. P.; Saunders, L. B.; Yu, J. Q., *J. AM. CHEM. SOC*. **2007**, *129*, 3510-3511.

[26] Zhu, Y.; Chen, X.; Yuan, C.; Li, G.; Zhang, J.; Zhao, Y., *Nat Commun.*, **2017**, *8*, 14904.

[27] Ghiringhelli, F.; Uttry, A.; Ghosh, K. K.; Gemmeren, M.; *Angew. Chem. Int. Ed*. **2020**, *59*, 23127 –23131.

[28] Zhuang, Z.; Herron, A. N.; Fan, Z.; Yu, J. Q., *J. Am. Chem. Soc*. **2020**, *142*, 6769−6776.

[29] Hu, L.; Meng, G.; Chen, X.; Yoon, J. S.; Shan, J. R.; Chekshin, N.; Strassfeld, D. A.; Sheng, T.; Zhuang, Z.; Jazzar, R.; Bertrand, G.; Houk, K. N.; Yu, J. Q., *J. Am. Chem. Soc*. **2023**, *145*, 16297 – 16304.

[30] Hu, L.; Meng, G.; Yu, J. Q., *J. Am. Chem. Soc*. **2022**, *144*, 20550−20553.

[31] Zhang, S. L.; Xie, H. X.; Zhu, J.; Li, H.; Zhang, X. S.; Li, J.; Wang, W., *Nat. Commun*. **2011**, *2*, 211.

[32] Petronijević, F. R.; Nappi, M.; MacMillan, D. W. C., *J. Am. Chem. Soc*. **2013**, *135*, 18323−18326.

[33] Jeffrey, J. L.; Petronijević, F. R.; MacMillan, D. W. C., *J. Am. Chem. Soc*. **2015**, *137*, 8404−8407.
[34] Treacy, S. M.; Rovis, T., *J. Am. Chem. Soc*. **2021**, *143*, 2729−2735.

Chapter 3
α-Trifluoromethylthiolation of Carboxylic Acids[35]

3.1 Introduction

Fluorine atom has the highest electronegativity, small van der Waals radius and high lipophilicity. Introducing fluorine atom in bioactive compounds has the potential to improve their pharmacokinetic properties.

Among fluorine-containing functional groups, SCF_3 is one of the most attractive. SCF_3 has Hansch parameter of 1.44, bestowing its high lipophilicity. The progress of installing this functional group to the molecules has been highly pursued in past decades. Some molecules have been proven to exhibit great value, such as vanilliprole or cefazaflur.

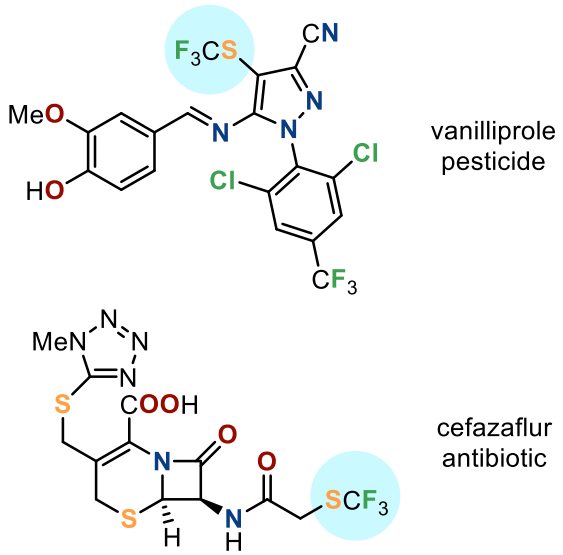

Fig 3.1 SCF_3-containing bioactive molecules

The installation of SCF_3 group at the α-position of ester or amide has been reported[36][37]. However, the direct introduction of SCF_3 group to α-position of carboxylic acid has not been documented but can have great synthetic utility in expanding the chemical space.

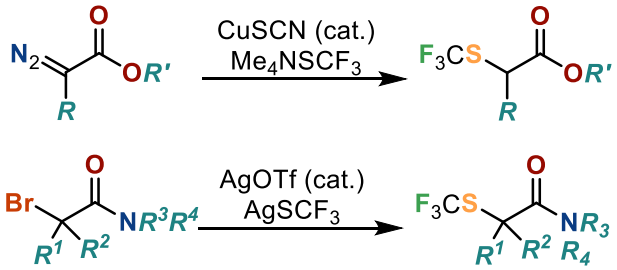

Fig 3.2 Installation of SCF_3 group

3.2 Hypothesis

It was envisioned that enolate generated from carboxylic acid by boron catalysts can be utilized to achieve this functionalization.

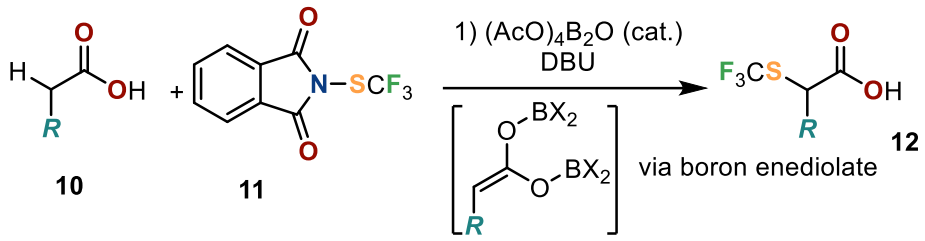

Fig 3.3 Working hypothesis

3.3 Screening

N-(Trifluoromethylthio)phthalimide was chosen to be the electrophilic source of F_3CS^+, which had been showcased in the literature[38].

Solvent screening was performed. It was found that the reaction was promoted by using 10 mol% $B_2O(OAc)_4$ as boron source, 2.4 equivalence of DBU as base, and toluene or THF as solvent. Acetonitrile or DCM was inferior as the solvent.

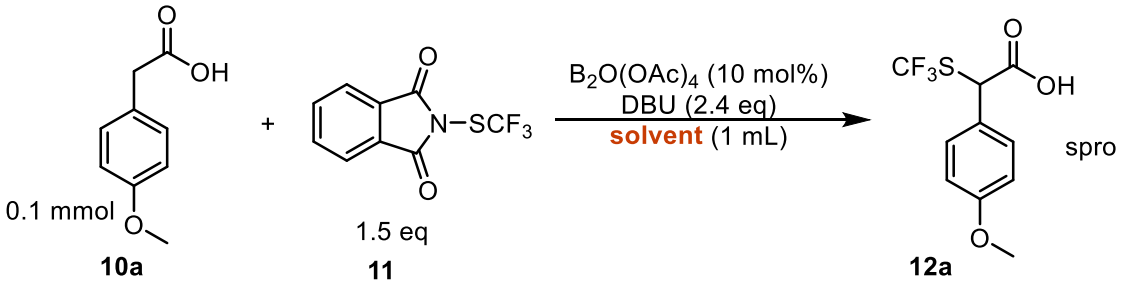

entry	solvent	yield / %
1	toluene	100
2	THF	100
3	MeCN	52.7
4	DCM	83.1

Fig 3.4 Solvent screening

3.4 Scope

α-Aryl carboxylic acids with an electron-donating substituent, such as methoxy (**13a**) or methyl (**13c**) groups, at the para position of the aryl groups were competent substrates, affording the desired products in high yields. However, electron-deficient substituents, such as chloro (**13j**) group, exhibited negative effect on the yields. It should

be noted that the reaction of 2-(4-chlorophenyl)acetic acid (**10j**) produced decarboxylated compound, namely, (4-chlorobenzyl)(trifluoromethyl)sulfane as the major side product. Sterically demanding o-methoxy (**13b**) and o-methyl (**13d**) substituents were well tolerated. In addition, carboxylic acids containing heteroaryl groups, thiophene (**13h**), and benzodioxol (**13g**) also showed high reactivity. The reaction was applicable to a wide variety of bioactive agrochemicals and pharmaceuticals, demonstrating its utility in complex molecule synthesis.

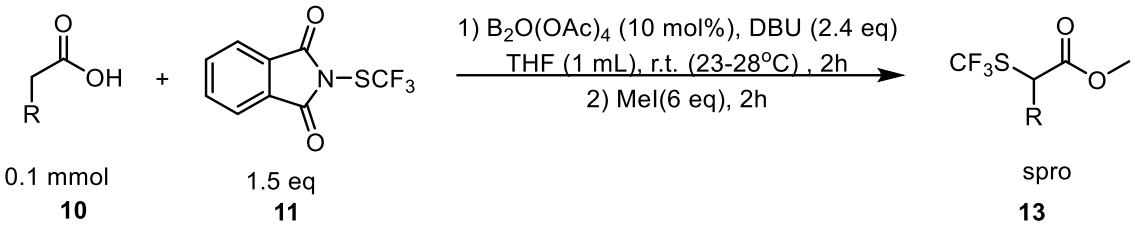

0.1 mmol
10

1.5 eq
11

spro
13

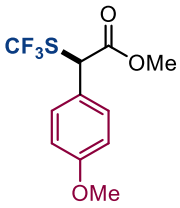

100% (93%)
13a

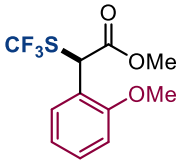

100% (88%)
13b

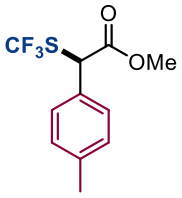

100% (80%)
13c

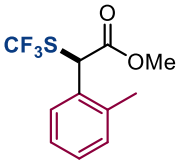

84% (86%)
13d

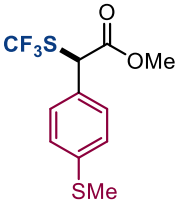

83% (82%)
13e

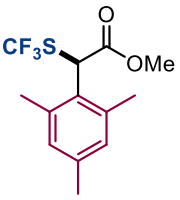

0%
13f

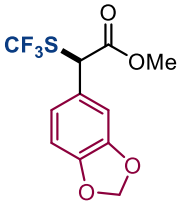

100% (98%)
13g

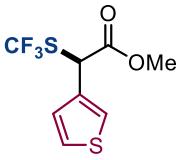

97% (32%)
13h

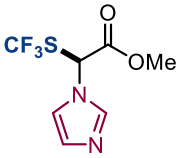

0%
13i

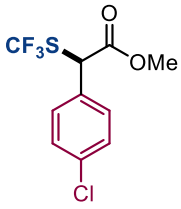

41% (26%)
13j

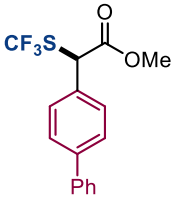

44% (34%)
13k

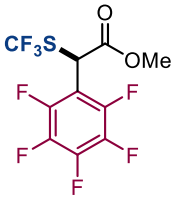

9%
13l

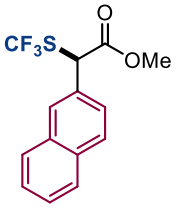

70% (54%)
Naproxen derivative
13m

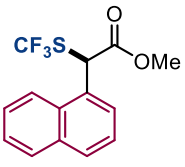

54% (44%)
from NAA
13n

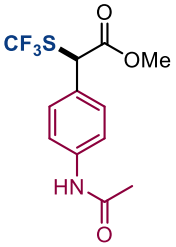

61% (59%)
from Actarit
13o

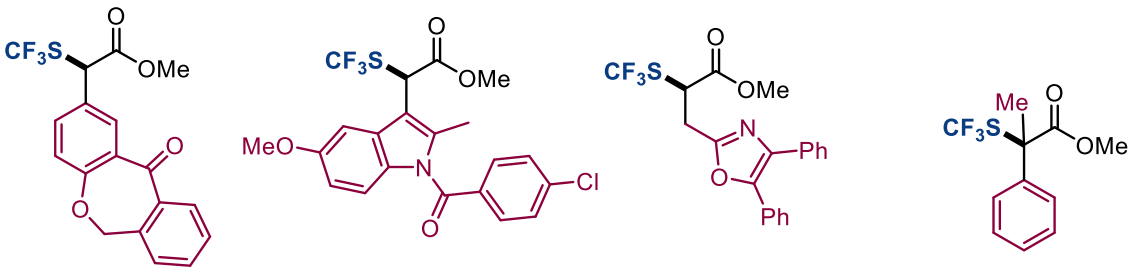

Fig 3.5 scope investigation

number inside the parenthesis is isolated yield, and number outside is NMR yield

3.5 Research with data science

The scope collected conveyed a message that substrates bearing electron-rich aryl group at α-position generally worked well, while others were moderate or incompatible. It was surmised that some descriptors can characterize the relationship between substrate structure and reaction outcome in a reasonable way.

To interrogate this presumption, analysis was conducted using the dataset of the full reaction scope of 29 substrates, including those did not provide good yield. 32 descriptors were obtained from DFT calculation of these carboxylic acids. This includes mainly electronic and energetic properties.

With these descriptors, univariate classification was first tested. This simple yet reliable method has been proved powerful in chemistry application[39][40]. As a result, it was found that 2 descriptors that can divide substrates into "yielding" group and "non-yielding" group with a threshold of 20% yield (Fig 3.6 (a),(b)). One descriptor is NBOC2, which is the NBO charge on α-carbon. Another is C12D, which is the absolute deviation of C1-C2 bond length from 1.508Å. These 2 descriptors were considered to be related to the reactivity as well as the stability of possible enolate intermediate.

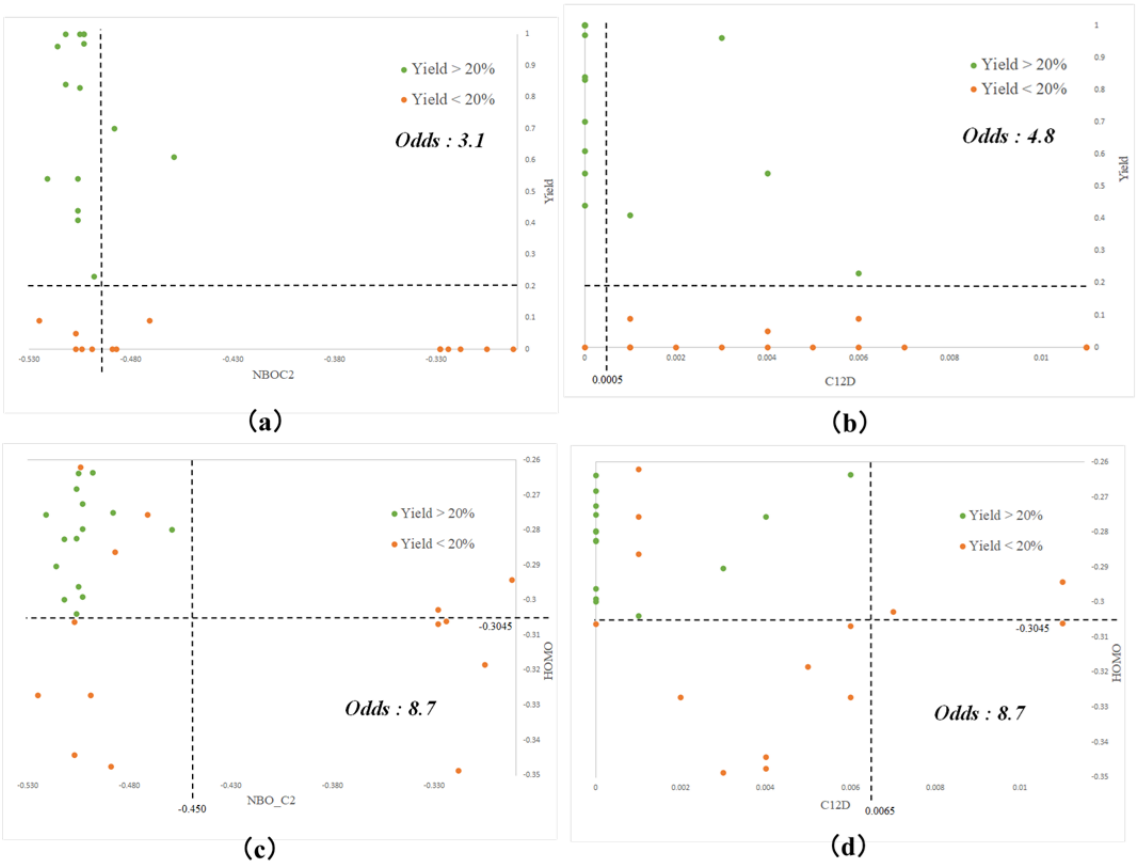

Fig 3.6 Classification models

To obtain a more accurate prediction, bivariate classification was consequently performed. Both classifications provided improved performance with another descriptor, namely HOMO energy, yielding an odds of 8.7 that was good enough for a simple classification (Fig 3.6 (c),(d)). Intriguingly, the substrates that both models failed to correctly classify were the same ones. This suggests a possibility that some unique mechanisms have been involved. These enigmatic factors which cannot be captured by the descriptors haunted the performance of these substrates. **A1** bears an active N-H bond on the aryl ring, which may induce side reactions. **A2** bears the most steric substituent on α-position, which may hinder the generation of an enolate intermediate. **A3** has a quite complicated structure, and its behavior can be difficult to predict accurately with a simple model.

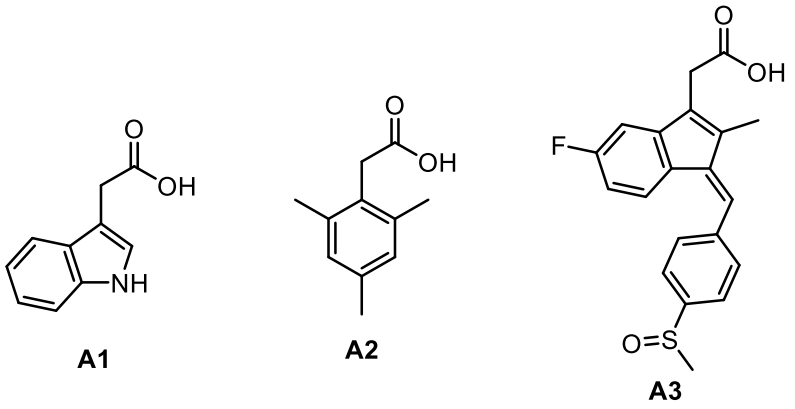

Fig. 3.7 Substrates wrongly classified by the model

In an application point of view, this classification can be used to screen substrates before fully engaging in the experimental works. In other words, before actually synthesizing the substrates, one may utilize this model to predict whether the targeted molecule is likely to work or not.

Logistic regression was further tested with only 2 or 3 descriptors. Logistic regression, as one of the simplest non-linear regression, provides people a convenient tool to comprehend the reaction[40][41]. Some fairly good models were identified, three of which are shown below (Fig 3.8 (a),(b),(c)). An ensemble model was also created with these 3 models by simply taking an average of each prediction. Interestingly, the ensemble model exhibited a better correlation than any of the single model (Fig 3.8 (d)). This delivers an inspiration that it is possible to create a good model by combining several simple models.

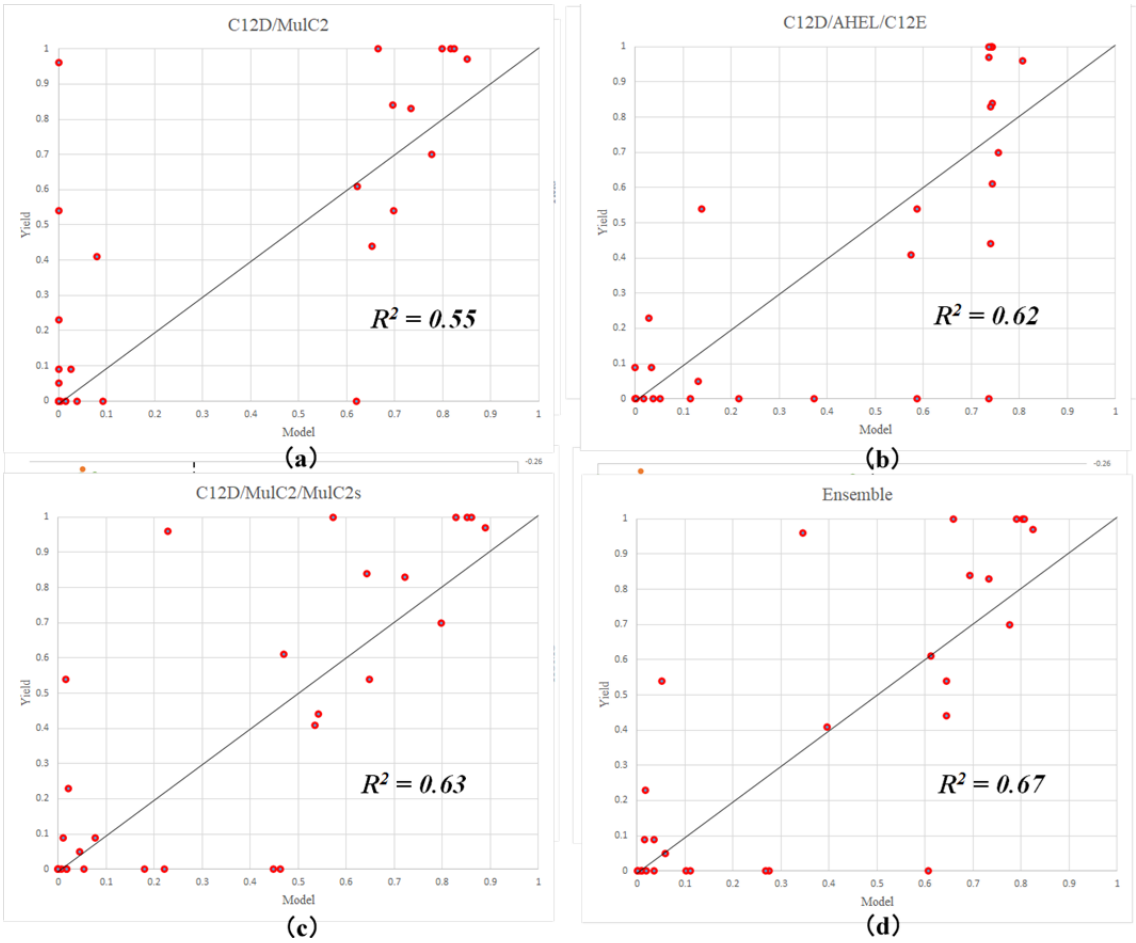

Fig 3.8 Regression models

In the trial with more complicated transformation of descriptors, the best model was found as shown below:

$$\begin{cases} Yield = \dfrac{1}{1+e^{-z}} \\ \mathrm{z} = 7.37656 * \mathrm{MulCC2} - 4364.12 * \mathrm{C12D} + 368.455 * \mathrm{AHEL(c)s} + 3.75559 \end{cases}$$

MulCC2 is the Mulliken charge on α-position, AHEL(c)s is the square of centralized lowest NBO energy of α-H. All these descriptors have a strong relationship to the α-position, which is the reaction site. This discovery transmitted an important enlightenment that the descriptors related to the possible mechanism are promising to be the component of a good model. In an outlook involving a more complicated machine learning approach and exquisite reaction system, such expert knowledge can be useful in choosing the suitable descriptors.

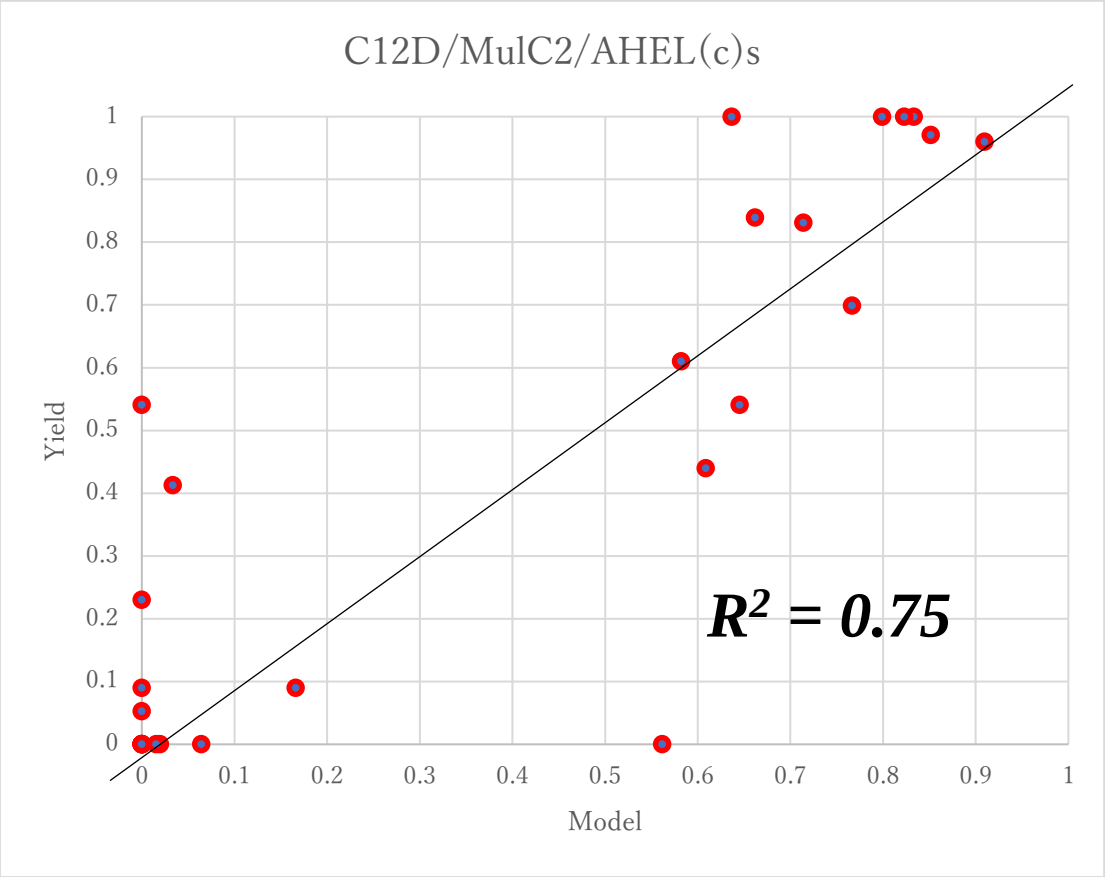

Fig 3.9 The best regression model

3.6 Mechanistic investigation

3.6.1 investigation of possible radical pathway

When TEMPO, the radical scavenger, was added to the reaction, the reaction proceeded normally. Although a small decrease of the yield was observed, this result indicates that the reaction does not go through a radical pathway.

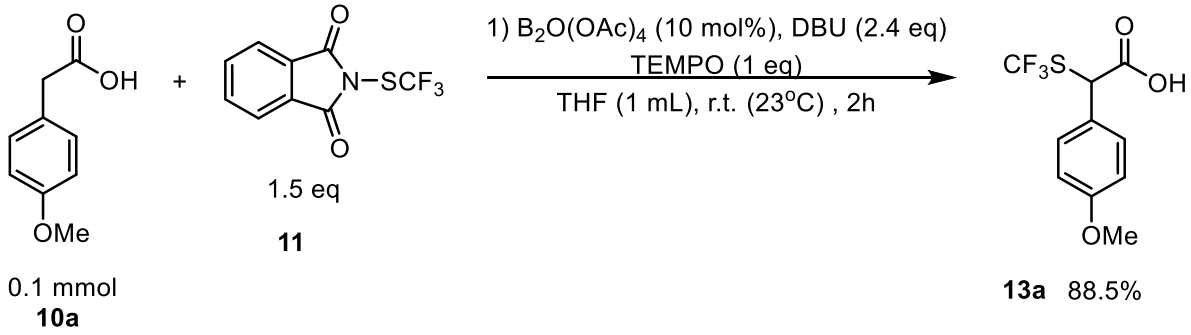

Fig 3.10 TEMPO addition

3.6.2 decarboxylation of the product

Experiments were performed to gain insight into the mechanism of decarboxylation mentioned in the scope section. An α-SCF_3 carboxylic acid was subjected to several reaction conditions. The decarboxylation was observed as long as DBU is present. The decarboxylation most likely occurs from α-SCF_3 carboxylic acids via carboxylate formation, followed by ionic decarboxylation to form the benzylic anion, which would be stabilized by a strongly electron-withdrawing SCF_3 group and electron-deficient aryl group.

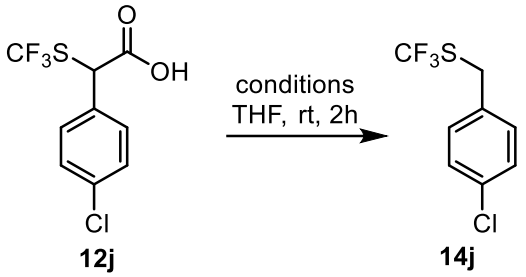

12j **14j**

entry	conditions	yield / %
1	DBU(2.4 eq), $(AcO)_4B_2O$(10 mol%)	30
2	DBU(2.4 eq)	26
3	$(AcO)_4B_2O$(10 mol%)	0

Fig 3.11 Decarboxylation experiments

3.6.3 competing experiment

A competition experiment was performed. As a result, equimolar amount of the products and the side product were obtained from the *para*-chloro substrate, while no decarboxylated product derived from *para*-methoxy substrate was obtained. This outcome suggests that the reaction rate of *para*-chloro substrate is higher, but rapid decarboxylation diminishes the yield.

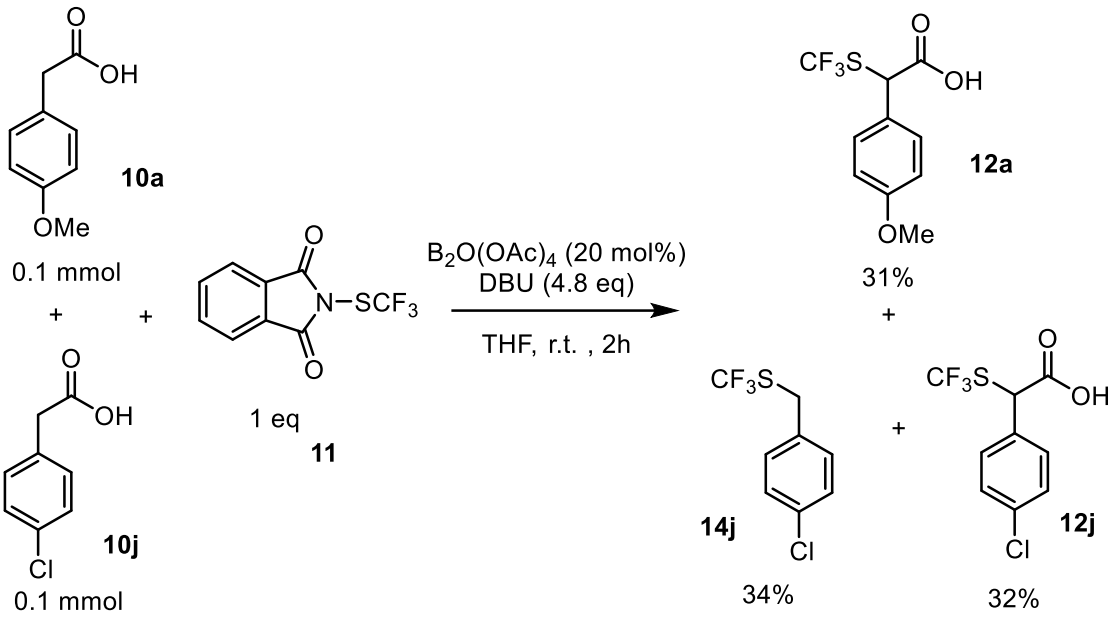

Fig 3.12 Competing experiment

3.7 Summary

A boron-catalyzed direct α-trifluoromethylthiolation of carboxylic acid was developed. Enediolate generated catalytically reacts with an electrophilic SCF_3 reagent, *N*-SCF_3-phtalimide, to furnish the desired product. This method is applicable to bioactive carboxylic acids. Suitable models for substrate classification or yield prediction were built with data science analyses.

3.8 General procedure

Carboxylic acid (0.1 mmol, 1.0 equiv) substrate was added to a 4mL vial and then brought into the glovebox. $B_2O(OAc)_4$ (2.7 mg, 0.1 equiv), THF (1 mL), DBU (35.7 μL, 2.4 equiv) and *N*-(trifluoromethylthio)phthalimide (37.1 mg, 1.5 equiv) were sequentially added. The vial was sealed and removed from the glovebox, and the resulting solution was stirred for 2 h at room temperature (23–28 °C). MeI (37.4 μL, 6 equiv) was consequently added, and the reaction mixture was left stirred for another 2 h. Then the reaction was worked up by adding 2 mL of 2:1:1 solution of brine, water and 4 M HCl, followed by extraction with EtOAc (3 times) in the vial. The combined organic layer was dried with Na_2SO_4 and evaporated on a rotavapor. To this crude product was added tetrabromoethane (11.6 μL, 0.1 mmol) and hexafluorobenzene (34.6 μL, 0.3 mmol) as the NMR standards for the determination of NMR yield.

The residue was then purified by silica gel chromatography on a Biotage Isolera One using a dry-load method.

3.9 Characterization of products

Methyl 2-(4-methoxyphenyl)-2-((trifluoromethyl)thio)acetate (13a)

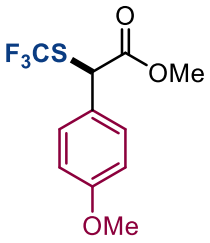

Silica gel chromatography was performed with EtOAc/Hex (0–10%).
26.1 mg, 93% yield, green tea color.
R_f = 0.58 (EtOAc : Hexane = 1 : 2)
^{1}H NMR (400 MHz, $CDCl_3$) δ (ppm) 7.36 (dt, J_1 = 9.5 Hz, J_2 = 2.7 Hz, 2H), 6.89 (dt, J_1 = 9.6 Hz, J_2 = 2.6 Hz, 2H), 5.04 (s, 1H), 3.81 (s, 3H), 3.76 (s, 3H).
^{19}F NMR (396 MHz, $CDCl_3$) δ (ppm) –41.13.
^{13}C NMR (100.5 MHz, $CDCl_3$) δ (ppm) 169.69, 160.11, 129.74 (q, J = 308.2 Hz), 129.44, 125.50, 114.49, 55.30, 53.34, 50.70 (d, J = 1.9 Hz).
HRMS-EI+ (*m/z*): $[M]^+$ calcd for $C_{11}H_{11}F_3O_3S$, 280.0376; found, 280.0384.

Methyl 2-(2-methoxyphenyl)-2-((trifluoromethyl)thio)acetate (13b)

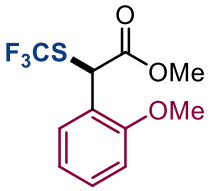

Silica gel chromatography was performed with EtOAc/Hex (0–10%).
24.6 mg, 88% yield, colorless oil.
R_f = 0.35 (EtOAc : Hexane = 1 : 5)
^{1}H NMR (400 MHz, $CDCl_3$) δ (ppm) 7.38 (dd, J_1 = 7.6 Hz, J_2 = 1.2 Hz, 1H), 7.33 (ddd, J_1 = J_2 = 7.9 Hz, J_3 = 1.6 Hz, 1H), 6.97 (ddd, J_1 = J_2 = 7.6 Hz, J_3 = 0.8 Hz, 1H), 6.91 (d, J = 8.4 Hz, 1H), 5.50 (s, 1H), 3.88 (s, 3H), 3.75 (s, 3H).
^{19}F NMR (396 MHz, $CDCl_3$) δ (ppm) –41.40.
^{13}C NMR (100.5 MHz, $CDCl_3$) δ (ppm) 169.79, 156.40, 131.05 (q, J = 307.9 Hz), 130.33, 129.18, 122.95, 120.99, 110.15, 55.78, 53.30, 45.20 (d, J = 1.9 Hz).

HRMS-EI+ (*m/z*): $[M]^+$ calcd for $C_{11}H_{11}F_3O_3S$, 280.0376; found, 280.0382.

Methyl 2-(*p*-tolyl)-2-((trifluoromethyl)thio)acetate (13c)

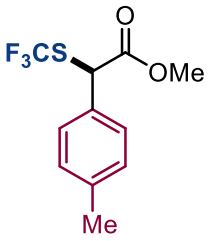

Silica gel chromatography was performed with EtOAc/Hex (0–3%). Crude sample was transferred to the column using wet-load method instead of dry-load (an attempt with dry loading gave only 25.8% yield, presumably due to the volatility of this product).
21.2 mg, containing 9 mol% EtOAc, 80% yield, ivory oil.
R_f = 0.45 (EtOAc : Hexane = 1 : 5)
^{1}H NMR (400 MHz, $CDCl_3$) δ (ppm) 7.33 (d, *J* = 8.0 Hz, 2H), 7.18 (d, *J* = 8.4 Hz, 2H), 5.05 (s, 1H), 3.76 (s, 3H), 2.35 (s, 3H).
^{19}F NMR (396 MHz, $CDCl_3$) δ (ppm) –41.14.
^{13}C NMR (100.5 MHz, $CDCl_3$) δ (ppm) 169.64, 139.17, 130.73, 129.83, 129.77 (q, *J* = 307.9 Hz), 128.01, 53.37, 51.00 (d, *J* = 1.9 Hz), 21.16.
HRMS-EI+ (*m/z*): $[M]^+$ calcd for $C_{11}H_{11}F_3O_2S$, 264.0426; found, 264.0425.

Methyl 2-(*o*-tolyl)-2-((trifluoromethyl)thio)acetate (13d)

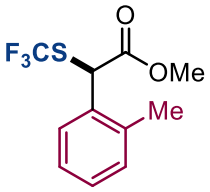

Silica gel chromatography was performed with EtOAc/Hex (0–5%).
24.3 mg, containing 20 mol% CH_2Cl_2 (determined by NMR), calculated to be 86% yield, colorless oil. NMR spectra was obtained after further purification by GPC (EtOAc)
R_f = 0.43 (EtOAc : Hexane = 1 : 5)
^{1}H NMR (400 MHz, $CDCl_3$) δ (ppm) 7.42-7.44 (m, 1H), 7.17-7.27 (m, 3H), 5.32 (s, 1H), 3.77 (s, 3H), 2.46 (s, 3H).
^{19}F NMR (396 MHz, $CDCl_3$) δ (ppm) –41.51.
^{13}C NMR (100.5 MHz, $CDCl_3$) δ (ppm) 169.78, 136.24, 131.86, 131.07, 129.85 (q, *J* = 308.2 Hz), 129.05, 127.83, 126.92, 53.41, 47.52 (d, *J* = 1.9 Hz), 19.27.

HRMS-EI+ (*m/z*): $[M]^+$ calcd for $C_{11}H_{11}F_3O_2S$, 264.0426; found, 264.0426.

Methyl 2-(4-(methylthio)phenyl)-2-((trifluoromethyl)thio)acetate (13e)

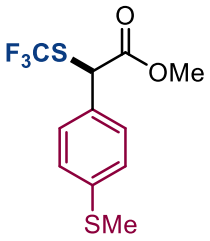

Silica gel chromatography was performed with EtOAc/Hex (0–5%).
24.2 mg, 82% yield, colorless oil.
R_f = 0.38 (EtOAc : Hexane = 1 : 5)
^{1}H NMR (400 MHz, $CDCl_3$) δ (ppm) 7.35 (dt, J_1 = 8.7 Hz, J_2 = 2.1 Hz, 2H), 7.22 (dt, J_1 = 8.8 Hz, J_2 = 2.1 Hz, 2H), 5.03 (s, 1H), 3.76 (s, 3H), 2.48 (s, 3H).
^{19}F NMR (396 MHz, $CDCl_3$) δ (ppm) –41.01.
^{13}C NMR (100.5 MHz, $CDCl_3$) δ (ppm) 169.37, 140.28, 130.14, 129.71 (q, J = 307.9 Hz), 128.52, 126.50, 53.44, 50.88 (d, J = 1.9 Hz), 15.29.
HRMS-EI+ (*m/z*): $[M]^+$ calcd for $C_{11}H_{11}F_3O_2S_2$, 296.0147; found, 296.0147.

Methyl 2-(benzo[d][1,3]dioxol-5-yl)-2-((trifluoromethyl)thio)acetate (13g)

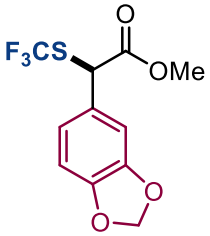

Reaction worked up with saturated NH_4Cl aqueous solution instead of mixture solution.
Silica gel chromatography was performed with EtOAc/Hex (0–5%).
28.8 mg, 98% yield, white solid.
R_f = 0.38 (EtOAc : Hexane = 1 : 5)
^{1}H NMR (400 MHz, $CDCl_3$) δ (ppm) 6.94 (d, J = 2.0 Hz, 1H), 6.89 (dd, J_1 = 8.2 Hz, J_2 = 1.8 Hz, 1H), 6.77 (d, J = 8.4 Hz, 1H), 5.98 (m, 2H), 4.99 (s, 1H), 3.77 (s, 3H).
^{19}F NMR (396 MHz, $CDCl_3$) δ (ppm) –41.08.
^{13}C NMR (100.5 MHz, $CDCl_3$) δ (ppm) 169.45, 148.35, 148.26, 129.79 (q, J = 307.9 Hz), 127.21, 122.14, 108.59, 108.30, 101.53, 53.42, 51.13 (d, J = 2.0 Hz).
HRMS-EI+ (*m/z*): $[M]^+$ calcd for $C_{11}H_9F_3O_4S$, 294.0168; found, 294.0168.

Methyl 2-(thiophen-3-yl)-2-((trifluoromethyl)thio)acetate (13h)

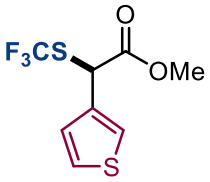

Silica gel chromatography was performed with EtOAc/Hex (0–3%).

8.1 mg, 32% yield, pale yellow oil. It is surmised that this product is volatile.

R_f = 0.44 (EtOAc : Hexane = 1 : 5)

^{1}H NMR (400 MHz, $CDCl_3$) δ (ppm) 7.40 (dd, J_1 = 2.8 Hz, J_2 = 1.6 Hz, 1H), 7.35 (dd, J_1 = 5.2 Hz, J_2 = 2.8 Hz, 1H), 6.77 (dd, J_1 = 5.4 Hz, J_2 = 1.4 Hz, 1H), 5.20 (s, 1H), 3.80 (s, 3H).

^{19}F NMR (396 MHz, $CDCl_3$) δ (ppm) –41.27.

^{13}C NMR (100.5 MHz, $CDCl_3$) δ (ppm) 169.34, 132.95, 129.65 (q, J = 308.1 Hz), 127.12, 126.87, 124.86, 53.44, 46.20 (d, J = 2.9 Hz).

HRMS-EI+ (*m/z*): $[M]^+$ calcd for $C_8H_7F_3O_2S_2$, 255.9834; found, 255.9839.

Methyl 2-(4-chlorophenyl)-2-((trifluoromethyl)thio)acetate (13j)

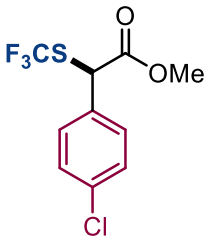

Silica gel chromatography was performed with EtOAc/Hex (0–2%).

7.5 mg, 26% yield, yellow oil.

R_f = 0.40 (EtOAc : Hexane = 1 : 5)

^{1}H NMR (400 MHz, $CDCl_3$) δ (ppm) 7.37 (dt, J_1 = J_2 = 7.9 Hz, 4H), 5.04 (s, 1H), 3.78 (s, 3H).

^{19}F NMR (396 MHz, $CDCl_3$) δ (ppm) –40.94.

^{13}C NMR (100.5 MHz, $CDCl_3$) δ (ppm) 169.04, 135.22, 132.56, 129.61 (q, J = 308.1 Hz), 129.52, 129.35, 53.58, 50.67.

HRMS-EI+ (*m/z*): $[M]^+$ calcd for $C_{10}H_8ClF_3O_2S$, 283.9880; found, 283.9887.

Methyl 2-([1,1'-biphenyl]-4-yl)-2-((trifluoromethyl)thio)acetate (13k)

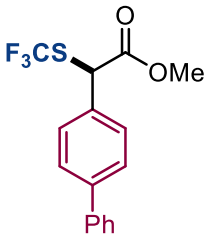

Silica gel chromatography was performed with EtOAc/Hex (0–5%).
11.2 mg, 34% yield, white solid. NMR spectra was obtained after further purification by GPC (EtOAc)
R_f = 0.48 (EtOAc : Hexane = 1 : 5)
^{1}H NMR (400 MHz, $CDCl_3$) δ (ppm) 7.56-7.62 (m, 4H), 7.52 (dt, J_1 = 8.1 Hz, J_2 = 2.0 Hz, 2H), 7.45 (tt, J_1 = 7.4 Hz, J_2 = 1.7 Hz, 2H), 7.37 (tt, J_1 = 7.2 Hz, J_2 = 1.7 Hz, 1H), 5.11 (s, 1H), 3.80 (s, 3H).
^{19}F NMR (396 MHz, $CDCl_3$) δ (ppm) –41.02.
^{13}C NMR (100.5 MHz, $CDCl_3$) δ (ppm) 169.47, 142.09, 140.06, 132.68, 129.75 (q, J = 307.2 Hz), 128.86, 128.58, 127.85, 127.74, 127.11, 53.50, 50.98 (d, J = 1.9 Hz).
HRMS-EI+ (*m/z*): $[M]^+$ calcd for $C_{16}H_{13}F_3O_2S$, 326.0583; found, 326.0579.

Methyl 2-(naphthalen-2-yl)-2-((trifluoromethyl)thio)acetate (13m)

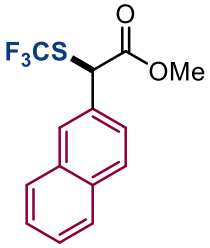

Silica gel chromatography was performed with EtOAc/Hex (0–5%).
16.1 mg, 54% yield, white solid.
R_f = 0.66 (EtOAc : Hexane = 1 : 2)
^{1}H NMR (400 MHz, $CDCl_3$) δ (ppm) 7.91 (d, J = 1.2 Hz, 1H), 7.87 (d, J = 8.8 Hz, 1H), 7.82-7.87 (m, 2H), 7.50-7.56 (m, 3H), 5.25 (s, 1H), 3.78 (s, 3H).
^{19}F NMR (396 MHz, $CDCl_3$) δ (ppm) –40.95.
^{13}C NMR (100.5 MHz, $CDCl_3$) δ (ppm) 169.46, 133.29, 133.12, 131.13, 129.76 (q, J = 308.2 Hz), 129.21, 128.10, 127.74, 126.96, 126.77, 125.12, 53.50, 51.58 (d, J = 1.9 Hz).
HRMS-EI+ (*m/z*): $[M]^+$ calcd for $C_{14}H_{11}F_3O_2S$, 300.0426; found, 300.0429.

Methyl 2-(naphthalen-1-yl)-2-((trifluoromethyl)thio)acetate (13n)

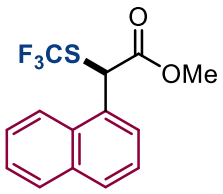

Silica gel chromatography was performed twice. EtOAc/Hex (0–5%) was used in the first time. Biotage Sfär Silica HC D - High Capacity Duo 20 µm (25 g) column and EtOAc/Hex (0–3%) was used in the second time.

13.2 mg, 44% yield, colorless oil.

R_f = 0.4 (EtOAc : Hexane = 1 : 5)

^{1}H NMR (400 MHz, $CDCl_3$) δ (ppm) 8.10 (d, J = 8.4 Hz, 1H), 7.91 (dd, J_1 = 7.8 Hz, J_2 = 1.2 Hz, 1H), 7.88 (d, J = 8.4 Hz, 1H), 7.66 (dd, J_1 = 7.2 Hz, J_2 = 1.6 Hz, 1H), 7.63 (ddd, J_1 = 8.8 Hz, J_2 = 8.4 Hz, J_3 = 1.6 Hz, 1H), 7.56 (ddd, J_1 = 8.1 Hz, J_2 = 6.9 Hz, J_3 = 1.1 Hz, 1H), 7.47 (dd, J_1 = 8.0 Hz, J_2 = 7.2 Hz, 1H), 5.84 (s, 1H), 3.77 (s, 3H).

^{19}F NMR (396 MHz, $CDCl_3$) δ (ppm) –41.49.

^{13}C NMR (100.5 MHz, $CDCl_3$) δ (ppm) 169.89, 134.07, 130.36, 130.05, 129.87 (q, J = 308.1 Hz), 129.24, 127.26, 127.00, 126.31, 125.37, 122.57, 53.57, 47.87.

HRMS-EI+ (*m/z*): $[M]^+$ calcd for $C_{14}H_{11}F_3O_2S$, 300.0426; found, 300.0432.

Methyl 2-(4-acetamidophenyl)-2-((trifluoromethyl)thio)acetate (13o)

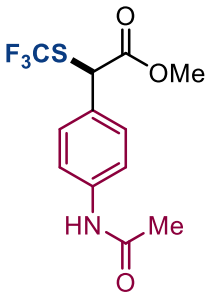

Silica gel chromatography was performed with EtOAc/Hex (20–40%).

18.2 mg, 59% yield, pink rose color solid.

R_f = 0.14 (EtOAc : Hexane = 1 : 1)

^{1}H NMR (400 MHz, $CDCl_3$) δ (ppm) 7.52 (d, J = 8.4 Hz, 2H), 7.49 (brs, 1H), 7.38 (d, J = 8.8 Hz, 2H), 5.04 (s, 1H), 3.76 (s, 3H), 2.17 (s, 3H).

^{19}F NMR (396 MHz, $CDCl_3$) δ (ppm) –41.03.

^{13}C NMR (100.5 MHz, $CDCl_3$) δ (ppm) 169.43, 168,51, 138.64, 129.79 (q, J = 308.2 Hz), 129.31, 128.91, 120.21, 53.45, 50.79 (d, J = 1.9 Hz), 24.58.

HRMS-EI+ (*m/z*): $[M]^+$ calcd for $C_{12}H_{12}F_3NO_3S$, 307.0484; found, 307.0489.

Methyl 2-(11-oxo-6,11-dihydrodibenzo[b,e]oxepin-2-yl)-2-((trifluoromethyl)thio)acetate (13p)

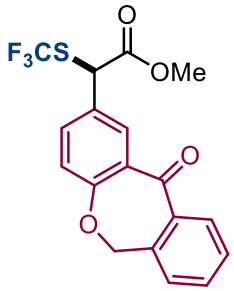

Silica gel chromatography was performed with EtOAc/Hex (0–10%).
35.6 mg, containing 19 mol% *N*-methyl phthalimide and 12.5 mol% CH_2Cl_2 (determined by NMR), calculated to be 84% yield, colorless oil.
NMR spectra was obtained after further purification by GPC (EtOAc), 19.1 mg recovered, white solid.
R_f = 0.18 (EtOAc : Hexane = 1 : 5)
^{1}H NMR (400 MHz, $CDCl_3$) δ (ppm) 8.27 (d, J = 2.8 Hz, 1H), 7.89 (dd, J_1 = 7.8 Hz, J_2 = 1.4 Hz, 1H), 7.61 (dd, J_1 = 8.8 Hz, J_2 = 2.4 Hz, 1H), 7.58 (ddd, J_1 = J_2 = 7.4 Hz, J_3 = 1.4 Hz, 1H), 7.49 (ddd, J_1 = J_2 = 7.5 Hz, J_3 = 1.1 Hz, 1H), 7.37 (dd, J_1 = 7.4 Hz, J_2 = 1.0 Hz, 1H), 7.09 (d, J = 8.8 Hz, 1H), 5.21 (s, 2H), 5.12 (s, 1H), 3.78 (s, 3H).
^{19}F NMR (396 MHz, $CDCl_3$) δ (ppm) –40.87.
^{13}C NMR (100.5 MHz, $CDCl_3$) δ (ppm) 190.34, 169.19, 161.61, 140.26, 135.10, 134.48, 133.00, 132.02, 129.66 (q, J = 308.2 Hz), 129.50, 129.43, 127.91, 127.71, 125.24, 122.02, 73.56, 53.51, 50.52 (d, J = 1.9 Hz).
HRMS-EI+ (*m/z*): $[M]^+$ calcd for $C_{18}H_{13}F_3O_4S$, 382.0481; found, 382.0475.

Methyl 2-(1-(4-chlorobenzoyl)-5-methoxy-2-methyl-1H-indol-3-yl)-2-((trifluoromethyl)thio)acetate (13q)

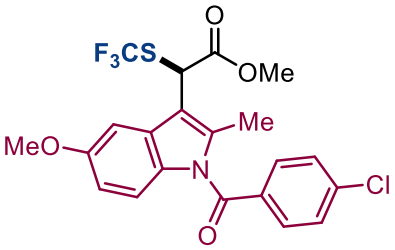

Silica gel chromatography was performed with EtOAc/Hex (0–10%).
25.3 mg, containing 10.2 mol% *N*-methyl phthalimide (determined by NMR), calculated

to be 52% yield, yellow oil.

NMR spectra was obtained after further purification by GPC (EtOAc), 16.8 mg recovered, pale yellow oil.

R_f = 0.26 (EtOAc : Hexane = 1 : 5)

^{1}H NMR (400 MHz, $CDCl_3$) δ (ppm) 7.66 (dd, J_1 = 8.8 Hz, J_2 = 2.4 Hz, 2H), 7.48 (d, J = 8.8 Hz, 2H), 7.14 (d, J = 2.8 Hz, 1H), 6.83 (d, J = 8.8 Hz, 1H), 6.70 (dd, J_1 = 9.2 Hz, J_2 = 2.8 Hz, 1H), 5.44 (s, 1H), 3.84 (s, 3H), 3.77 (s, 3H), 2.45(s, 3H).

^{19}F NMR (396 MHz, $CDCl_3$) δ (ppm) –40.71.

^{13}C NMR (100.5 MHz, $CDCl_3$) δ (ppm) 168.67, 168.26, 155.91, 139.93, 136.78, 133.18, 131.36, 130.90, 130.15 (q, J = 305.7 Hz), 129.28, 127.74, 114.88, 112.37, 112.02, 102.05, 55.67, 53.59, 44.23 (d, J = 1.9 Hz), 13.00.

HRMS-EI+ (*m/z*): $[M]^+$ calcd for $C_{21}H_{17}ClF_3NO_4S$, 471.0513; found, 471.0508.

Methyl 3-(4,5-diphenyloxazol-2-yl)-2-((trifluoromethyl)thio)propanoate (13r)

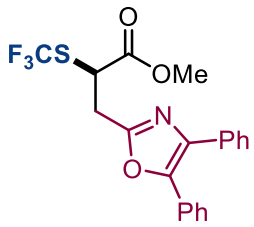

Silica gel chromatography was performed with EtOAc/Hex (0–10%). The sample was further purified by GPC (EtOAc).

6.1 mg, 15% yield, white solid.

R_f = 0.24 (EtOAc : Hexane = 1 : 5)

^{1}H NMR (400 MHz, $CDCl_3$) δ (ppm) 7.60-7.63 (m, 2H), 7.55-7.58 (m, 2H), 7.30-7.39 (m, 6H), 4.42 (dd, J_1 = 8.4 Hz, J_2 = 6.4 Hz, 1H), 3.83 (s, 3H), 3.60 (dd, J_1 = 16.0 Hz, J_2 = 8.4 Hz, 1H), 3.44 (dd, J_1 = 16.2 Hz, J_2 = 6.2 Hz, 1H).

^{19}F NMR (396 MHz, $CDCl_3$) δ (ppm) –40.12.

^{13}C NMR (100.5 MHz, $CDCl_3$) δ (ppm) 169.85, 158.38, 146.02, 135.24, 132.03, 129.87 (q, J = 307.7 Hz), 128.73, 128.69, 128.60, 128.56, 128.20, 127.79, 126.56, 53.39, 43.29, 31.32.

HRMS-EI+ (*m/z*): $[M]^+$ calcd for $C_{20}H_{16}F_3NO_3S$, 407.0798; found, 407.0796.

Synthesis of carboxylic acid **12j**

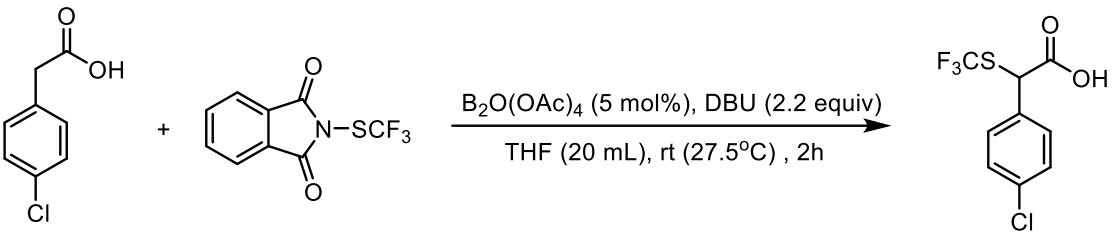

2-(4-Chlorophenyl)acetic acid (2.0 mmol, 1 equiv) substrate was added to a 50 mL flask and then brought into the glovebox. $B_2O(OAc)_4$ (27.4 mg, 0.05 equiv), THF (20 mL), DBU (656.7 µL, 2.2 equiv) and *N*-(trifluoromethylthio)phthalimide (271.9 mg, 1.1 equiv) were sequentially added. The resulting solution was removed from the glove box and stirred for 1 h at room temperature (27.5 °C). The resulting reaction mixture was worked up by adding 10 mL of 2:1:1 solution of brine, water and 4M HCl and then 20mL of saturated NH_4Cl aqueous solution, followed by extraction with EtOAc (3 times). The organic layer was dried over Na_2SO_4 and evaporated on a rotavapor. Crude NMR was then measured, which showed remaining starting material.

The crude product was then purified by silica gel chromatography on a Biotage Isolera One using dry-load method and eluted with first EtOAc/Hex (0–50%) then with MeOH/DCM (0–20%). Further purification was conducted by GPC (EtOAc).

Finally, 46.4 mg product was obtained as white crystal, 9% yield.

2-(4-Chlorophenyl)-2-((trifluoromethyl)thio)acetic acid (12j)

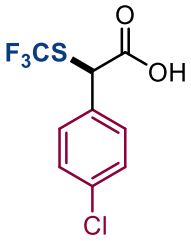

R_f = 0.05 (EtOAc : Hexane = 1 : 2), 0.23 (MeOH : DCM = 1 : 5)

^{1}H NMR (400 MHz, $CDCl_3$) δ (ppm) 11.50 (brs, 1H), 7.38 (dt, $J_1 = J_2$ = 7.6 Hz, 4H), 5.04 (s, 1H).

^{19}F NMR (396 MHz, $CDCl_3$) δ (ppm) –40.86.

^{13}C NMR (100.5 MHz, $CDCl_3$) δ (ppm) 174.76, 135.62, 131.68, 129.57, 129.50, 129.42 (q, J = 308.2 Hz), 50.49.

unsuccessful substrates

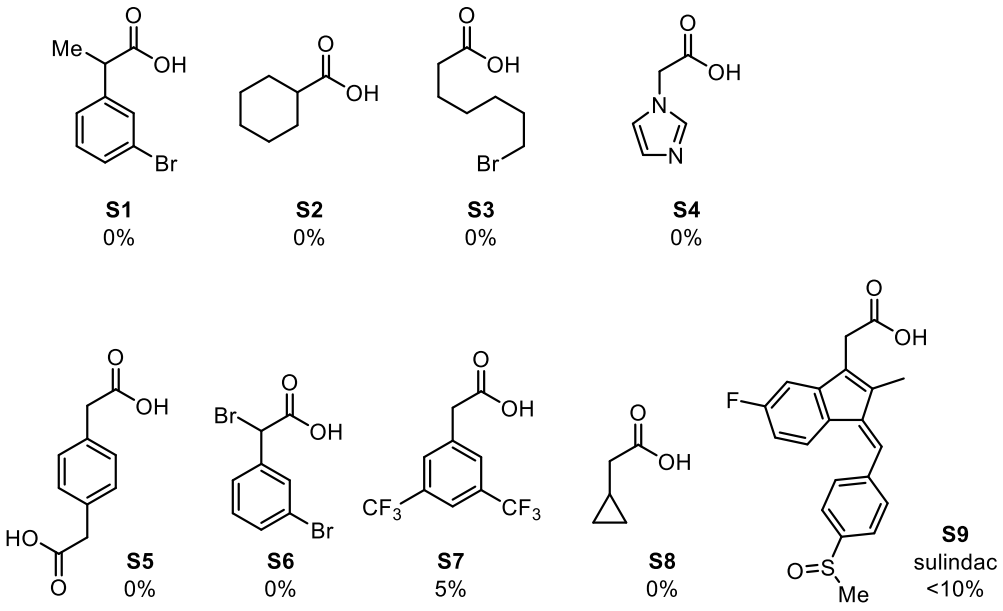

Fig 3.13 Unsuccessful substrates

3.10 Descriptors and mathematical modelling

Descriptor Name	**Description**
NBOC1	NBO charge on C1 (C of carboxy group)
NBOC2	NBO charge on C2 (α-C of carboxy group)
NBO=O	NBO charge on carbonyl O of carboxy group
NBO-O	NBO charge on hydroxy O of carboxy group
vC=O	IR wave number of C=O bond of carboxy group
IC=O	IR vibrational intensity of C=O bond of carboxy group
C12Len	C1-C2 bond length
MulCC2	Mulliken charge on C2
APTC2	APT charge on C2
NBOHH	highest NBO charge on α-H
NBOHL	lowest NBO charge on α-H
MulHH	highest Mulliken charge on α-H
MulHL	lowest Mulliken charge on α-H
APTHH	highest APT charge on α-H
APTHL	lowest APT charge on α-H
E	E (RM062X)
Dip	dipole moment
Pol	Polarizability (α)

Et	E (Thermal)
CV	Heat Capacity (Cv)
S	Entropy (S)
HOMO	HOMO energy
LUMO	LUMO energy
C12Occ	C1-C2 σ-bond NBO electron occupation
C12E	C1-C2 σ-bond NBO energy
AHOccH	highest NBO electron occupation of αH-αC σ-bond
AHOccL	lowest NBO electron occupation of αH-αC σ-bond
AHEH	highest NBO energy of αH-αC σ-bond
AHEL	lowest NBO energy of αH-αC σ-bond
C12D	C1-C2 bond length deviation from 1.508 Å
HLG	HOMO-LUMO energy gap
AHEa	average of NBO energy of αH-αC σ-bond

The program used for logistic regression can be found here:
https://github.com/DWs-code-drink/SCF3_Logistic

3.11 DFT calculation of substrates

All density functional theory (DFT) calculations were carried out in Gaussian 16 program at the M062x levels of theory with the aug-cc-pvtz basis set. The descriptors were obtained from the optimized geometry optimizations of each molecule (listed below).

2-(4-Methoxyphenyl)acetic acid (10a)

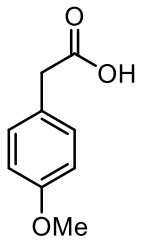

1 6 0 0.072514 1.376527 -0.404206
2 6 0 -1.262855 1.437977 -0.061050
3 6 0 -2.017511 0.268588 0.021794
4 6 0 -1.417637 -0.957655 -0.242333
5 6 0 -0.071517 -0.999966 -0.587585
6 6 0 0.687520 0.156023 -0.678245
7 6 0 2.157682 0.081637 -1.022470
8 6 0 2.947682 -0.257463 0.216235
9 8 0 3.179648 0.828898 0.977408
10 8 0 3.307636 -1.356982 0.531512
11 8 0 -3.321406 0.424461 0.363018
12 6 0 -4.115724 -0.736759 0.461608
13 1 0 0.651567 2.289724 -0.459654
14 1 0 -1.747867 2.381044 0.148216
15 1 0 -1.978569 -1.877842 -0.184616
16 1 0 0.393237 -1.958066 -0.785173
17 1 0 2.344047 -0.703624 -1.750797
18 1 0 2.502207 1.035482 -1.417280
19 1 0 3.633423 0.528785 1.776515
20 1 0 -5.109465 -0.402786 0.743660
21 1 0 -4.166882 -1.262156 -0.494835
22 1 0 -3.729655 -1.415031 1.225974

2-(2-Methoxyphenyl)acetic acid (10b)

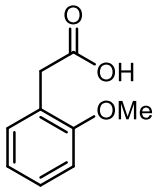

1 6 0 0.058582 -1.840841 0.337261
2 6 0 1.226339 -2.406703 -0.158337
3 6 0 2.288488 -1.582482 -0.483911
4 6 0 2.192342 -0.205813 -0.319701
5 6 0 1.017784 0.352349 0.173630
6 6 0 -0.063325 -0.471647 0.511250
7 6 0 -1.354049 0.117973 1.029332
8 6 0 -2.379834 0.147117 -0.075429
9 8 0 -2.138238 1.125245 -0.967344
10 8 0 -3.297351 -0.617558 -0.189424
11 8 0 0.840191 1.684211 0.365258
12 6 0 1.895234 2.549848 0.010672
13 1 0 -0.785052 -2.470664 0.592851

14 1 0	1.301407	-3.476962	-0.285960
15 1 0	3.206594	-2.004050	-0.869814
16 1 0	3.032546	0.419849	-0.578947
17 1 0	-1.759005	-0.501378	1.825180
18 1 0	-1.188333	1.129513	1.391000
19 1 0	-2.805209	1.046406	-1.662616
20 1 0	1.546607	3.555683	0.223584
21 1 0	2.791376	2.342994	0.600050
22 1 0	2.132878	2.464618	-1.051859

2-(*p*-Tolyl)acetic acid (10c)

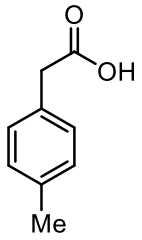

1 6 0	-0.491154	-1.261413	0.446461
2 6 0	-1.820603	-1.181533	0.053213
3 6 0	-2.432012	0.047776	-0.160608
4 6 0	-1.670374	1.200356	0.025784
5 6 0	-0.345459	1.125656	0.419133
6 6 0	0.258247	-0.109701	0.638927
7 6 0	1.714197	-0.180880	1.041812
8 6 0	2.580675	0.108453	-0.157751
9 6 0	-3.876984	0.143049	-0.564362
10 8 0	2.770359	-0.986469	-0.917433
11 8 0	3.029756	1.182270	-0.446292
12 1 0	-0.032394	-2.229909	0.601594
13 1 0	-2.390161	-2.091242	-0.090548
14 1 0	-2.124617	2.169454	-0.141342
15 1 0	0.234080	2.031265	0.550902
16 1 0	1.941643	0.570813	1.794043
17 1 0	1.951028	-1.170050	1.427791
18 1 0	-4.261554	-0.823723	-0.883662
19 1 0	-4.489839	0.489012	0.269455
20 1 0	-4.008707	0.851329	-1.381928
21 1 0	3.280400	-0.713929	-1.692166

2-(*o*-Tolyl)acetic acid (10d)

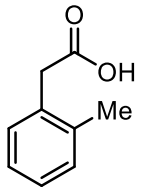

1 6 0	0.721135	-1.451691	0.365145
2 6 0	1.997518	-1.662330	-0.131861
3 6 0	2.776062	-0.572678	-0.489957
4 6 0	2.269342	0.710521	-0.350845
5 6 0	0.987542	0.938707	0.142663
6 6 0	0.210989	-0.165718	0.509228
7 6 0	-1.200517	-0.007254	1.036689
8 6 0	-2.186639	-0.267227	-0.073954
9 8 0	-2.320257	0.796067	-0.892100
10 8 0	-2.773023	-1.296451	-0.255867
11 6 0	0.470809	2.345464	0.276376
12 1 0	0.101532	-2.295436	0.643962
13 1 0	2.379555	-2.668255	-0.236667
14 1 0	3.775150	-0.719413	-0.877016
15 1 0	2.879178	1.559573	-0.632923
16 1 0	-1.395849	-0.740998	1.814318
17 1 0	-1.364217	0.992002	1.433138
18 1 0	-2.920823	0.535990	-1.603861
19 1 0	1.197069	3.056953	-0.110386
20 1 0	-0.463584	2.476867	-0.268912
21 1 0	0.280780	2.599026	1.321185

2-(4-(Methylthio)phenyl)acetic acid (10e)

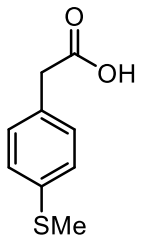

1 6 0	-0.444352	1.414906	0.412129
2 6 0	0.902897	1.463834	0.106756
3 6 0	1.661786	0.293194	0.064996
4 6 0	1.040264	-0.922266	0.333340
5 6 0	-0.313205	-0.959211	0.639713
6 6 0	-1.070406	0.202858	0.688388
7 6 0	-2.549302	0.137707	0.993614
8 6 0	-3.295908	-0.294475	-0.243539
9 8 0	-3.531226	0.737802	-1.074636
10 8 0	-3.619276	-1.420150	-0.500258
11 16 0	3.371868	0.474333	-0.328399
12 6 0	3.964821	-1.226369	-0.311250
13 1 0	-1.020097	2.331579	0.434832
14 1 0	1.375570	2.414885	-0.102279
15 1 0	1.596883	-1.847117	0.308881
16 1 0	-0.787829	-1.912181	0.839432
17 1 0	-2.750465	-0.599040	1.767480
18 1 0	-2.912996	1.112536	1.311850
19 1 0	-3.954459	0.379573	-1.866635
20 1 0	5.021068	-1.172609	-0.561904
21 1 0	3.855336	-1.671389	0.675174
22 1 0	3.451551	-1.827835	-1.058181

2-Mesitylacetic acid (10f)

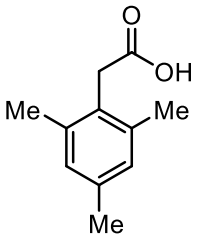

1 6 0	-0.540551	1.213801	-0.354486
2 6 0	-1.878417	1.131841	0.020502
3 6 0	-2.504831	-0.085904	0.242190
4 6 0	-1.758921	-1.245481	0.069879
5 6 0	-0.421766	-1.207745	-0.303867
6 6 0	0.192443	0.034002	-0.514289
7 6 0	1.655346	0.080664	-0.909994
8 6 0	2.547959	-0.044728	0.300519
9 6 0	-3.942865	-0.156057	0.675165
10 8 0	2.547154	1.075791	1.049855
11 8 0	3.187352	-1.013509	0.604501
12 6 0	0.334619	-2.495606	-0.495774
13 6 0	0.076113	2.566665	-0.593455
14 1 0	-2.444943	2.048034	0.140586
15 1 0	-2.231363	-2.208130	0.229940
16 1 0	1.908182	-0.739577	-1.576331
17 1 0	1.887717	1.020686	-1.406151
18 1 0	-4.455035	0.787461	0.495594
19 1 0	-4.475001	-0.943009	0.141569
20 1 0	-4.014384	-0.377724	1.741279
21 1 0	3.104915	0.903895	1.820589
22 1 0	-0.277724	-3.343976	-0.198451
23 1 0	0.608107	-2.634258	-1.544239
24 1 0	1.258501	-2.515893	0.081048
25 1 0	-0.640103	3.354734	-0.371735
26 1 0	0.957461	2.718711	0.028291
27 1 0	0.382854	2.682077	-1.635161

2-(Benzo[d][1,3]dioxol-5-yl)acetic acid (10g)

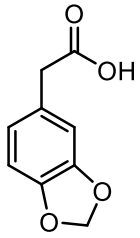

1 6 0	0.222490	1.697956	-0.249198
2 6 0	-1.128817	1.822557	0.098349
3 6 0	-1.873102	0.673365	0.096983

4 6 0	-1.320021	-0.555376	-0.237306
5 6 0	-0.003273	-0.690759	-0.585875
6 6 0	0.779357	0.475737	-0.588901
7 6 0	2.245967	0.369023	-0.945813
8 6 0	2.972625	-0.394573	0.132230
9 8 0	3.392972	0.408166	1.126528
10 8 0	3.135916	-1.582904	0.146090
11 8 0	-3.206752	0.513018	0.353658
12 6 0	-3.401621	-0.892810	0.444124
13 8 0	-2.293944	-1.513483	-0.196012
14 1 0	0.847838	2.580399	-0.249459
15 1 0	-1.565649	2.776606	0.353062
16 1 0	0.421093	-1.652326	-0.840655
17 1 0	2.374068	-0.183418	-1.874592
18 1 0	2.680756	1.360315	-1.046910
19 1 0	3.795422	-0.155865	1.800875
20 1 0	-3.422071	-1.188120	1.497544
21 1 0	-4.318619	-1.166672	-0.069547

2-(Thiophen-3-yl)acetic acid (10h)

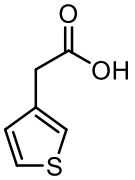

1 6 0	-0.176618	-0.111191	0.516141
2 6 0	1.210690	-0.390065	1.031756
3 6 0	2.223189	0.018247	-0.009223
4 8 0	2.517907	-0.986399	-0.852731
5 8 0	2.696072	1.115303	-0.115741
6 6 0	-0.640596	1.195044	0.178316
7 6 0	-1.922945	1.193788	-0.268041
8 16 0	-2.586090	-0.387870	-0.287835
9 6 0	-1.127218	-1.061963	0.307453
10 1 0	1.409073	0.201713	1.923820
11 1 0	1.322611	-1.446837	1.260860
12 1 0	3.125026	-0.635080	-1.518296
13 1 0	-0.029578	2.082148	0.262638
14 1 0	-2.517456	2.032975	-0.587010
15 1 0	-1.043089	-2.123381	0.472715

2-(4-Chlorophenyl)acetic acid (10j)

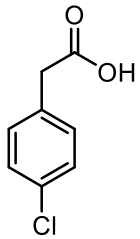

1 6 0	0.084868	1.284787	0.492685
2 6 0	1.428379	1.222385	0.153445
3 6 0	2.024342	-0.016281	-0.010052
4 6 0	1.300933	-1.186492	0.157968
5 6 0	-0.039550	-1.107551	0.498030
6 6 0	-0.659488	0.125892	0.673360
7 6 0	-2.129843	0.189738	1.018504
8 6 0	-2.943986	-0.126080	-0.212011
9 17 0	3.707795	-0.106615	-0.431797
10 8 0	-3.122269	0.958718	-0.987167
11 8 0	-3.359089	-1.211430	-0.505964
12 1 0	-0.388367	2.250294	0.616685
13 1 0	2.010033	2.122448	0.016818
14 1 0	1.785680	-2.142574	0.024015
15 1 0	-0.615086	-2.016159	0.623357
16 1 0	-2.379222	-0.553677	1.771828
17 1 0	-2.390773	1.181548	1.380762
18 1 0	-3.597857	0.673888	-1.779449

2-([1,1'-Biphenyl]-4-yl)acetic acid (10k)

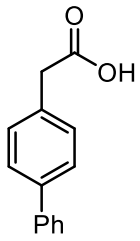

1 6 0	-1.231249	1.429439	-0.011900
2 6 0	0.136173	1.295126	-0.194022
3 6 0	0.802898	0.142098	0.216443
4 6 0	0.055976	-0.873451	0.814342
5 6 0	-1.309443	-0.738327	0.998214
6 6 0	-1.968014	0.417543	0.590521
7 6 0	-3.463654	0.542090	0.772431
8 6 0	-4.164801	-0.285608	-0.275639
9 8 0	-4.279497	0.374704	-1.442714
10 8 0	-4.549832	-1.411161	-0.126571
11 6 0	2.263696	-0.001457	0.023920
12 6 0	2.817844	-1.228526	-0.340477
13 6 0	4.185505	-1.363706	-0.521852
14 6 0	5.024981	-0.273437	-0.340786
15 6 0	4.485638	0.952622	0.022433
16 6 0	3.117655	1.086809	0.202490
17 1 0	-1.733583	2.326916	-0.350209
18 1 0	0.690421	2.085574	-0.682792
19 1 0	0.555912	-1.768214	1.161131
20 1 0	-1.874367	-1.535397	1.465677
21 1 0	-3.765111	0.157509	1.743826
22 1 0	-3.771046	1.581239	0.676730
23 1 0	-4.681689	-0.231983	-2.079058
24 1 0	2.167318	-2.077238	-0.506525
25 1 0	4.595818	-2.321083	-0.813072
26 1 0	6.091860	-0.378611	-0.481549
27 1 0	5.132885	1.805693	0.174466
28 1 0	2.706969	2.039956	0.508954

2-(Perfluorophenyl)acetic acid (10l)

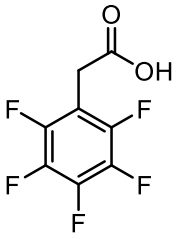

1 6 0	0.320219	1.279469	-0.260252
2 6 0	1.658311	1.103463	0.047247
3 6 0	2.170263	-0.177880	0.141863
4 6 0	1.345194	-1.269788	-0.072362
5 6 0	0.014649	-1.060341	-0.378793
6 6 0	-0.527558	0.209832	-0.484886
7 6 0	-1.980433	0.392999	-0.789713
8 6 0	-2.858790	0.024103	0.387019
9 9 0	3.448108	-0.361378	0.434894
10 8 0	-4.156148	0.177365	0.076214
11 8 0	-2.476210	-0.353892	1.454982
12 9 0	1.836601	-2.497866	0.017792
13 9 0	-0.766945	-2.118689	-0.583438
14 9 0	-0.147164	2.525791	-0.337789
15 9 0	2.447622	2.149569	0.251684
16 1 0	-2.196292	1.424763	-1.061513
17 1 0	-2.285785	-0.229757	-1.631233
18 1 0	-4.674186	-0.070780	0.854152

2-(Naphthalen-2-yl)acetic acid (10m)

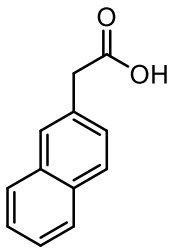

1 6 0	0.005963	-0.937475	0.545552
2 6 0	-1.320089	-0.564075	0.216342
3 6 0	-1.610527	0.802110	-0.021887
4 6 0	-0.561138	1.749020	0.076350
5 6 0	0.705462	1.359158	0.396588
6 6 0	1.000735	-0.005924	0.640775
7 6 0	2.418670	-0.400886	0.985257
8 6 0	3.312752	-0.155001	-0.204273

9 8 0	3.336904	-1.205906	-1.043244
10 8 0	3.911752	0.861437	-0.420322
11 6 0	-2.363867	-1.514647	0.117275
12 6 0	-3.633772	-1.124934	-0.202105
13 6 0	-3.923321	0.236750	-0.438499
14 6 0	-2.935022	1.175954	-0.350089
15 1 0	0.222514	-1.984530	0.722746
16 1 0	-0.782342	2.792792	-0.107831
17 1 0	1.505148	2.086456	0.461526
18 1 0	2.794905	0.211384	1.802793
19 1 0	2.460956	-1.451369	1.262640
20 1 0	3.879808	-0.955819	-1.803245
21 1 0	-2.137564	-2.557748	0.299207
22 1 0	-4.424207	-1.859271	-0.275684
23 1 0	-4.932562	0.532116	-0.690577
24 1 0	-3.150981	2.221453	-0.530761

2-(Naphthalen-1-yl)acetic acid (10n)

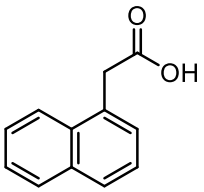

1 6 0	0.832073	-0.266492	-0.035183
2 6 0	1.796708	0.773196	0.014846
3 6 0	1.367979	2.122924	0.012398
4 6 0	0.040426	2.422480	-0.041558
5 6 0	-0.921938	1.389980	-0.089687
6 6 0	-0.553874	0.073049	-0.081986
7 6 0	-1.571746	-1.046732	-0.137773
8 6 0	-2.989008	-0.548049	-0.074464
9 8 0	-3.400943	-0.356991	1.193316
10 8 0	-3.691189	-0.322336	-1.019509
11 6 0	1.289731	-1.607201	-0.043243
12 6 0	2.625373	-1.897290	0.001225
13 6 0	3.580218	-0.862045	0.057041
14 6 0	3.171121	0.440940	0.062893
15 1 0	2.113243	2.907010	0.051018
16 1 0	-0.289003	3.452236	-0.048335
17 1 0	-1.968309	1.662452	-0.139589
18 1 0	-1.463750	-1.601961	-1.069521
19 1 0	-1.409200	-1.730976	0.695461
20 1 0	-4.305923	-0.018751	1.153636
21 1 0	0.575754	-2.417516	-0.089346
22 1 0	2.953282	-2.927752	-0.007157
23 1 0	4.633505	-1.103718	0.093352
24 1 0	3.895075	1.245039	0.102979

2-(4-Acetamidophenyl)acetic acid (10o)

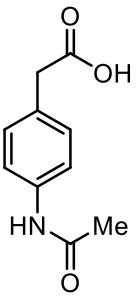

1 6 0	-0.572311	-1.127675	-0.614990
2 6 0	0.779737	-0.944543	-0.357397
3 6 0	1.266159	0.345250	-0.160141
4 6 0	0.382788	1.424883	-0.225128
5 6 0	-0.958250	1.224058	-0.484047
6 6 0	-1.454950	-0.060532	-0.687872
7 6 0	-2.928820	-0.272424	-0.950364
8 6 0	-3.703350	-0.008025	0.315902
9 7 0	2.614966	0.635851	0.105487
10 8 0	-3.783468	-1.100490	1.096620
11 8 0	-4.167873	1.051429	0.633612
12 6 0	3.677278	-0.225328	0.218022
13 8 0	3.587610	-1.425802	0.094069
14 6 0	4.988118	0.469051	0.514709
15 1 0	-0.942328	-2.134486	-0.762377
16 1 0	1.449857	-1.785416	-0.309048
17 1 0	0.755428	2.430458	-0.070722
18 1 0	-1.632282	2.070760	-0.521698
19 1 0	-3.289060	0.426884	-1.701854
20 1 0	-3.110007	-1.292130	-1.282088
21 1 0	2.824561	1.612407	0.230765
22 1 0	-4.237290	-0.841366	1.910066
23 1 0	4.925652	1.018853	1.453894
24 1 0	5.767291	-0.281876	0.585933
25 1 0	5.234875	1.175580	-0.277853

2-(11-Oxo-6,11-dihydrodibenzo[b,e]oxepin-2-yl)acetic acid (10p)

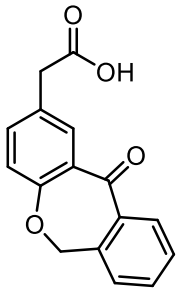

1 6 0	2.294163	1.248331	-0.813151
2 6 0	1.098565	1.907734	-0.664908
3 6 0	-0.040231	1.238914	-0.205939
4 6 0	0.021396	-0.132292	0.069781
5 6 0	1.268752	-0.765734	-0.066727
6 6 0	2.398587	-0.110764	-0.498660
7 6 0	3.700046	-0.842381	-0.652109
8 6 0	4.825036	-0.280520	0.185130
9 8 0	5.883574	-1.114008	0.186857
10 8 0	4.829983	0.768128	0.763521
11 8 0	-1.125802	2.035316	-0.056296
12 6 0	-2.096271	1.662316	0.908694
13 6 0	-3.025849	0.611580	0.384772
14 6 0	-2.540235	-0.669126	0.132759
15 6 0	-1.115998	-1.061917	0.378547
16 8 0	-0.884505	-2.198114	0.731819
17 6 0	-4.368699	0.888835	0.167989
18 6 0	-5.223586	-0.094855	-0.306647
19 6 0	-4.738543	-1.371062	-0.557820
20 6 0	-3.403622	-1.658925	-0.327512
21 1 0	3.166744	1.791787	-1.150557
22 1 0	1.008732	2.964612	-0.871510
23 1 0	1.302919	-1.822692	0.160787
24 1 0	3.592520	-1.897715	-0.405465
25 1 0	4.053489	-0.809055	-1.686887
26 1 0	6.577923	-0.695045	0.713077
27 1 0	-2.642237	2.573697	1.140910
28 1 0	-1.584500	1.319664	1.813383
29 1 0	-4.745642	1.882190	0.375696
30 1 0	-6.266611	0.133437	-0.478050
31 1 0	-5.401334	-2.141177	-0.927231
32 1 0	-3.009072	-2.651080	-0.496567

2-(1-(4-Chlorobenzoyl)-5-methoxy-2-methyl-1H-indol-3-yl)acetic acid (10q)

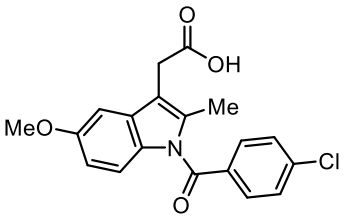

1 6 0	2.261055	-0.866230	-0.632158
2 6 0	3.628280	-1.143692	-1.180944
3 6 0	4.578949	-1.471669	-0.056649
4 8 0	5.006033	-0.362974	0.578460
5 8 0	4.904796	-2.575808	0.276412
6 6 0	1.762308	0.430252	-0.258220
7 6 0	0.444414	0.262340	0.176832
8 7 0	0.143377	-1.107823	0.076443
9 6 0	1.284660	-1.779941	-0.387565
10 6 0	-1.037850	-1.752821	0.469178
11 8 0	-1.022391	-2.870090	0.922215
12 6 0	-2.318991	-1.024756	0.244681

13 6 0	-3.371895	-1.268506	1.119859
14 6 0	-4.602218	-0.667542	0.918605
15 6 0	-4.774962	0.155737	-0.184431
16 6 0	-3.743916	0.389257	-1.082252
17 6 0	-2.510969	-0.198990	-0.858171
18 17 0	-6.316071	0.903849	-0.451943
19 6 0	2.371404	1.689034	-0.238585
20 6 0	1.635667	2.760087	0.233868
21 6 0	0.322720	2.577087	0.699299
22 6 0	-0.280459	1.338491	0.687144
23 6 0	1.315385	-3.251790	-0.603015
24 8 0	2.102928	4.034696	0.310209
25 6 0	3.424272	4.266444	-0.120839
26 1 0	3.619372	-1.993463	-1.858097
27 1 0	3.994708	-0.267966	-1.716102
28 1 0	5.554670	-0.649651	1.321321
29 1 0	-3.214498	-1.934849	1.956762
30 1 0	-5.424568	-0.835952	1.598298
31 1 0	-3.910496	1.024931	-1.939300
32 1 0	-1.695345	-0.014604	-1.544216
33 1 0	3.399019	1.795008	-0.552789
34 1 0	-0.202083	3.440258	1.082956
35 1 0	-1.281940	1.227685	1.073435
36 1 0	0.441445	-3.592491	-1.157095
37 1 0	2.215145	-3.515903	-1.153378
38 1 0	1.322036	-3.785921	0.344956
39 1 0	3.609120	5.327561	0.015825
40 1 0	4.139562	3.692398	0.473206
41 1 0	3.545362	4.008947	-1.176030

3-(4,5-Diphenyloxazol-2-yl)propanoic acid (10r)

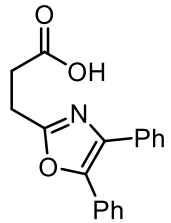

1 6 0	2.948773	-0.991802	-0.005866
2 6 0	3.914789	0.177777	0.015471
3 6 0	5.342840	-0.285959	-0.002257
4 8 0	6.202811	0.748406	0.029446
5 8 0	5.708750	-1.428279	-0.040514
6 6 0	1.538879	-0.524230	-0.000989
7 8 0	0.570810	-1.459058	-0.006429
8 6 0	-0.610621	-0.763718	0.003496
9 6 0	-0.294819	0.559626	-0.012097
10 7 0	1.093143	0.681805	0.003511
11 6 0	-1.834915	-1.555499	0.069099
12 6 0	-1.874347	-2.829512	-0.498237
13 6 0	-3.030280	-3.590824	-0.428494
14 6 0	-4.158009	-3.092435	0.208231
15 6 0	-4.120481	-1.829670	0.785832
16 6 0	-2.966625	-1.066937	0.723272
17 6 0	-1.146261	1.753204	-0.075623
18 6 0	-0.725208	2.927912	0.545196
19 6 0	-1.507576	4.070873	0.488641
20 6 0	-2.715044	4.057698	-0.195609
21 6 0	-3.131761	2.895964	-0.832361
22 6 0	-2.351346	1.752453	-0.777108
23 1 0	3.121388	-1.611627	-0.886993
24 1 0	3.117811	-1.643183	0.852807
25 1 0	3.765418	0.801597	0.897310
26 1 0	3.756105	0.839384	-0.836837
27 1 0	7.096510	0.380308	0.014450
28 1 0	-0.995341	-3.217192	-0.994155
29 1 0	-3.050121	-4.575694	-0.874528
30 1 0	-5.059469	-3.687121	0.261081
31 1 0	-4.990345	-1.441550	1.297694
32 1 0	-2.933698	-0.091953	1.189834
33 1 0	0.222060	2.933314	1.066393
34 1 0	-1.172699	4.975029	0.978523
35 1 0	-3.324095	4.950070	-0.240887
36 1 0	-4.062351	2.883424	-1.383224
37 1 0	-2.670068	0.854482	-1.289637

2-Phenylpropanoic acid (10s)

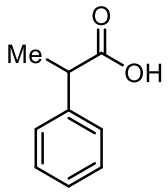

1 6 0	-0.842587	-1.078521	0.106761
2 6 0	-2.169866	-1.240369	0.473184
3 6 0	-3.050255	-0.168685	0.406149
4 6 0	-2.593467	1.067008	-0.025805
5 6 0	-1.263667	1.227881	-0.390024
6 6 0	-0.376591	0.158648	-0.332780
7 6 0	1.071570	0.354929	-0.744531
8 6 0	1.950845	0.311043	0.487628
9 8 0	2.195897	-0.947206	0.906504
10 8 0	2.384246	1.271235	1.059485
11 6 0	1.523976	-0.646346	-1.808077
12 1 0	-0.161682	-1.916667	0.172789
13 1 0	-2.517899	-2.206206	0.813510
14 1 0	-4.085457	-0.296943	0.690988
15 1 0	-3.270608	1.908546	-0.079082
16 1 0	-0.909154	2.195469	-0.722010
17 1 0	1.178263	1.369198	-1.124406
18 1 0	2.724069	-0.879679	1.713345
19 1 0	2.562883	-0.472665	-2.086637
20 1 0	0.902045	-0.538606	-2.695007
21 1 0	1.436646	-1.668209	-1.446431

Benzoylglycine (1s)

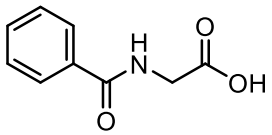

1 6 0	2.324704	0.672629	0.000038
2 6 0	3.345653	-0.430733	0.000000
3 8 0	4.593596	0.051448	-0.000052
4 8 0	3.089111	-1.603516	0.000079
5 7 0	1.009833	0.098063	0.000038
6 6 0	-0.079800	0.903465	-0.000022
7 6 0	-1.426267	0.240604	-0.000013
8 8 0	0.039661	2.115395	-0.000089
9 6 0	-2.536279	1.079262	0.000053
10 6 0	-3.815541	0.548164	0.000067
11 6 0	-3.996228	-0.828320	0.000011
12 6 0	-2.893503	-1.670631	-0.000061
13 6 0	-1.612763	-1.138905	-0.000074
14 1 0	2.488856	1.308331	0.873265
15 1 0	2.488809	1.308386	-0.873153
16 1 0	5.201108	-0.700792	-0.000031
17 1 0	0.952796	-0.905880	0.000181
18 1 0	-2.368768	2.146971	0.000093
19 1 0	-4.672656	1.207313	0.000120
20 1 0	-4.994245	-1.244976	0.000020
21 1 0	-3.029181	-2.743229	-0.000113
22 1 0	-0.774356	-1.822383	-0.000149

2-(1*H*-Indol-3-yl)acetic acid (1t)

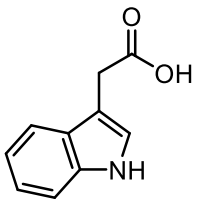

1 6 0	0.585820	0.733205	0.514401
2 6 0	1.918589	0.241014	0.990946
3 6 0	2.690710	-0.379695	-0.147802
4 8 0	2.277009	-1.634302	-0.411076
5 8 0	3.554209	0.160961	-0.779410
6 6 0	-0.601720	-0.047134	0.303946
7 6 0	-1.599368	0.836605	-0.155834
8 7 0	-1.036612	2.087673	-0.226562
9 6 0	0.274443	2.015921	0.177451
10 6 0	-0.913956	-1.401525	0.468239
11 6 0	-2.193186	-1.827643	0.181104
12 6 0	-3.173258	-0.929523	-0.274152
13 6 0	-2.892845	0.409400	-0.449612

14 1 0	2.515207	1.064911	1.373755
15 1 0	1.786517	-0.503708	1.776499
16 1 0	2.770163	-1.944364	-1.182687
17 1 0	-1.509109	2.923721	-0.516655
18 1 0	0.896096	2.895643	0.195515
19 1 0	-0.158355	-2.099947	0.802322
20 1 0	-2.450862	-2.870581	0.302380
21 1 0	-4.166675	-1.296328	-0.492558
22 1 0	-3.647818	1.099924	-0.800883

2-(3-Bromophenyl)propanoic acid (S1)

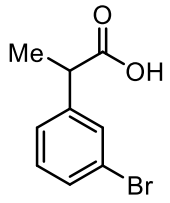

1 6 0	0.999848	1.569592	-0.059299
2 6 0	-0.145659	2.263917	-0.413897
3 6 0	-1.385968	1.640506	-0.399489
4 6 0	-1.453137	0.309661	-0.027044
5 6 0	-0.316622	-0.399824	0.327136
6 6 0	0.922326	0.230885	0.317113
7 6 0	2.159930	-0.551043	0.718062
8 6 0	3.023663	-0.785784	-0.504679
9 8 0	3.753231	0.297275	-0.839885
10 8 0	3.064273	-1.805889	-1.131540
11 35 0	-3.133427	-0.566992	0.000157
12 6 0	2.938119	0.123852	1.848582
13 1 0	1.959866	2.066473	-0.085386
14 1 0	-0.077259	3.302723	-0.706367
15 1 0	-2.282987	2.176235	-0.673082
16 1 0	-0.397073	-1.440697	0.608835
17 1 0	1.845063	-1.545000	1.029345
18 1 0	4.241728	0.073824	-1.643777
19 1 0	3.814571	-0.464413	2.117882
20 1 0	2.298350	0.217716	2.724247
21 1 0	3.272639	1.116180	1.555308

Cyclohexanecarboxylic acid (S2)

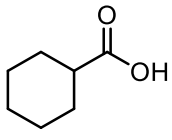

1 6 0	-0.355695	-0.007369	-0.372356
2 6 0	-1.807153	-0.138447	0.004813
3 8 0	-2.556733	0.854099	-0.520334
4 8 0	-2.280805	-0.989550	0.706033
5 6 0	0.412175	-1.292554	-0.084759
6 6 0	1.888453	-1.133450	-0.436599
7 6 0	2.509487	0.046128	0.307400
8 6 0	1.738929	1.334320	0.030648
9 6 0	0.260987	1.184369	0.379993
10 1 0	-0.319973	0.219436	-1.442316
11 1 0	-3.462150	0.721612	-0.209208
12 1 0	0.305158	-1.529098	0.976541
13 1 0	-0.032876	-2.122710	-0.633791
14 1 0	2.425982	-2.053640	-0.206123
15 1 0	1.988848	-0.970391	-1.514335
16 1 0	2.489670	-0.158667	1.382155
17 1 0	3.556448	0.164602	0.025963
18 1 0	2.168257	2.164739	0.592271
19 1 0	1.830050	1.587580	-1.030078
20 1 0	0.155742	1.006680	1.454801
21 1 0	-0.287941	2.095480	0.143694

7-Bromoheptanoic acid (S3)

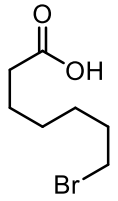

1 6 0	-2.902948	0.494555	-0.785387
2 6 0	-1.912772	1.569748	-0.366920
3 6 0	-0.471881	1.071964	-0.366845
4 6 0	0.490165	2.128495	0.162345
5 8 0	-3.753800	-1.636389	-0.216290
6 6 0	-3.074183	-0.575176	0.260299
7 8 0	-2.689453	-0.519077	1.395586
8 6 0	1.971775	1.774719	0.063111
9 6 0	2.385059	0.526463	0.827429
10 35 0	2.204090	-1.121422	-0.217848
11 1 0	-3.898025	0.909621	-0.962315
12 1 0	-2.606596	0.010831	-1.717693
13 1 0	-2.005189	2.420905	-1.044349
14 1 0	-2.175663	1.922996	0.631927
15 1 0	-0.405358	0.170635	0.244592
16 1 0	-0.182512	0.781906	-1.381480
17 1 0	0.326146	3.064438	-0.378495
18 1 0	0.244197	2.333500	1.208551
19 1 0	-3.843882	-2.268249	0.509726
20 1 0	2.550820	2.605158	0.475507
21 1 0	2.272751	1.675963	-0.981019
22 1 0	3.433365	0.548593	1.102909
23 1 0	1.781533	0.372606	1.718236

2-(1*H*-Imidazol-1-yl)acetic acid (S4)

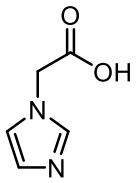

1 7 0	0.538800	-0.224478	0.458116
2 6 0	-0.807426	-0.378848	0.934399
3 6 0	-1.891241	0.029780	-0.048707
4 8 0	-1.454426	0.868597	-0.992189
5 8 0	-3.025092	-0.342951	0.045794
6 6 0	1.198101	-1.061630	-0.409050
7 6 0	2.405144	-0.471166	-0.640171
8 7 0	2.502568	0.707459	0.055049
9 6 0	1.370477	0.825486	0.692319
10 1 0	-1.001165	-1.411275	1.217558
11 1 0	-0.942593	0.234844	1.825921
12 1 0	-2.207466	1.094046	-1.555850
13 1 0	0.753610	-1.975220	-0.762615
14 1 0	3.209173	-0.828641	-1.259753
15 1 0	1.084676	1.638474	1.341004

2,2'-(1,4-Phenylene)diacetic acid (S5)

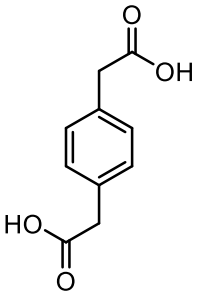

1 6 0	-0.581322	-0.829945	1.256628
2 6 0	0.799071	-0.831548	1.131161
3 6 0	1.393349	-0.839122	-0.126085
4 6 0	0.581306	-0.834054	-1.254212
5 6 0	-0.799091	-0.835315	-1.128741
6 6 0	-1.393367	-0.838775	0.128518
7 6 0	-2.900358	-0.818061	0.252280
8 6 0	-3.407978	0.566547	-0.064861
9 6 0	2.900343	-0.818792	-0.249874
10 8 0	-3.344802	1.381102	1.004030
11 8 0	-3.791009	0.933924	-1.139864
12 6 0	3.408014	0.566717	0.063207
13 8 0	3.344571	1.378226	-1.007984
14 8 0	3.791299	0.937169	1.137065
15 1 0	-1.032908	-0.822011	2.240452
16 1 0	1.424229	-0.821284	2.015410
17 1 0	1.032889	-0.829316	-2.238058
18 1 0	-1.424250	-0.827967	-2.013017
19 1 0	-3.353072	-1.500672	-0.462916
20 1 0	-3.200606	-1.090791	1.261573

21 1 0	3.353021	-1.499330	0.467316
22 1 0	3.200612	-1.094480	-1.258358
23 1 0	-3.628243	2.259313	0.715530
24 1 0	3.628050	2.257259	-0.722034

2-Bromo-2-(3-bromophenyl)acetic acid (S6)

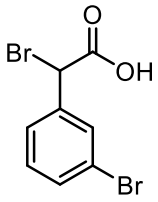

1 6 0	0.282784	0.886122	1.409964
2 6 0	-0.914299	1.141767	2.054166
3 6 0	-2.125555	0.783949	1.473810
4 6 0	-2.116130	0.164306	0.237761
5 6 0	-0.926841	-0.098590	-0.424195
6 6 0	0.278371	0.267077	0.162693
7 6 0	1.543982	-0.015043	-0.583035
8 6 0	2.412146	1.203387	-0.843046
9 8 0	3.113916	1.050774	-1.975300
10 8 0	2.481340	2.171903	-0.145886
11 35 0	-3.752975	-0.344865	-0.568333
12 35 0	2.704422	-1.262936	0.401650
13 1 0	1.221765	1.163233	1.866126
14 1 0	-0.912219	1.624010	3.021685
15 1 0	-3.061539	0.980172	1.975976
16 1 0	-0.943849	-0.585858	-1.389602
17 1 0	1.345525	-0.515628	-1.524046
18 1 0	3.680877	1.827848	-2.075482

2-(3,5-Bis(trifluoromethyl)phenyl)acetic acid (S7)

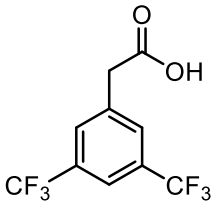

1 6 0	-0.841264	-1.005672	-0.529274
2 6 0	0.455206	-1.308709	-0.142075
3 6 0	1.384290	-0.306815	0.082016
4 6 0	0.991352	1.011279	-0.085672
5 6 0	-0.301907	1.326072	-0.472067
6 6 0	-1.228703	0.316371	-0.702838
7 6 0	-2.645896	0.661253	-1.093246
8 6 0	-3.476090	0.865081	0.153377
9 8 0	-3.835267	-0.307988	0.703616
10 8 0	-3.760036	1.926911	0.626876
11 9 0	2.145916	-2.928129	0.142565
12 6 0	0.824909	-2.751598	0.063845
13 9 0	0.374203	-3.520956	-0.935168
14 9 0	0.291496	-3.235702	1.194154
15 9 0	2.479441	2.539402	-1.073143
16 6 0	1.985727	2.123776	0.102324
17 9 0	3.023977	1.747022	0.853532
18 9 0	1.429283	3.189750	0.687345
19 1 0	-1.553623	-1.804076	-0.695177
20 1 0	2.393928	-0.547388	0.380765
21 1 0	-0.592223	2.362713	-0.589145
22 1 0	-2.674256	1.587655	-1.659891
23 1 0	-3.080112	-0.143865	-1.682863
24 1 0	-4.315865	-0.115141	1.520493

2-Cyclopropylacetic acid (S8)

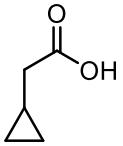

1 6 0	0.158901	-0.480602	1.093847
2 6 0	-1.254585	-0.432745	0.537727
3 8 0	1.838340	-0.793600	-0.552970
4 6 0	1.156006	0.132464	0.149199
5 8 0	1.333614	1.309410	-0.007911
6 6 0	-1.792767	0.791952	-0.132437
7 6 0	-1.522687	-0.448274	-0.935974
8 1 0	0.206489	0.084479	2.024331
9 1 0	0.445057	-1.512592	1.287299
10 1 0	-1.957684	-0.981746	1.148492
11 1 0	2.435993	-0.317499	-1.145947
12 1 0	-2.821068	1.057390	0.060846
13 1 0	-1.117247	1.624307	-0.264008
14 1 0	-0.673404	-0.433744	-1.604848
15 1 0	-2.362973	-1.023835	-1.293291

(*Z*)-2-(5-Fluoro-2-methyl-1-(4-(methylsulfinyl)benzylidene)-1*H*-inden-3-yl)acetic acid (S9)

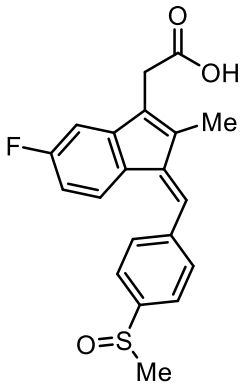

1 6 0	3.181690	-0.655008	-0.598101
2 6 0	4.632189	-0.907513	-0.888801
3 6 0	5.369588	-1.178215	0.400099
4 8 0	5.652692	-0.042016	1.062199
5 8 0	5.648484	-2.265116	0.821299
6 6 0	2.618794	0.679594	-0.363601
7 6 0	1.234394	0.552899	-0.143401
8 6 0	0.917089	-0.889900	-0.238001
9 6 0	2.204587	-1.576405	-0.482801
10 6 0	-0.242513	-1.554297	-0.130301
11 6 0	3.253498	1.905992	-0.296601
12 6 0	2.466502	3.004195	0.007999
13 6 0	1.112502	2.913599	0.262599
14 6 0	0.488997	1.669801	0.191699
15 9 0	3.054006	4.209893	0.079199
16 6 0	-1.603511	-1.009092	-0.037001
17 6 0	-2.513113	-1.567189	0.861799
18 6 0	-3.813112	-1.092285	0.949699
19 6 0	-4.211208	-0.071483	0.105599
20 6 0	-3.331406	0.492914	-0.808201
21 6 0	-2.034508	0.016909	-0.882601
22 16 0	-5.899306	0.540222	0.242999
23 6 0	-6.520209	-0.256576	-1.261101
24 8 0	-6.531809	-0.199876	1.380599
25 6 0	2.335482	-3.056505	-0.602201
26 1 0	4.756886	-1.779513	-1.524701
27 1 0	5.072392	-0.040014	-1.379401
28 1 0	6.069591	-0.287417	1.899599
29 1 0	-0.186217	-2.638897	-0.120701
30 1 0	4.318899	2.025788	-0.436501
31 1 0	0.563404	3.807301	0.520499
32 1 0	-0.565103	1.598205	0.413699
33 1 0	-2.191016	-2.373490	1.508399
34 1 0	-4.526513	-1.494582	1.657299
35 1 0	-3.655704	1.296315	-1.459101
36 1 0	-1.342207	0.434607	-1.601401
37 1 0	-5.974108	0.118822	-2.123801
38 1 0	-6.387212	-1.329476	-1.141901
39 1 0	-7.574808	-0.002772	-1.333501
40 1 0	1.735681	-3.441303	-1.429001
41 1 0	3.371181	-3.351608	-0.752901
42 1 0	1.988380	-3.547104	0.309099

3.12 References

[35] Sun, K.; Huang, C.Y. (D.); Sawamura, M.; Shimizu, Y., *Synlett.* **2023**, *34*, 2210-2214.
[36] Lübcke, M.; Yuan, W.; Szabó, K. J., *Org. Lett*. **2017**, *19*, 4548.
[37] Mizuta, S.; Kitamura, K.; Morii, Y.; Ishihara, J.; Yamaguchi, T.; Ishikawa, T., *J. Org. Chem*. **2021**, *86*, 18017.
[38] Pluta, R.; Nikolaienko, P.; Rueping, M., *Angew. Chem. Int. Ed*. **2014**, *53*, 1650 –1653.
[39] Dotson, J. J.; Dijk, L.; Timmerman, J. C.; Grosslight, S.; Walroth, R. C.; Gosselin, F.; Püntener, K.; Mack, K. A.; Sigman, M. S., *J. Am. Chem. Soc*. **2023**, *145*, 110–121.
[40] Newman-Stonebraker, S. H,; Smith, S. R.; Borowski, J. E.; Peters , E.; Gensch, T.; Johnson, H. C.; Sigman, M. S.; Doyle, A. G., *Science*, **2021**, *374*, 301–308.
[41] Boni, Y. T.; Cammarota, R. C.; Liao, K.; Sigman, M. S.; Davies, H. M. L., *J. Am. Chem. Soc.* **2022**, *144*, 15549–15561.

Outlook

Boron catalysis has been proven to bring about tremendous convenience and efficiency to the functionalization of carboxylic acid. I have in the course of five years developed three methodologies in this area. The combination of photocatalysis and data science has provided unique results that can expand the utilization of boron catalysis as well as direct functionalization of carboxylic acid. I believe my research here can be the source of greater achievements in the future.

Acknowledgement

I would like to thank my professors and families for their support to me.